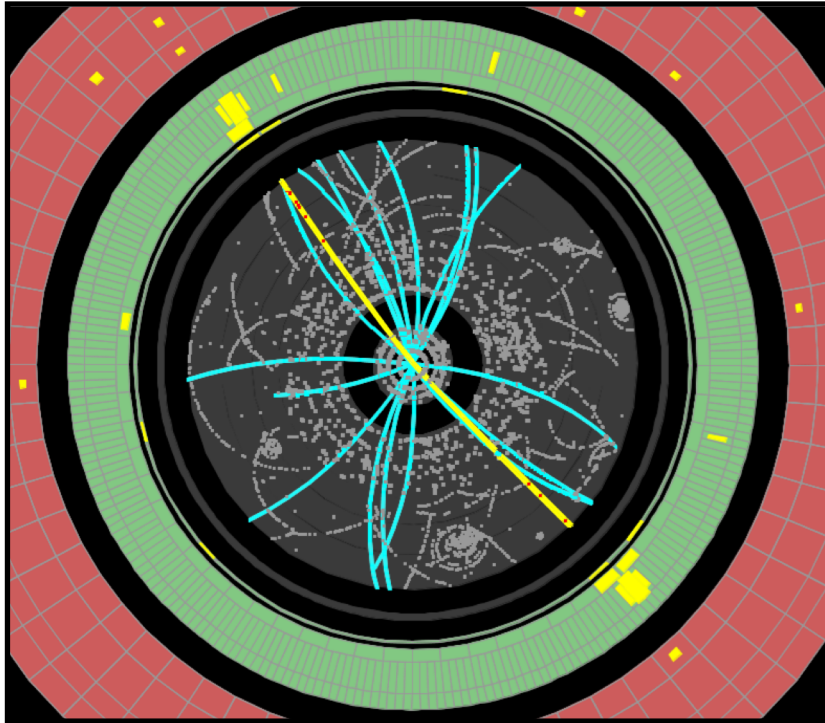


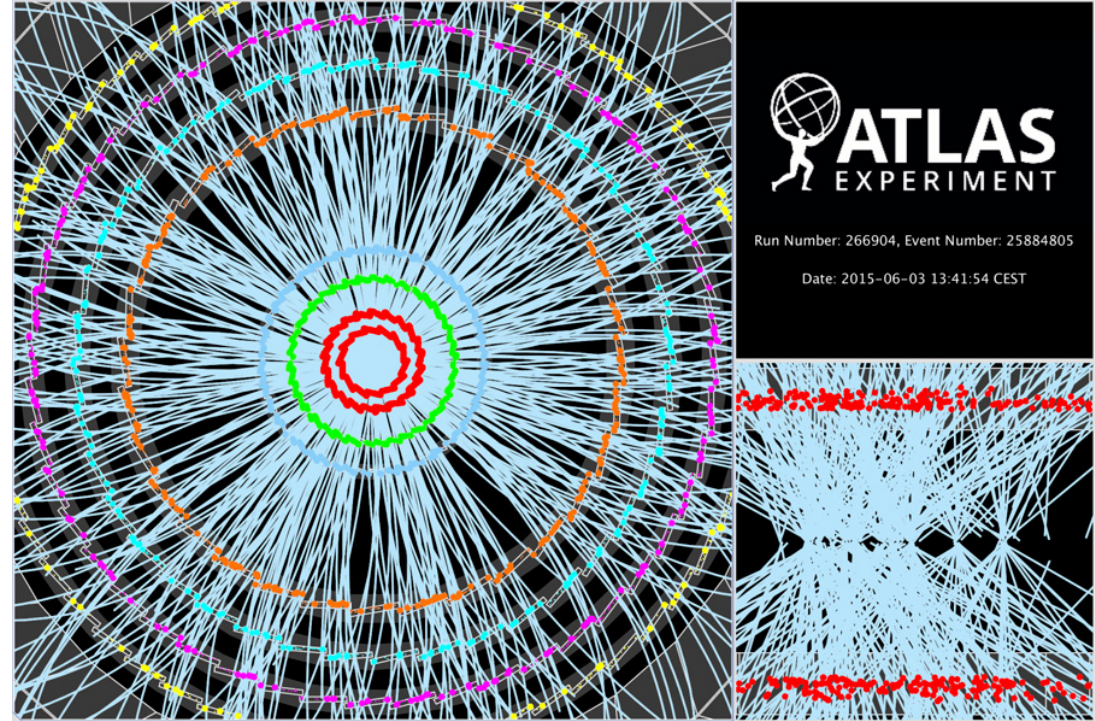


Lecture 1: Experiments & Accelerators

Toni Baroncelli Experimental High Energy Physics at Colliders 2019-20



Z \rightarrow ee Candidate
[September 2010]



Display of a proton-proton collision event recorded by ATLAS on 3 June 2015, with the first LHC stable beams at a collision energy of 13 TeV. Tracks reconstructed by the tracking detector are shown as light blue lines, and hits in the layers of the silicon tracking detector are shown as colored filled circles. The four inner layers are part of the silicon pixel detector and the four outer layers are part of the silicon strip detector. The layer closest to the beam, called IBL, is new for Run 2. In the view in the bottom right it is seen that this event has multiple pp collisions. The total number of reconstructed collision vertices is 17 but they are not all resolvable on the scale of this picture.

Toni Baroncelli
INFN RomaTRE

Originally inspired by Hans-Christian Schultz-Coulon *but also Material from many different sources*
Kirchhoff-Institut für Physik



Introduction & Motivation

The LHC and its Experiments





LHC: motivations

- Is the mass of elementary particles being generated by the Higgs mechanism via **EW symmetry breaking**? The ATLAS and CMS experiments discovered the Higgs boson, which is strong evidence that the Standard Model has the correct mechanism of giving mass to elementary particles. **Check couplings!**
- Is **supersymmetry**, extension of the SM, realised in nature, implying that all known particles have supersymmetric partners?
- Are there **extra dimensions**, as predicted by various models based on string theory, and can we detect them?
- What is the nature of the **dark matter** that appears to account for 27% of the mass-energy of the universe?
- What about **dark energy**?

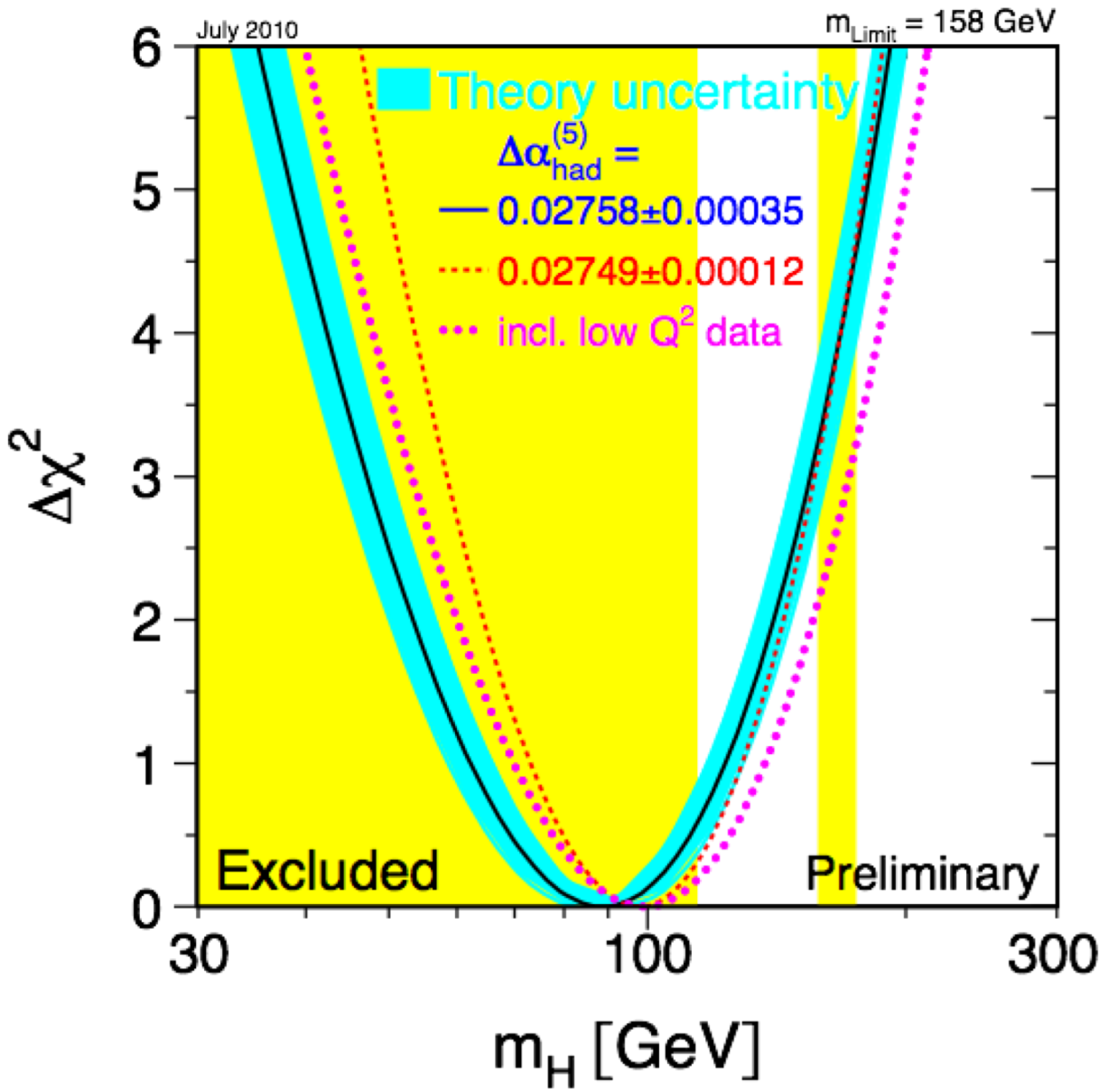
Other open questions that may be explored using high-energy particle collisions:

- Why is the **gravity** force so many orders of magnitude weaker than the other three fundamental forces?
- Why are there apparent violations of the symmetry between **matter and antimatter**?
- What are the nature and properties of **quark-gluon plasma**, thought to have existed in the early universe and in certain compact and strange and strange astronomical objects today? This will be investigated by *heavy ion collisions*, mainly in ALICE, but also in CMS, ATLAS and LHCb. First observed in 2010, findings published in 2012 confirmed the phenomenon of jet quenching in heavy-ion collisions.



Our Knowledge about the Higgs before its discovery

Toni Baroncelli Experimental High Energy Physics at Colliders 2019-20



EW-Fits:
 $M_H = 89 \text{ GeV}$
 $M_H < 158 \text{ GeV @ 95\% CL}$

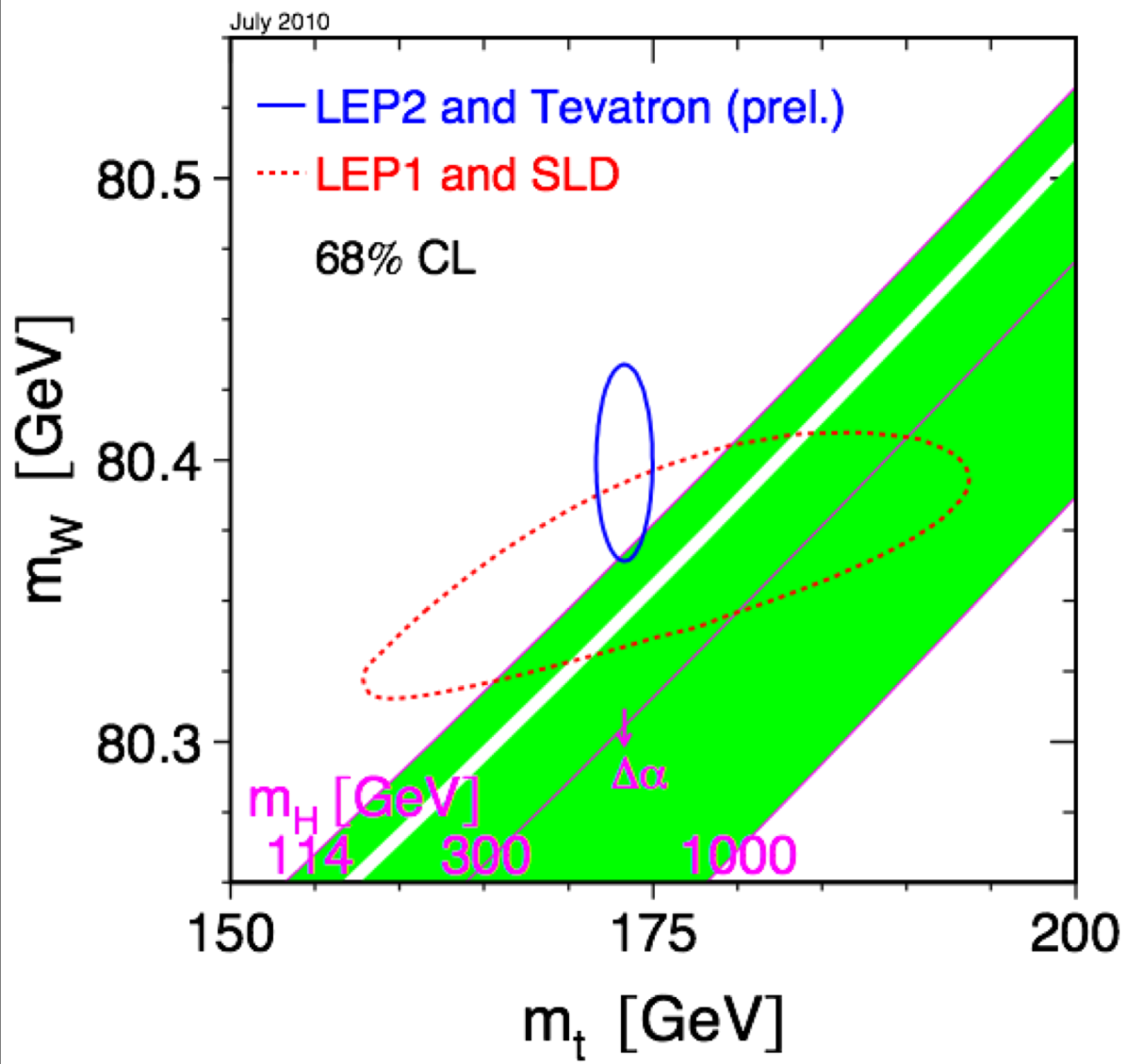
From direct search at LEP:
 $M_H > 114 \text{ GeV @ 95\% CL}$

From direct search at Tevatron:
 $158 < M_H < 175 \text{ GeV @ 95\% CL}$



Our Knowledge about the Higgs before its discovery

Toni Baroncelli Experimental High Energy Physics at Colliders 2019-20



EW-Fits:

$$M_H = 89^{+35}_{-26} \text{ GeV}$$

$$M_H < 158 \text{ GeV @ 95\% CL}$$

From direct search at LEP:

$$M_H > 114 \text{ GeV @ 95\% CL}$$

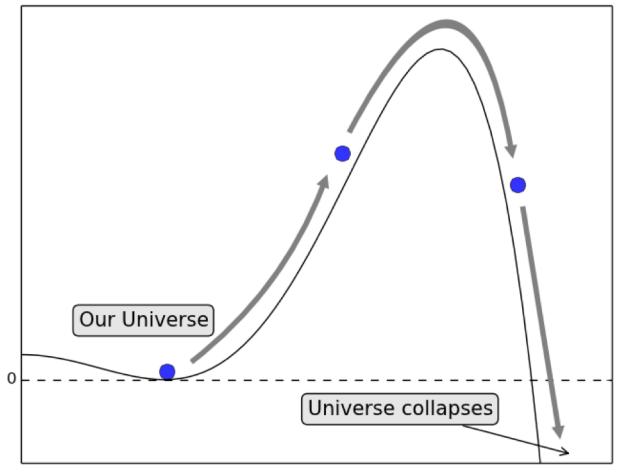
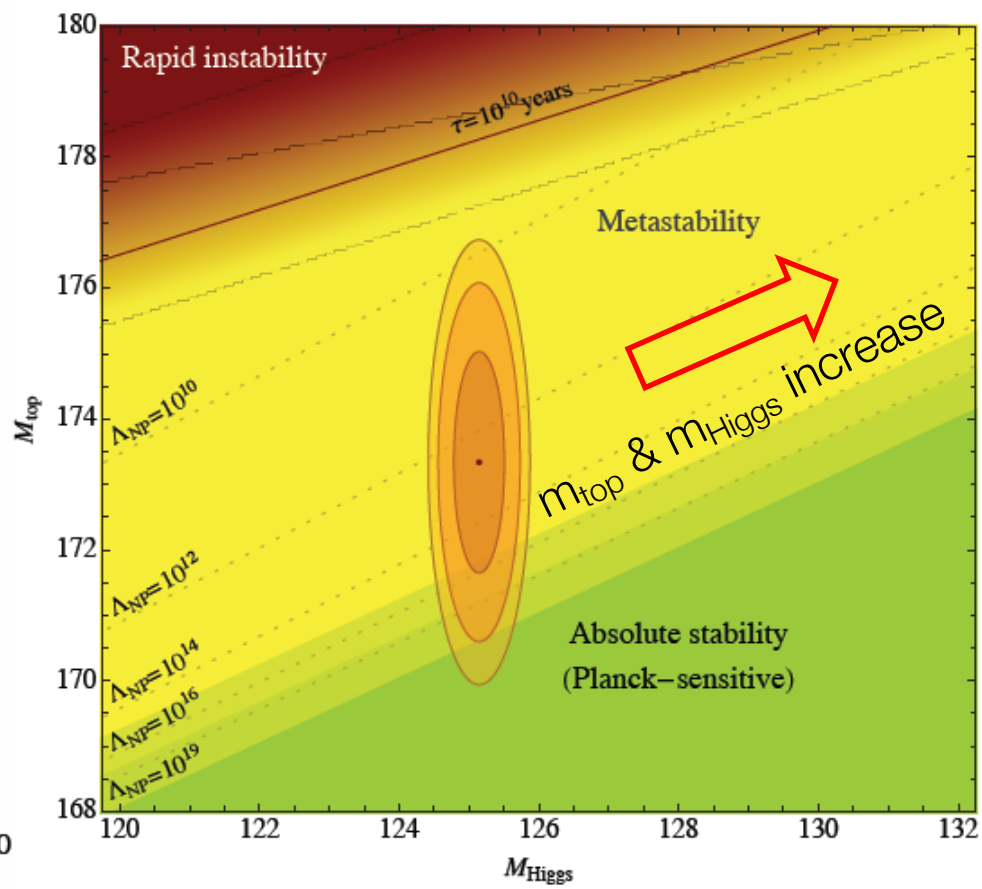
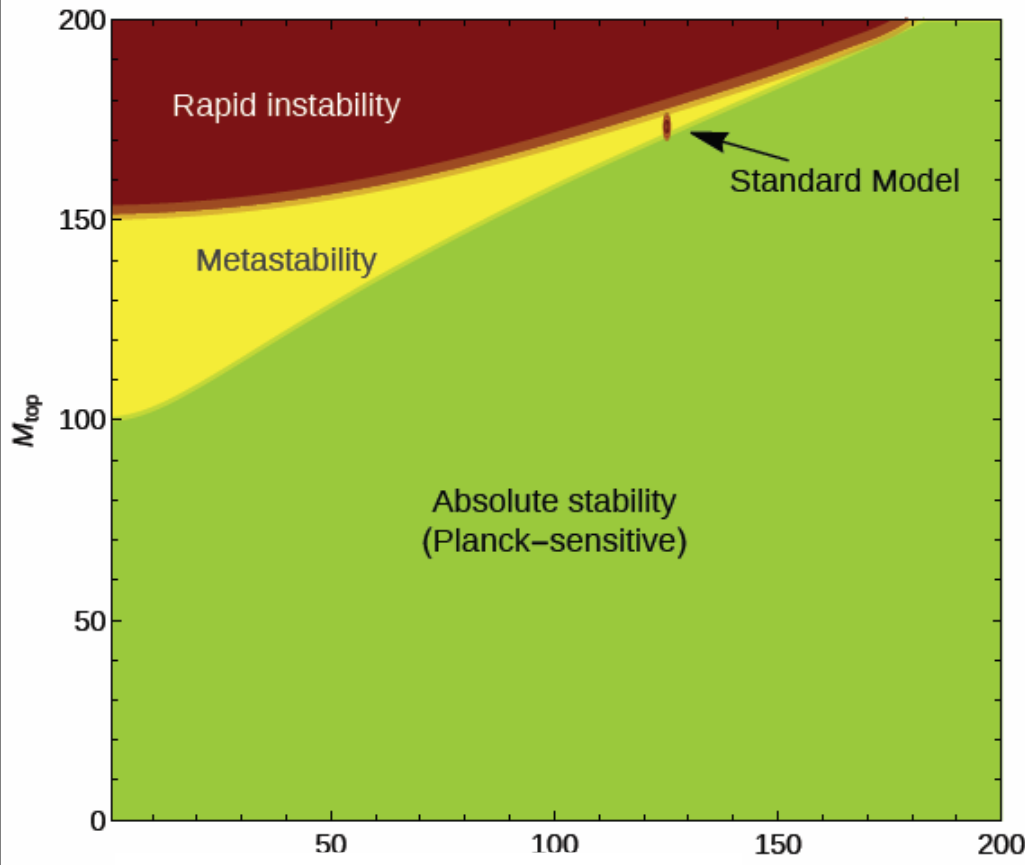
From direct search at Tevatron:

$$158 < M_H < 175 \text{ GeV @ 95\% CL}$$



After the Higgs discovery: m_{top} vs m_{Higgs} and stability of the Universe

Toni Baroncelli Experimental High Energy Physics at Colliders 2019-20



$$m_h^{\text{pole}} = (125.14 \pm 0.23) \text{ GeV}$$

$$m_t^{\text{pole}} = (173.34 \pm 1.12) \text{ GeV}$$

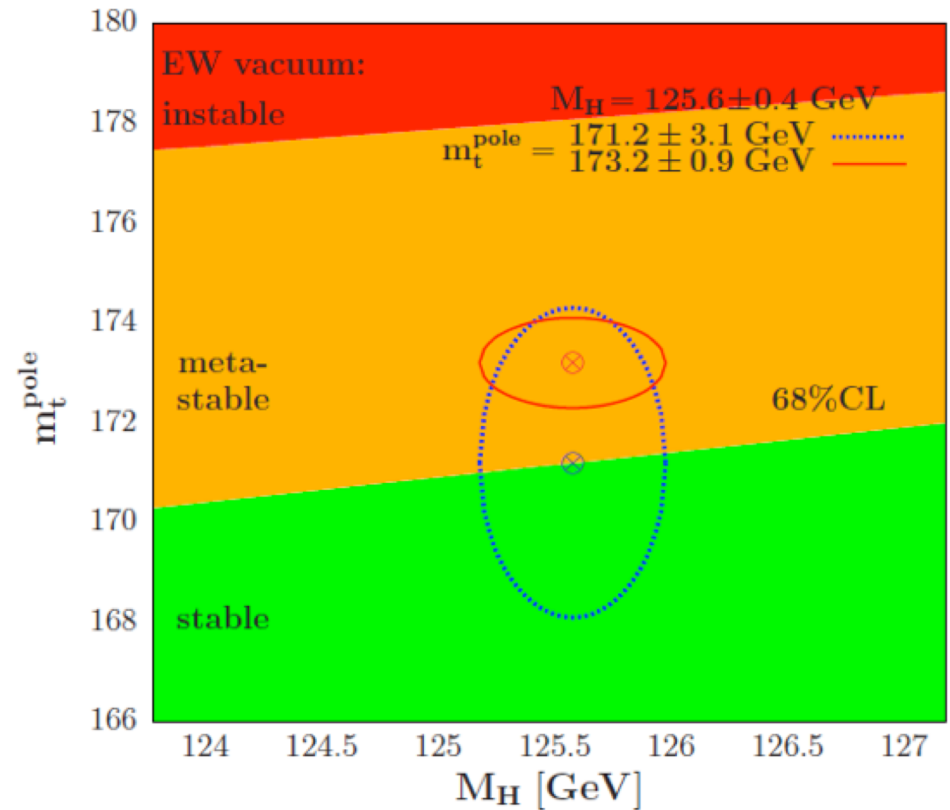
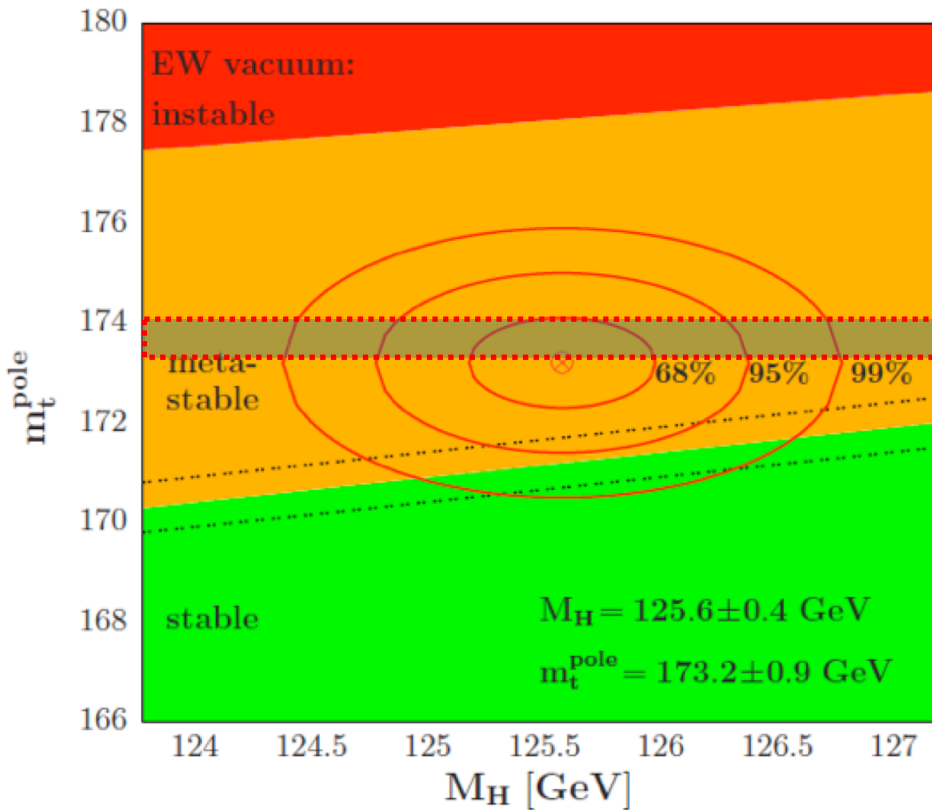


After the Higgs discovery:

m_{top} vs m_{Higgs} and stability of the Universe

$$m_{\text{top}} = 173.0 \pm 0.4 \text{ GeV}$$

$$m_{\text{top}} = 173.1 \pm 0.9 \text{ GeV}$$

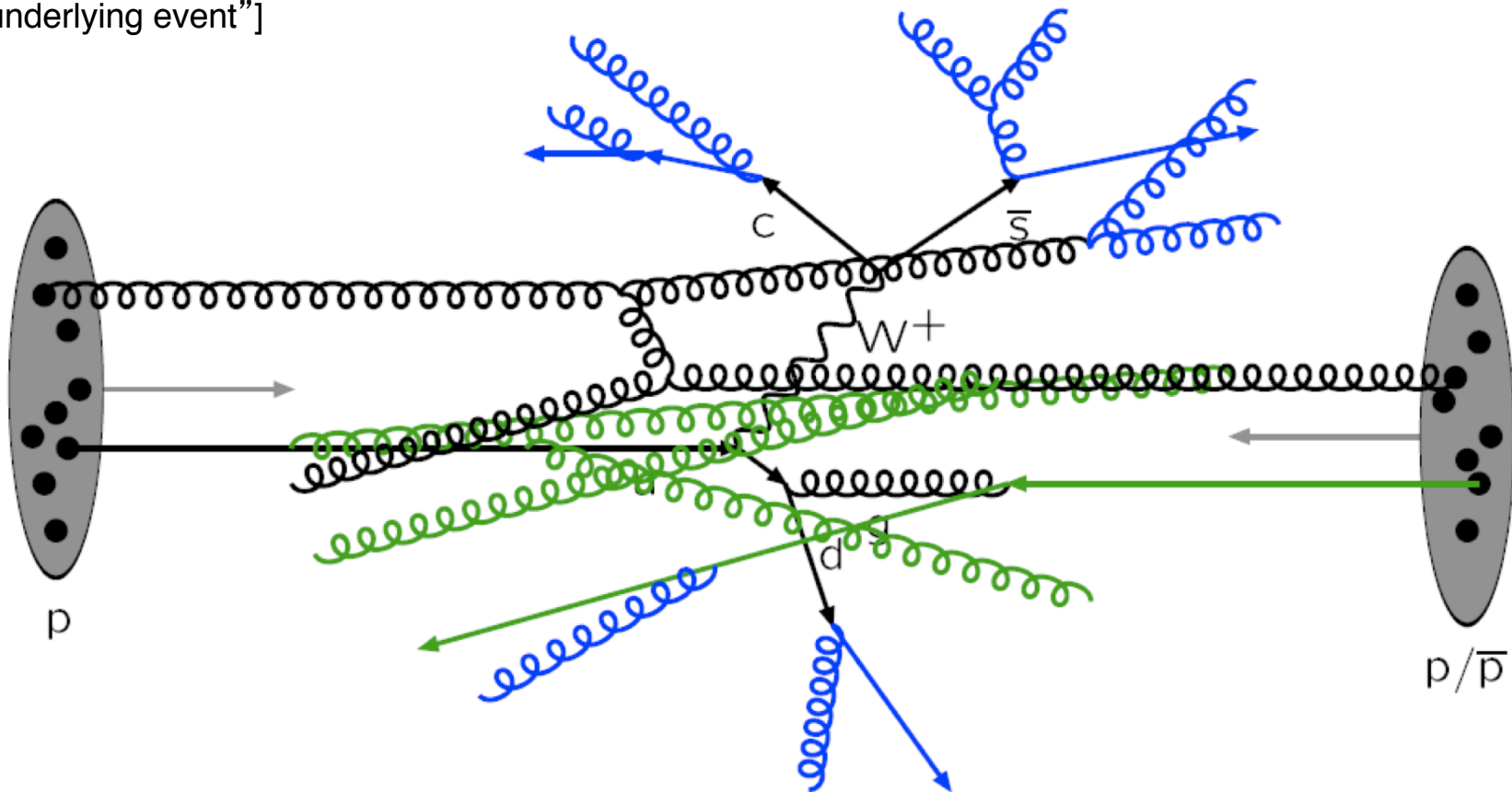


The ellipses in the $[M_H, m_{t^{\text{pole}}}]$ plane with the inputs $M_H = 125 \pm 0.4 \text{ GeV}$ and $\alpha_s = 0.1187$ are confronted with the areas in which the SM vacuum is absolutely stable, metastable and unstable up to the Planck scale. Left plot $m_{t^{\text{pole}}}$ is identified with the Tevatron measured top mass $m_t = 173.2 \pm 0.9 \text{ GeV}$, Right: $m_{t^{\text{pole}}}$ is taken as the one measured at the Tevatron $m_t = 171.2 \pm 3.1 \text{ GeV}$ extracted for the $t\bar{t}$ production cross section

Proton-Proton Scattering @ LHC

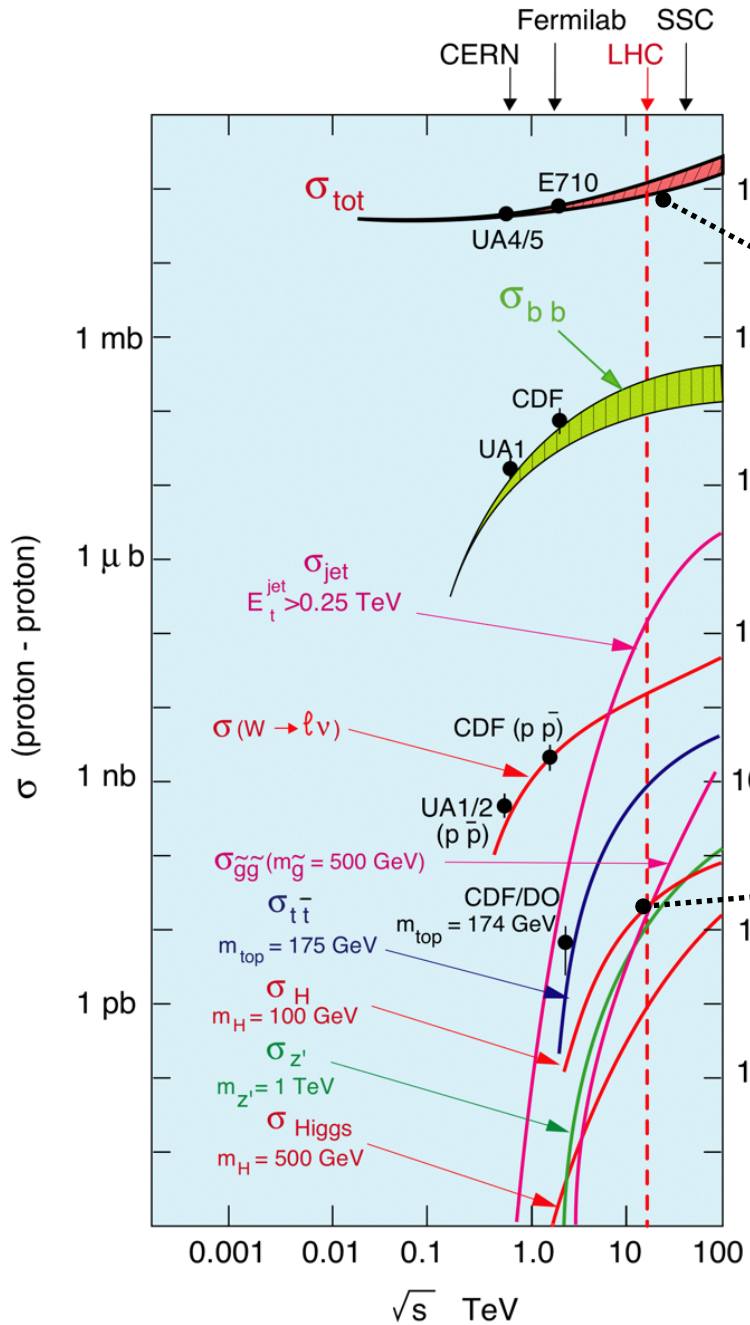
Very complex topologies!
(very different from e^+e^- collisions)

- Hard interaction: qq , gg , qg fusion
- **Initial** and **final** state radiation (ISR,FSR)
- Secondary interaction
[“underlying event”]





Needle in a Haystack



Events / sec for $\mathcal{L} = 10^{34} \text{ cm}^{-2} \text{ sec}^{-1}$

10^9 Events/sec
[1 Mbyte/Event]

$\sim 10^{10}$ reduction needed

Efficient rate reduction needed
[Storage rate: 100 Hz]

10 Events/min
[$m_H \approx 100 \text{ GeV}$]

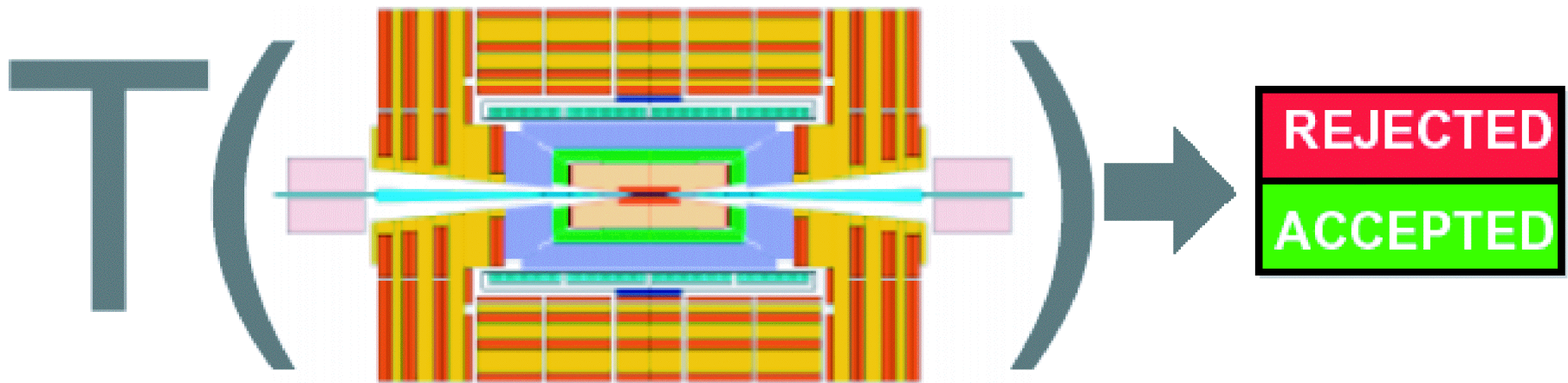
with 0.2% $H \rightarrow \gamma\gamma$
1.5% $H \rightarrow ZZ$

Trigger !



Challenge 1: Fast Trigger System

Fast selection of interesting Events
Number of necessary decisions: 40 million/sec



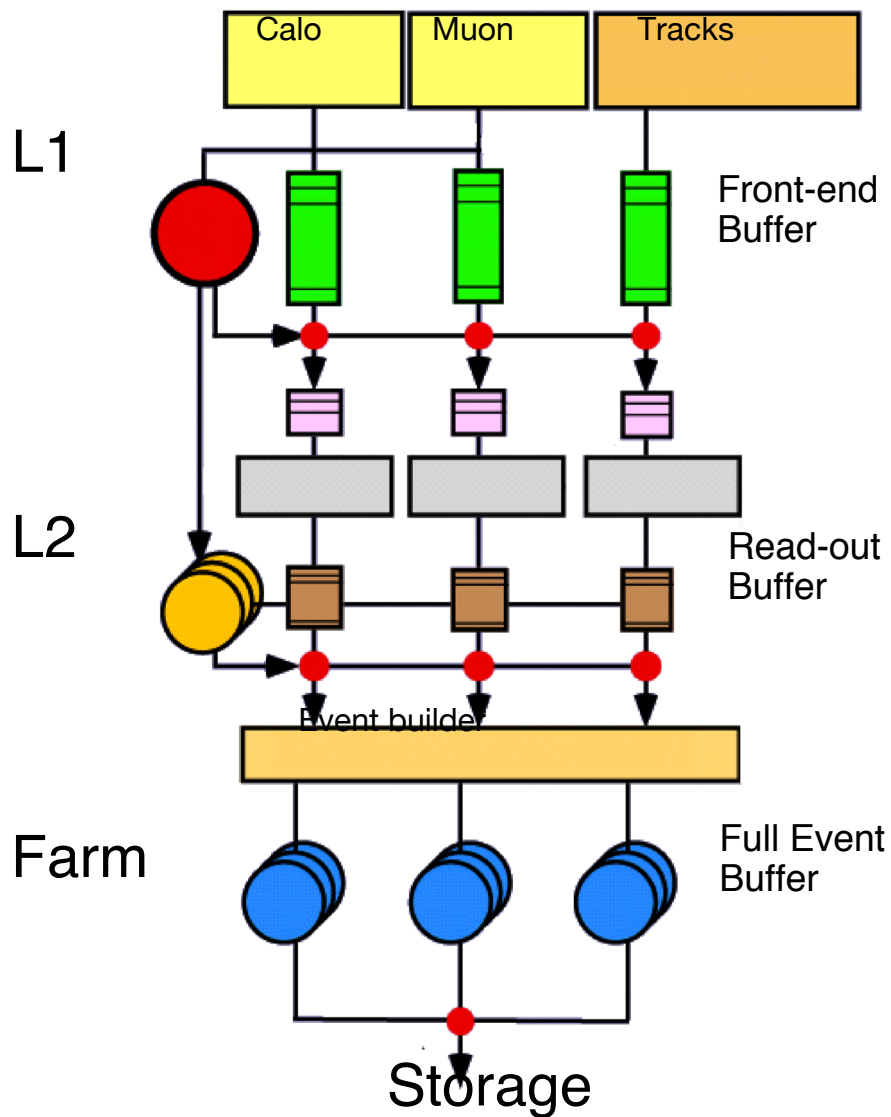
Function $T(\dots)$ is highly complex
Detector data not directly available

→ Stepwise decision

→ Trigger Levels



Challenge 1: Fast Trigger System



**Out-dated schema!
Now two levels only**

LEVEL-1 TRIGGER

- Hardware-Trigger [FPGAs & ASICs]
- Information from calorimeters & muon systems; low granularity
- 2 μ s latency [2.5 μ s pipelines]

40 MHz

LEVEL-2 TRIGGER

- Regions-of-Interest
- In principle full information of all subdetectors; high granularity
- Decision time: O(10 ms)

~75 kHz

EVENT FILTER

- Complete detector information
- Full event reconstruction
- Decision time: O(1 s)

~2 kHz

~ 200 Hz



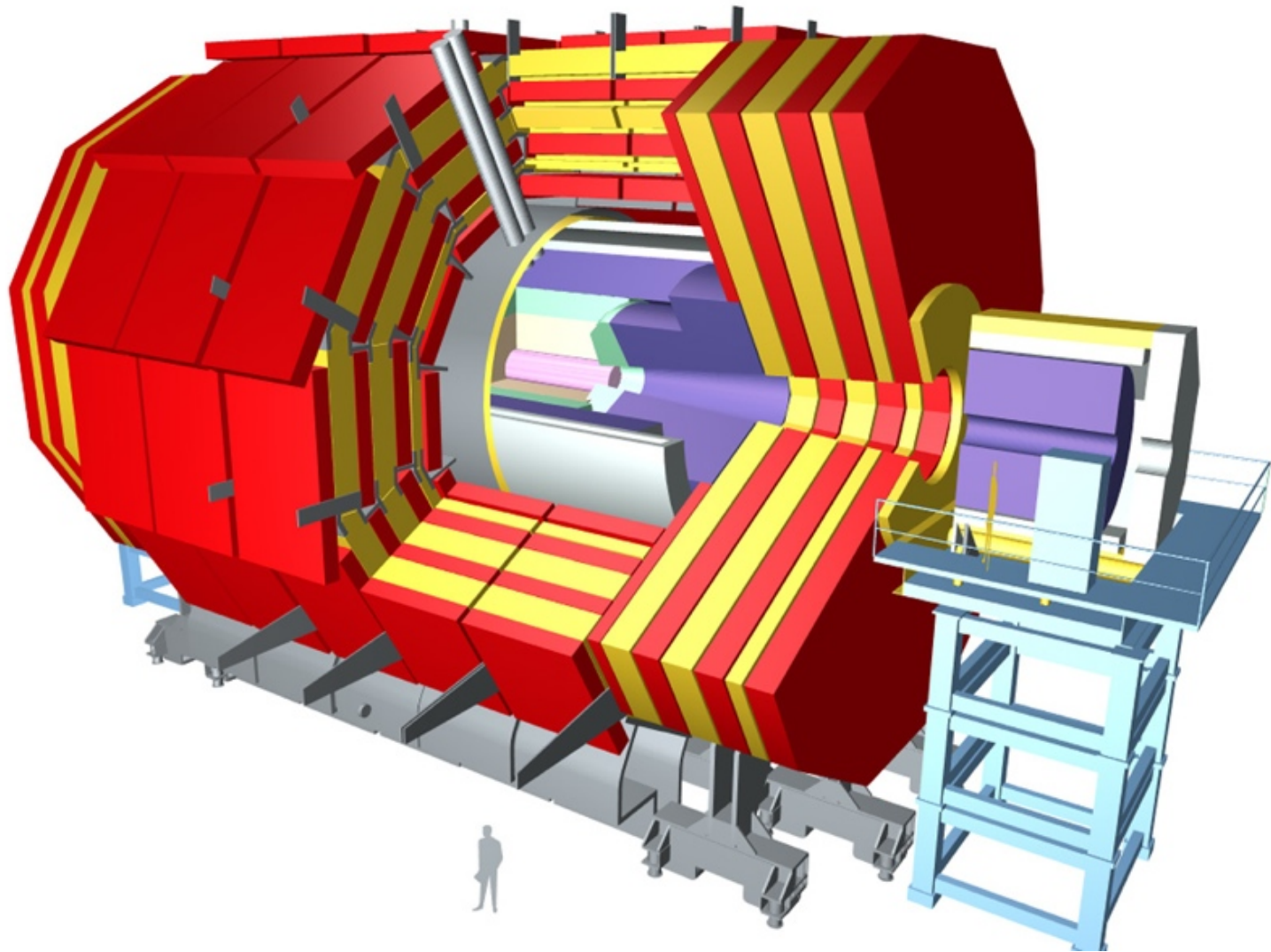
Experiments

The LHC and its Experiments





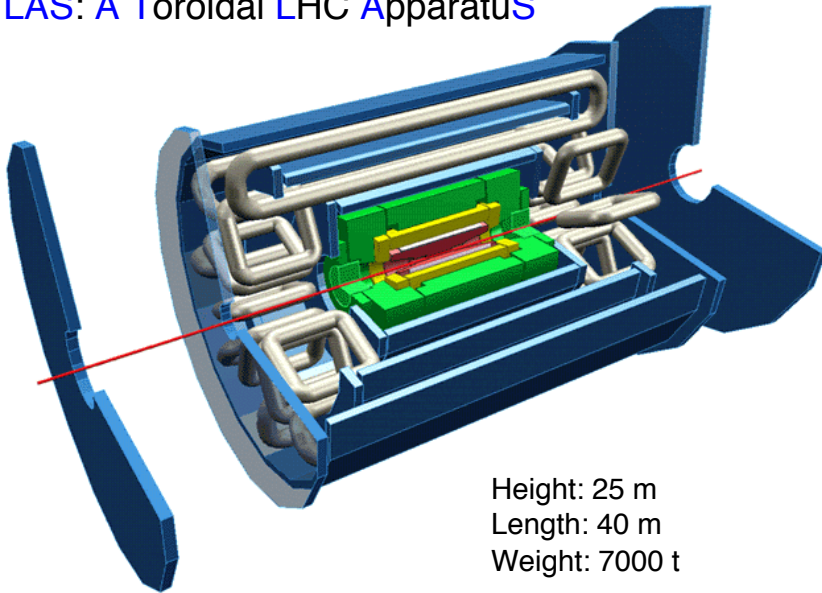
LHC Detectors, mostly ATLAS & CMS





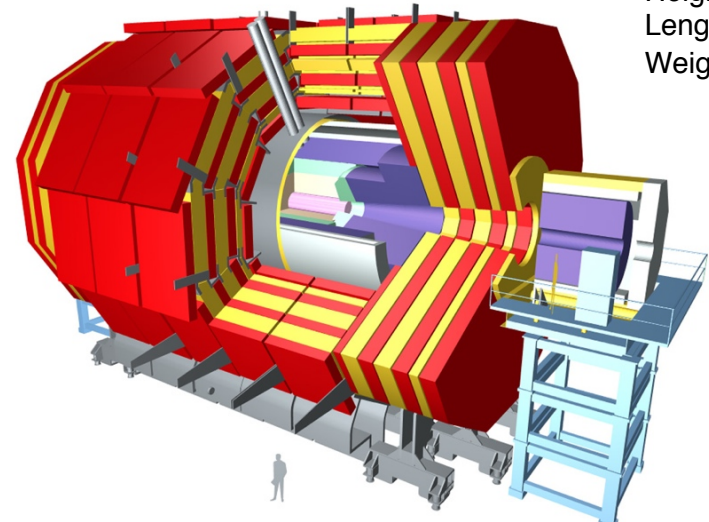
Basic Design Concepts

ATLAS: A Toroidal LHC Apparatus

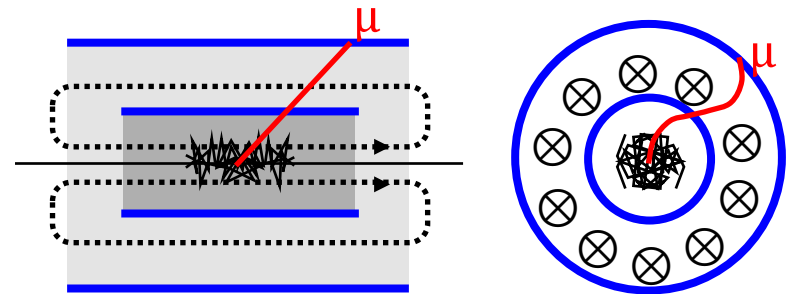
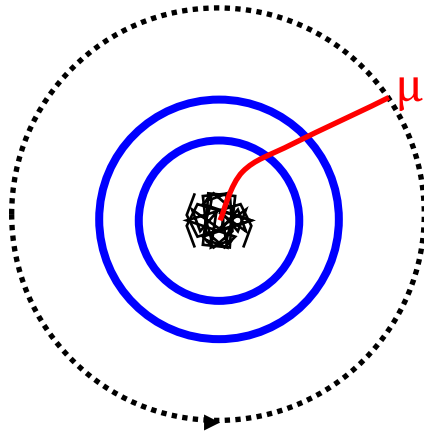
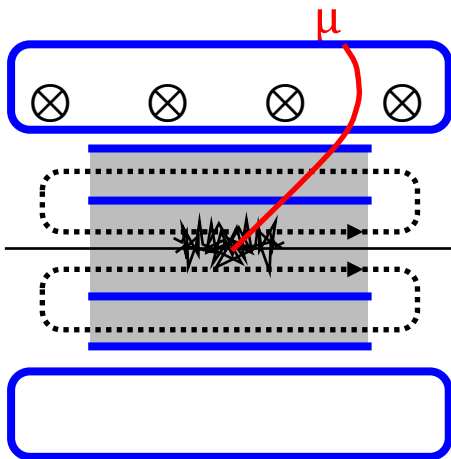


Height: 25 m
Length: 40 m
Weight: 7000 t

CMS: Compact Muon Solenoid



Height: 15 m
Length: 22 m
Weight: 12500 t





The ATLAS (and ~ CMS) Detector

The basic design criteria of the detector included the following points:

1. Excellent electromagnetic calorimetry for **electron and photon identification** and measurements, complemented by full-coverage hadronic calorimetry for accurate jet and ETmiss measurements;
2. High-precision **muon momentum measurements**, with the capability of accurate measurements at the highest collision rates using the external muon spectrometer alone;
3. Efficient **charged particle tracking at high luminosity** for high transverse momentum (p_T) lepton-momentum measurements, electron and photon identification, τ -lepton and heavy-flavour identification, and full event reconstruction capability at lower luminosity;
4. **Large acceptance in pseudorapidity (η)** with almost full azimuthal angle (ϕ) coverage everywhere. The azimuthal angle is measured around the beam axis z , whereas pseudorapidity relates to the polar angle (θ) where θ is the angle from the z direction, $\eta = -\ln(\tan\theta/2)$.
5. **Triggering and measurements of particles at low- p_T thresholds**, providing high efficiencies for most physics processes of interest at the LHC.

The main active detector components of the ATLAS detector, from the beam line towards the outside. The total readout channels for each component is given, as well as its pseudorapidity coverage.

Detector component	Position	Channels (total)	η - coverage [Collapse]
Tracking			
Pixel B-layer (IBL, added for Run 2)	1 cylindrical barrel layer	6 million	± 2.5
	Average radius 33 mm		
Pixel	3 cylindrical barrel layers	80.4 million	± 2.5
	3 end-cap disks on each side		
	Radial envelope 45.5 - 242 mm		
SCT strips	4 cylindrical barrel layers	6.3 million	± 2.5
	9 end-cap disks on each side		
	Radial envelope 251 - 610 mm		
TRT	73 barrel straw planes	351,000	± 2.0
	80 end-cap straw planes		
	Radial envelope 554 - 1106 mm		
Calorimetry			
EM presampler	Barrel	7,808	± 1.52
	End-caps	1,536	$1.5 < \eta < 1.8$
EM calorimeter	3 depth samples barrel	101,760	± 1.48
	3 depth layers end-caps	62,208	$1.375 < \eta < 3.2$
Hadronic tile calorimeter	3 depth samples barrel	5,760	± 1.0
	3 depth samples extended barrel	4,092	$0.8 < \eta < 1.7$
LAr hadronic end-caps	4 depth layers	5,632	$1.5 < \eta < 3.2$
LAr forward hadronic calorimeter	3 depth layers	3,524	$3.1 < \eta < 4.9$
Muon spectrometer			
MDT precision tracking	3 multi-layer stations	354,000	± 2.7
CSC precision tracking	1 innermost station end-caps	31,000	$2.0 < \eta < 2.7$
RPC trigger chambers	2 multi-layer stations barrel	373,000	± 1.05
TGC trigger chambers	2 multi-layer stations end-cap	318,000	$1.05 < \eta < 2.4$



The ATLAS Detector

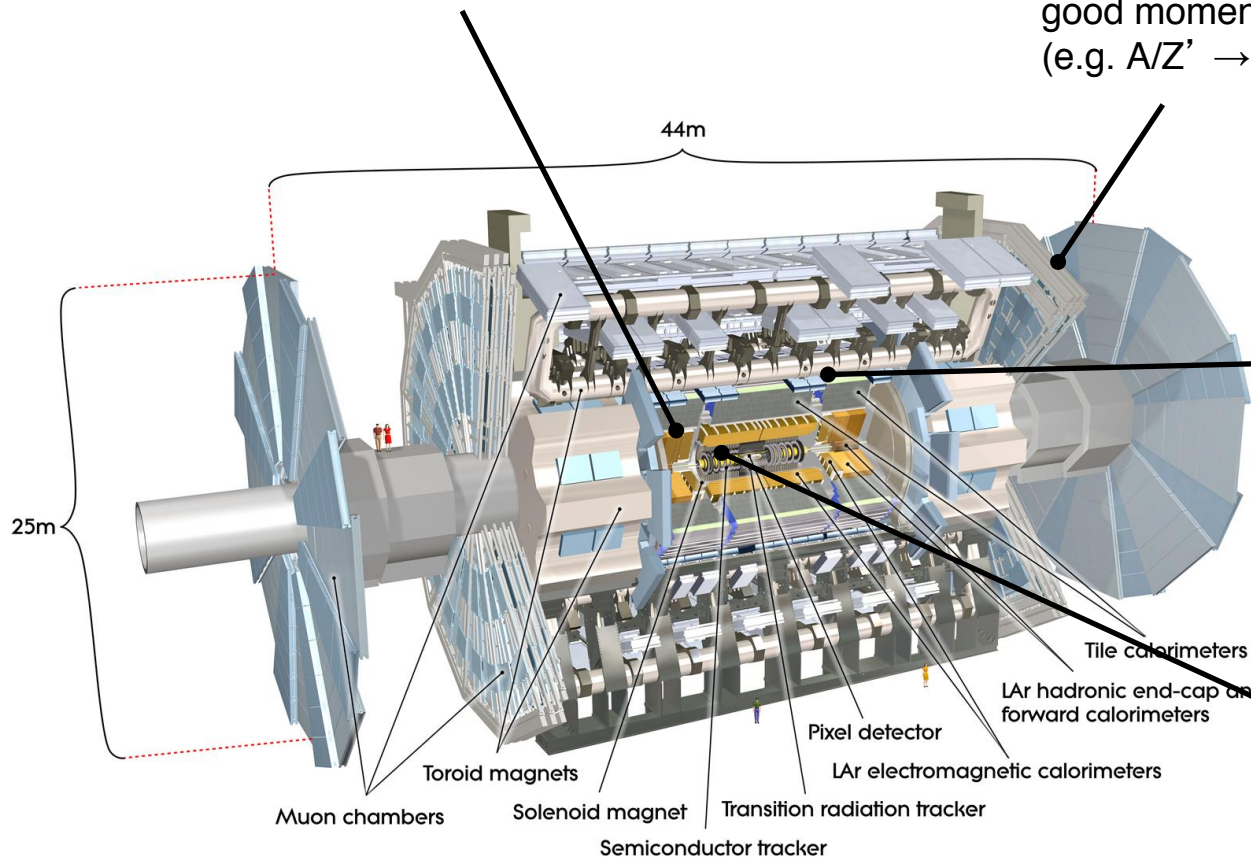
(http://www.scholarpedia.org/article/The_ATLAS_experiment)

Upgrades! → Detector evolves with time

EM Calorimeters: $\sigma/E \approx 10\%/ \sqrt{E} \oplus 0.7\%$
excellent e/ γ identification
good energy resolution (e.g. for $H \rightarrow \gamma\gamma$)

Precision Muon Spectrometer: $\sigma/p_t \approx 10\% @ 1 \text{ TeV}$
fast trigger response
good momentum resolution
(e.g. $A/Z' \rightarrow \mu\mu$, $H \rightarrow 4\mu$)

Hadron Calorimeter:
 $\sigma/E \approx 50\%/ \sqrt{E} \oplus 3\%$
good jet resolution
good missing E_T resolution
(e.g. $H \rightarrow \tau\tau$)



Inner Detector:
Si Pixel & strips; TRT
 $\sigma/p_t \approx 5 \cdot 10^{-4} p_t \oplus 0.001$
good impact parameter res., i.e.
 $\sigma(d_0) \approx 15 \mu\text{m} @ 20 \text{ GeV}$
(e.g. $H \rightarrow b\bar{b}$)

Magnets:

Solenoid (inner detector): 2 T

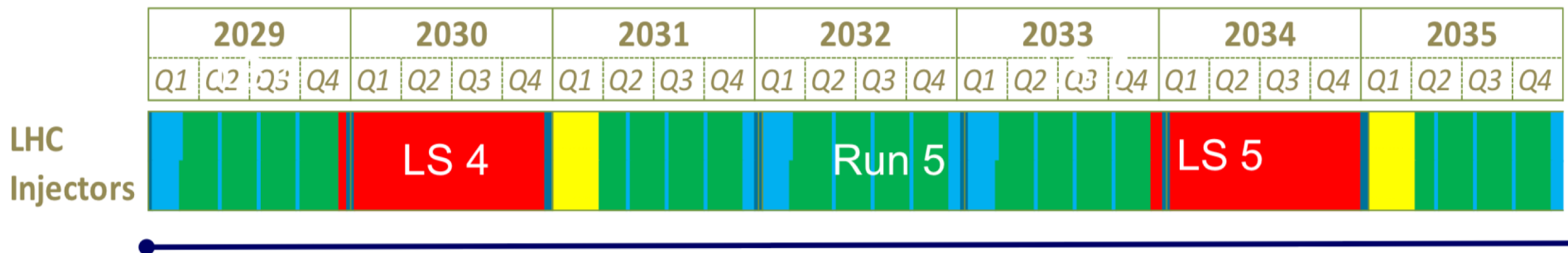
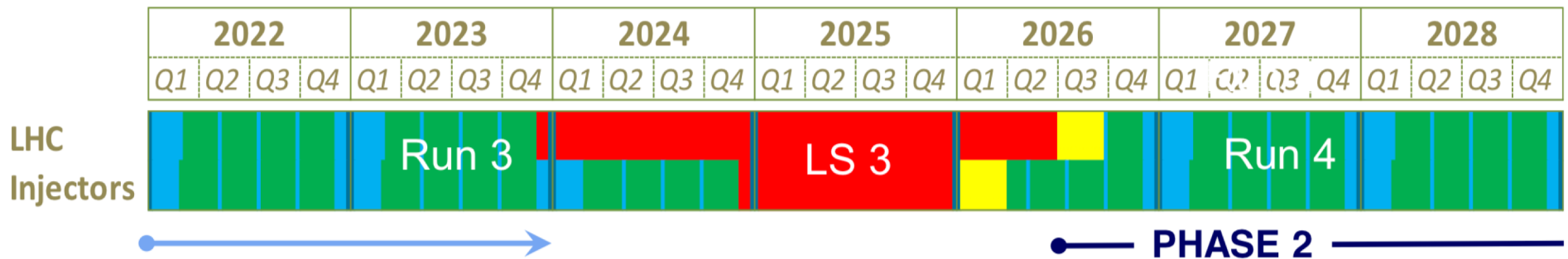
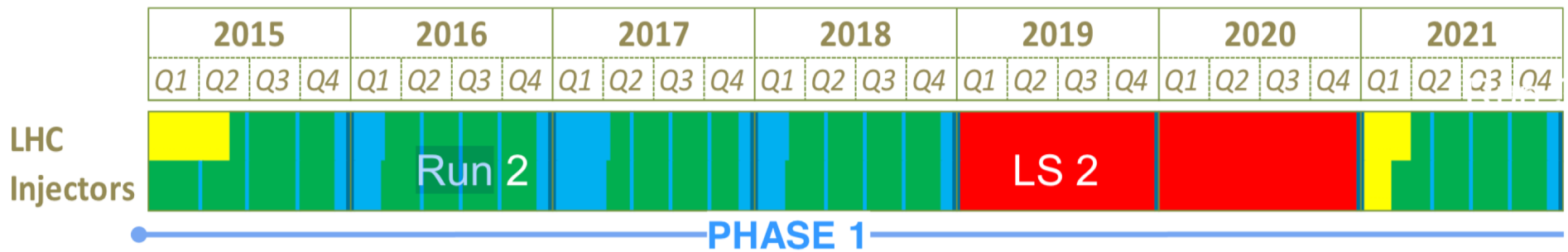
Toroid (muon spectrometer): 0.5 T



LHC Schedule as of Jan 2019

LHC roadmap: according to MTP 2016-2020 V1

LS2 starting in 2019 => 24 months + 3 months BC
 LS3 LHC: starting in 2024 => 30 months + 3 months BC
 Injectors: in 2025 => 13 months + 3 months BC





The ATLAS Detector

Indicative resolutions of the ATLAS detector components. The units for energy E and transverse momentum p_T are in GeV. The symbol \oplus means adding both parts in quadrature.

Detector component	Resolution
Tracking	$\sigma_{p_T}/p_T = 0.05\% p_T \oplus 1\%$
EM calorimetry	$\sigma_E/E = 10\%/\sqrt{E} \oplus 0.7\%$
Hadronic calorimetry (jets)	
barrel and end-caps	$\sigma_E/E = 50\%/\sqrt{E} \oplus 3\%$
forward	$\sigma_E/E = 100\%/\sqrt{E} \oplus 10\%$
Muon spectrometer	$\sigma_{p_T}/p_T = 10\%$ at $p_T = 1$ TeV



The CMS Detector

(https://en.wikipedia.org/wiki/Compact_Muon_Solenoid)

EM Calorimeters:

$$\sigma/E \approx 3\%/ \sqrt{E} \oplus 0.5\%$$

[cf. ATLAS: $\sigma/E \approx 10\%/ \sqrt{E} \oplus 0.7\%$]

Inner Detector:

$$\sigma/p_t \approx 5 \cdot 10^{-4} p_t \oplus 0.001$$

[cf. ATLAS $\sigma/p_t \approx 5 \cdot 10^{-4} p_t \oplus 0.001$]

Hadron Calorimeter:

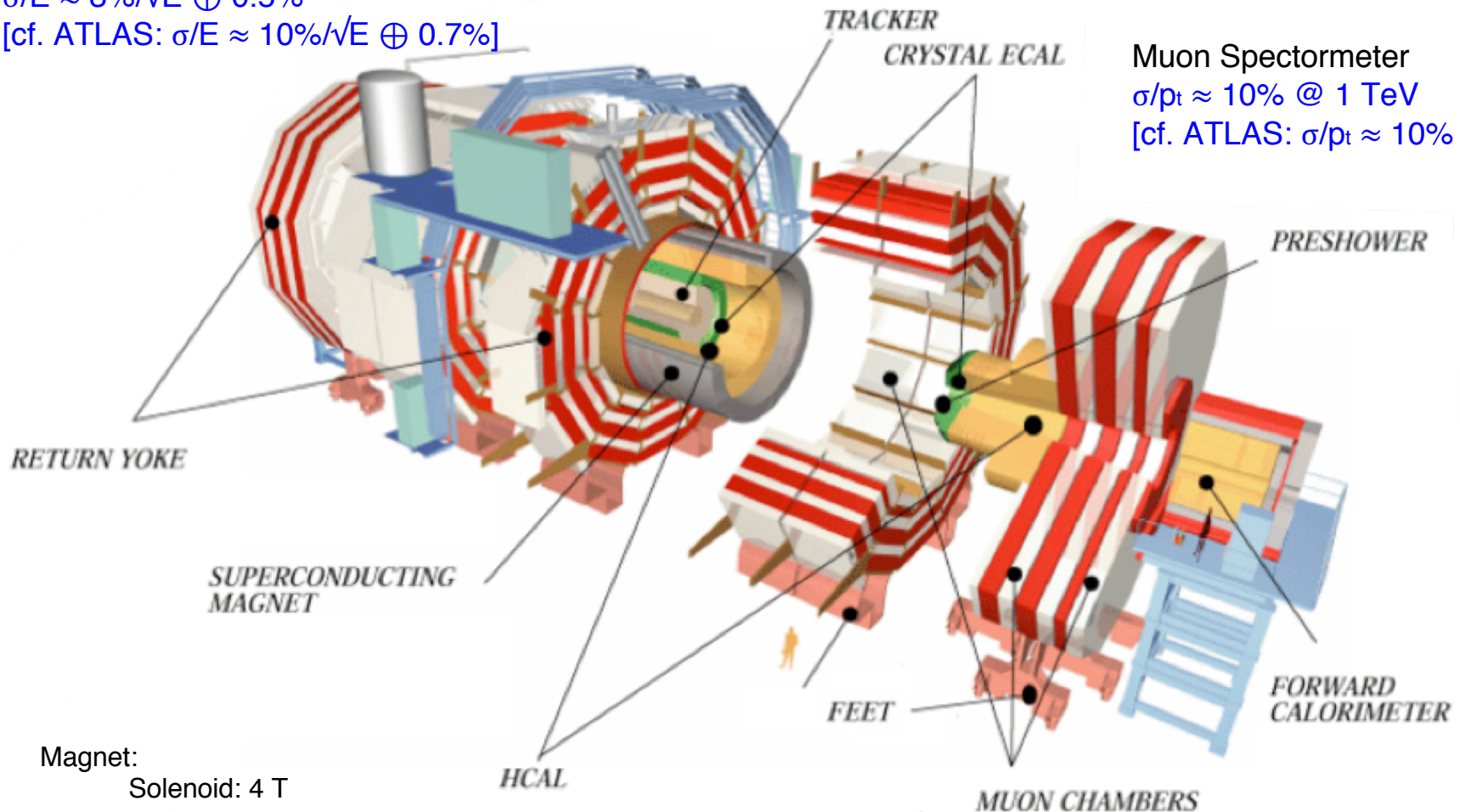
$$\sigma/E \approx 100\%/ \sqrt{E} \oplus 5\%$$

[cf. ATLAS: $\sigma/E \approx 50\%/ \sqrt{E} \oplus 3\%$]

Muon Spectrometer

$$\sigma/p_t \approx 10\% @ 1 \text{ TeV}$$

[cf. ATLAS: $\sigma/p_t \approx 10\% @ 1 \text{ TeV}$]

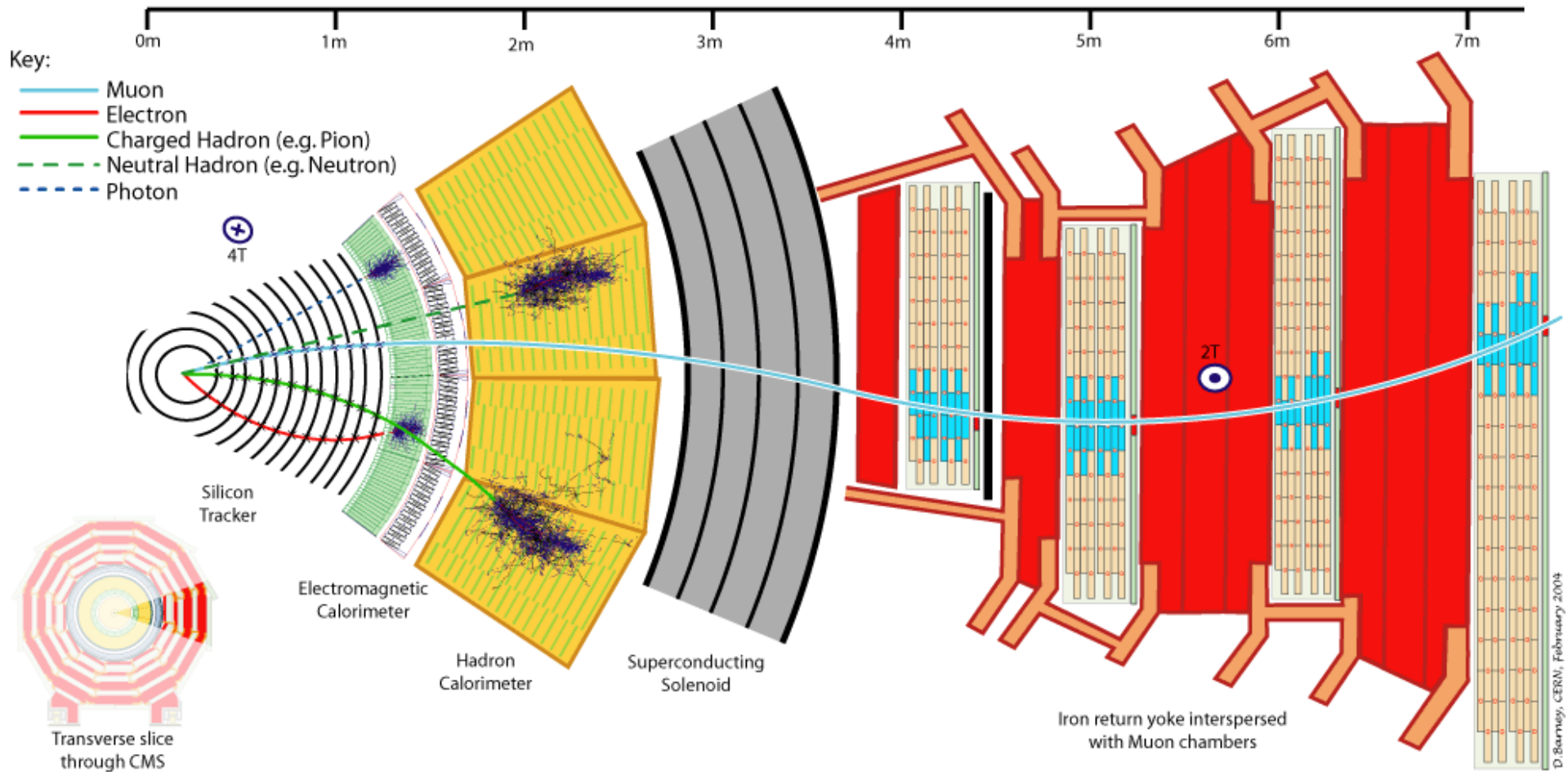


Magnet:

Solenoid: 4 T



The CMS Detector - 2





ATLAS vs CMS

ATLAS

CMS

Silicon pixels; Silicon strips;
Transition Radiation Tracker;
2 T magnetic field

Inner
Detector

Silicon pixels, Silicon strips,
4 T magnetic field

Lead plates as absorbers;
active medium: **liquid argon**;
outside solenoid

Electrom.
Calorimeter

Lead tungsten (PbWO_4) **crystals**;
both absorber and scintillator;
inside solenoid

Central region: Iron absorber
with plastic scintillating tiles;
Endcaps: copper and tungsten
absorber with liquid argon

Hadronic
Calorimeter

Stainless steel and copper with
plastic scintillating tiles

Large **air-core toroid** magnet;
muon chambers: drift tubes
and resistive plate
chambers; 0.5 T magnetic field

Muon
Chambers

Magnetic field from **return
yoke** (solenoid field: 4 T);
muon chambers: drift tubes
and resistive plate chambers



Accelerators

The LHC and its Experiments





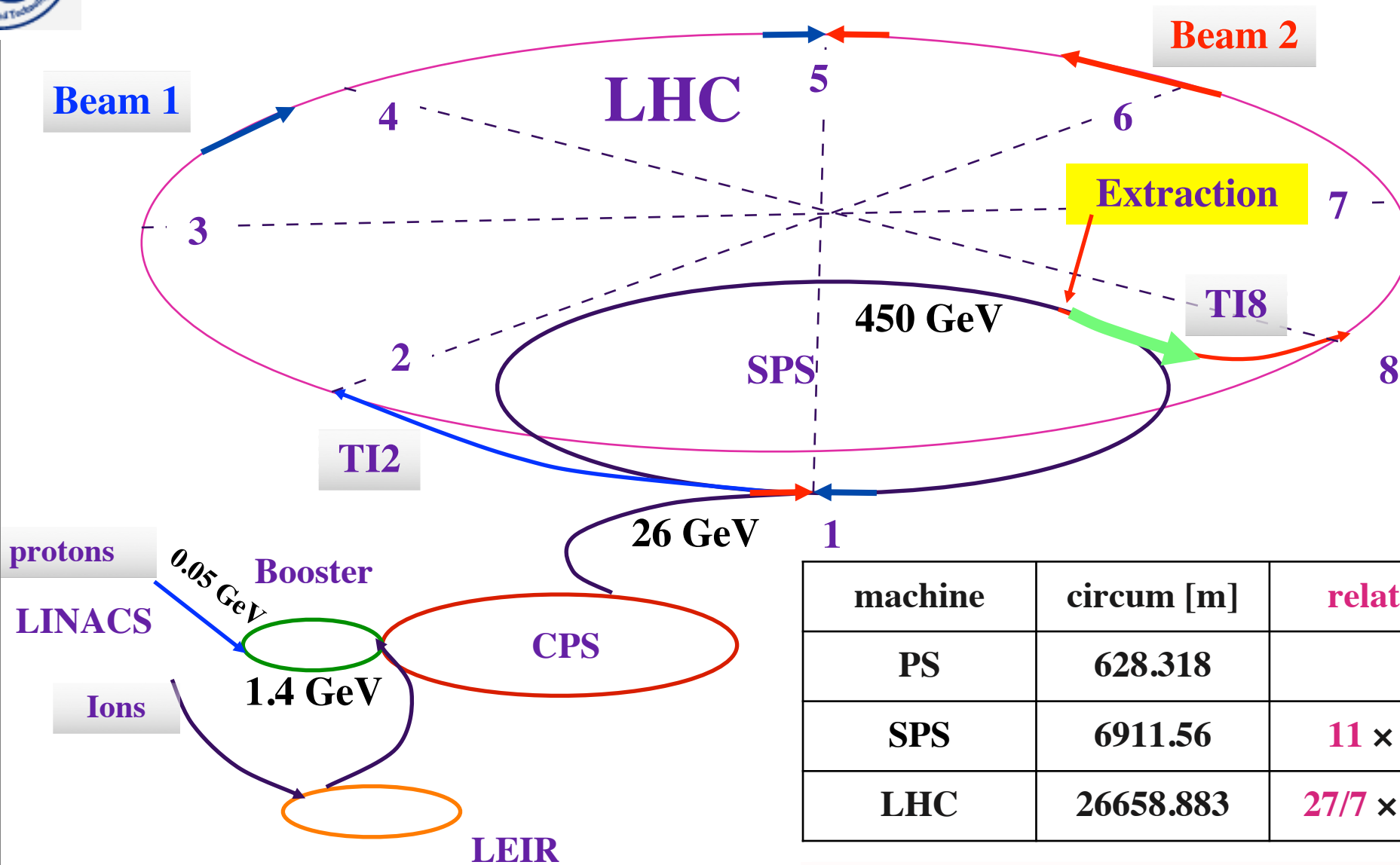
The Large Hadron Collider





The CERN accelerator complex : injectors and transfer

Toni Baroncelli Experimental High Energy Physics at Colliders 2019-20



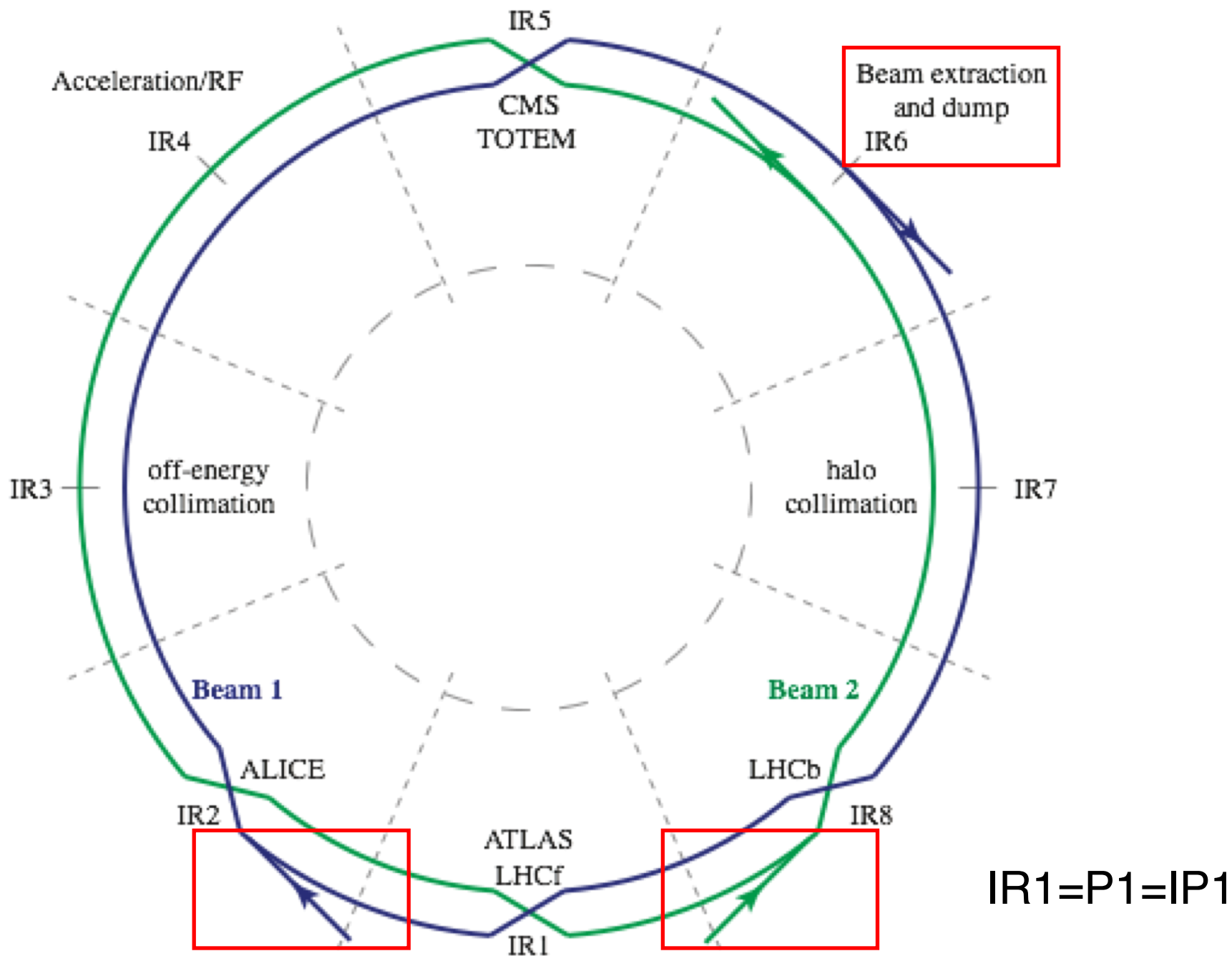
machine	circum [m]	relative
PS	628.318	
SPS	6911.56	11 × PS
LHC	26658.883	27/7 × SPS

simple rational fractions for **synchronization** based on a single frequency generator at injection

Beam size of protons decreases with energy : area $\sigma^2 \propto 1 / E$
 Beam size largest at injection, using the full aperture



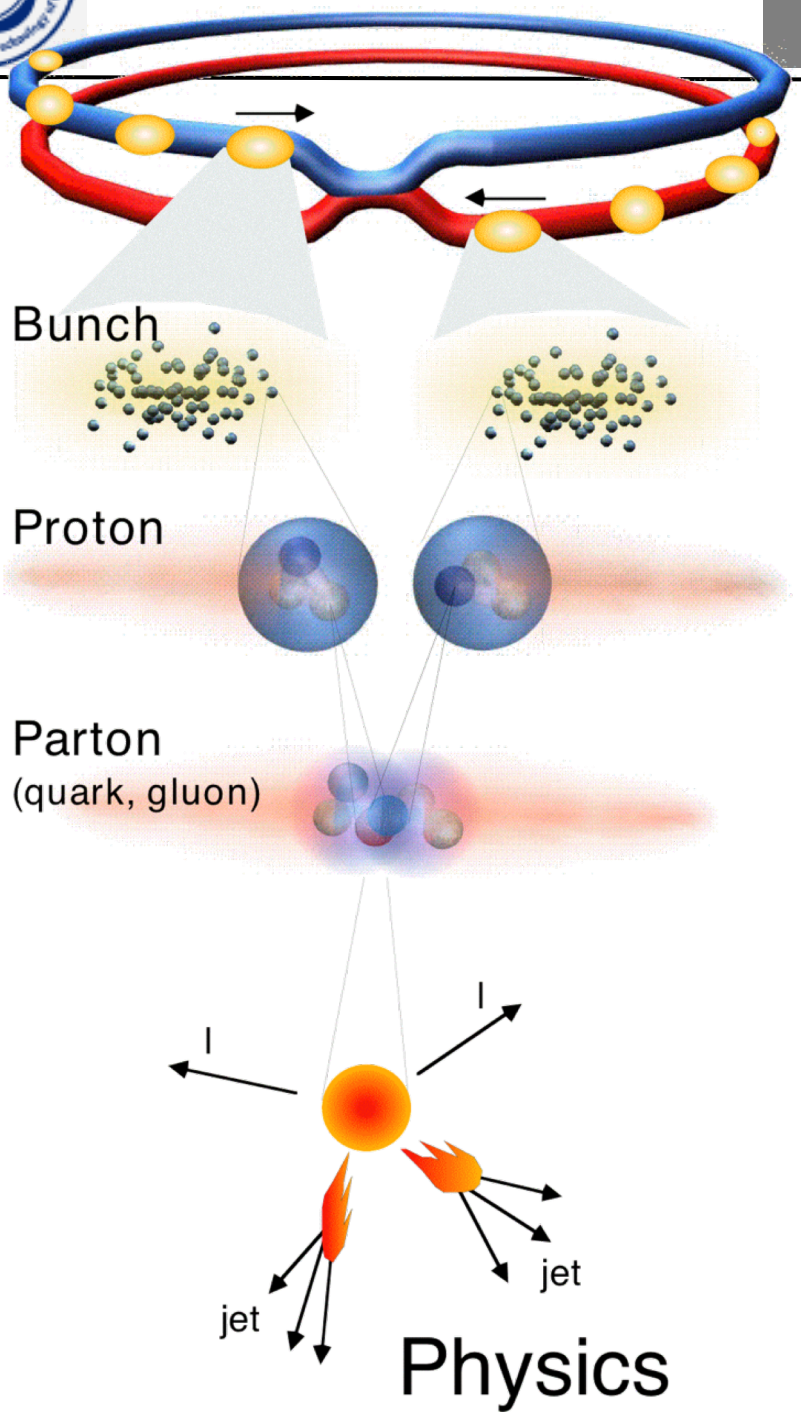
Layout of the LHC: Experiments





Proton-Proton

Some numbers (relevant for ATLAS & CMS)



total number of bunches (some empty) 3564x3564

2835 x 2835 proton bunches
distance: 7.5 m [25 ns]

(1.7*) 10¹¹ protons/bunch
bunch crossing rate: 40 MHz

10⁹ pp-collisions/sec
[i.e.: 23 pp-interactions/bunch crossing.]

Dominant Interactions:
gluon-gluon, quark-quark and
quark-gluon scattering



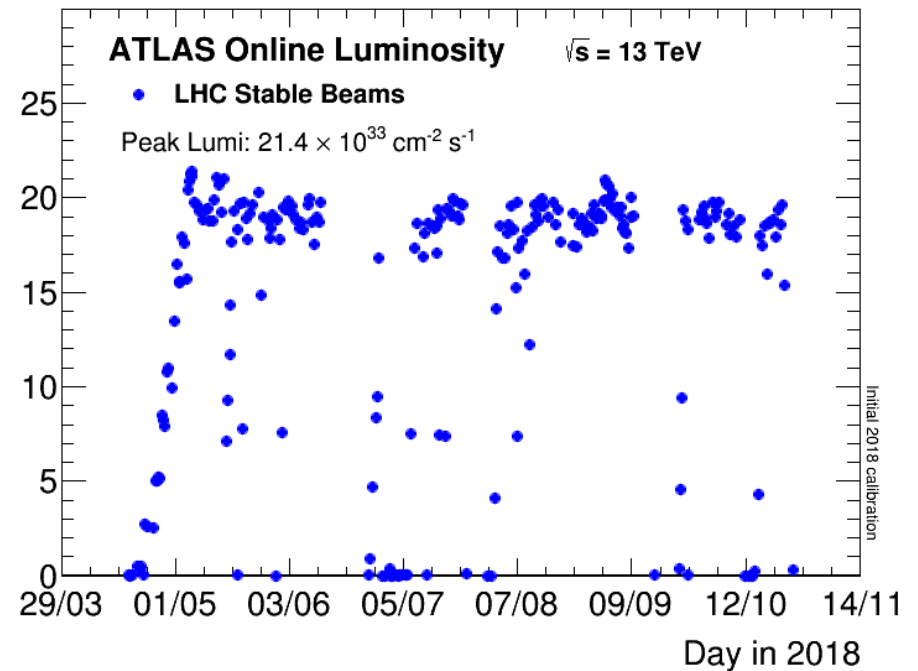
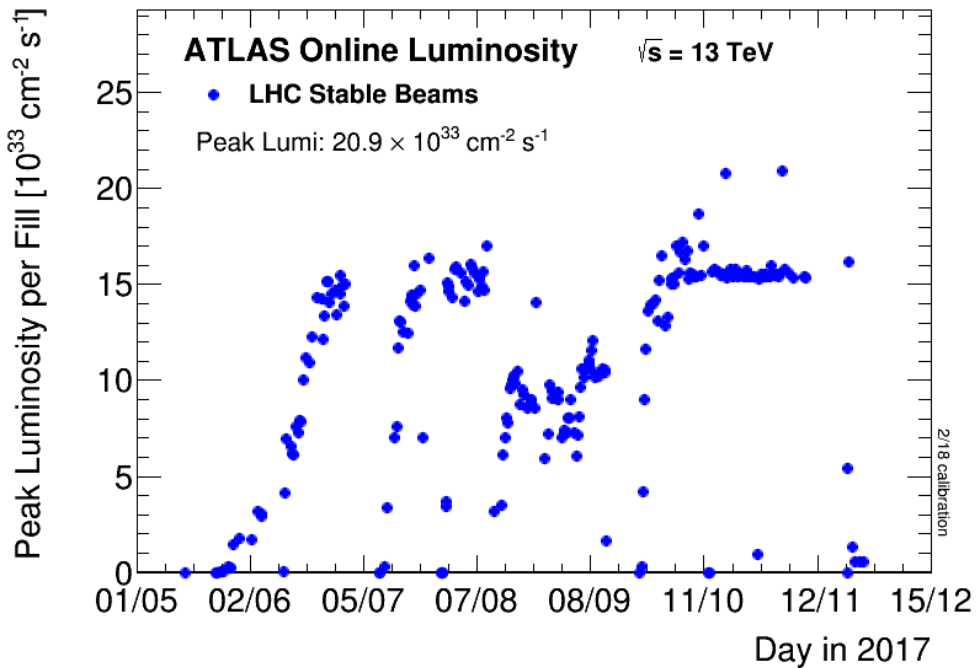
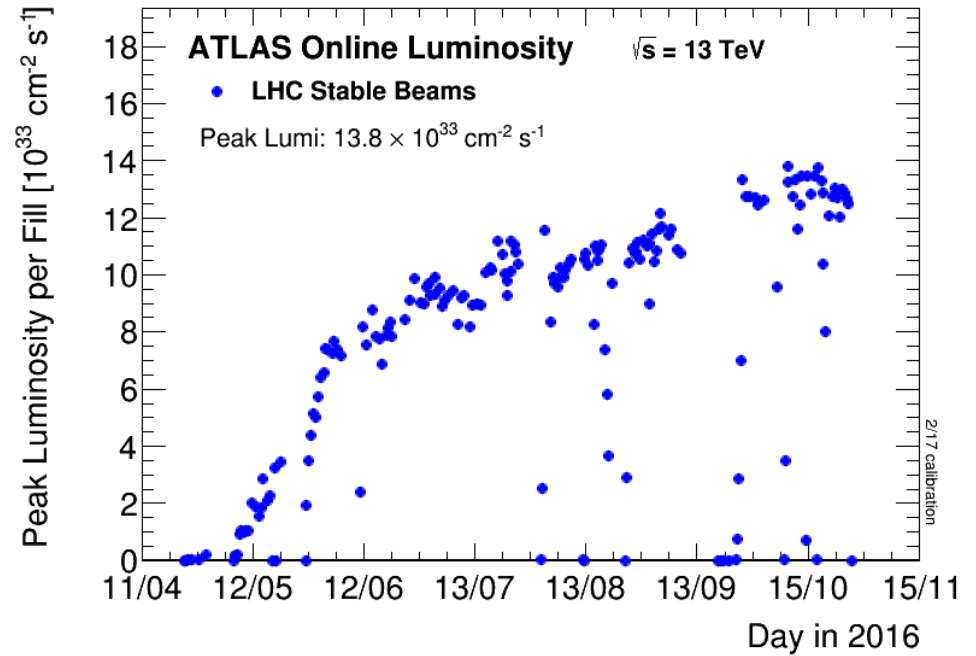
2016,2017,2018 LHC performance

$$N = L \cdot \sigma$$

Number of Events

Integrated Luminosity

X-Sec.





LHC status, a bit of story!

β^* indicates longitudinal size of the bunch

LHC :

2009 first collisions, mostly at injection energy 2×450 GeV

2010 2×3.5 TeV, $\beta^* = 3.5$ m, $L_{\text{peak}} = 0.2 \times 10^{33} \text{ cm}^{-2}\text{s}^{-1}$ $\int L dt = 0.044 \text{ fb}^{-1}$ 368 bunches

2011 2×3.5 TeV, $\beta^* = 1.0$ m, $L_{\text{peak}} = 3.5 \times 10^{33} \text{ cm}^{-2}\text{s}^{-1}$ $\int L dt = 6.1 \text{ fb}^{-1}$ 1380 bunches

2012 2×4.0 TeV, $\beta^* = 0.6$ m, $L_{\text{peak}} = 7.7 \times 10^{33} \text{ cm}^{-2}\text{s}^{-1}$ $\int L dt = 23.3 \text{ fb}^{-1}$ 1380 bunches

2013 **2014 shutdown**, magnet interconnections

2015 2×6.5 TeV, $\beta^* = 0.6$ m, $L_{\text{peak}} = 0.5 \times 10^{34} \text{ cm}^{-2}\text{s}^{-1}$ $\int L dt = 4.2 \text{ fb}^{-1}$ 2232 bunches

2016 2×6.5 TeV, $\beta^* = 0.4$ m, $L_{\text{peak}} = 1.4 \times 10^{34} \text{ cm}^{-2}\text{s}^{-1}$ $\int L dt = 35.6 \text{ fb}^{-1}$ 2208 bunches

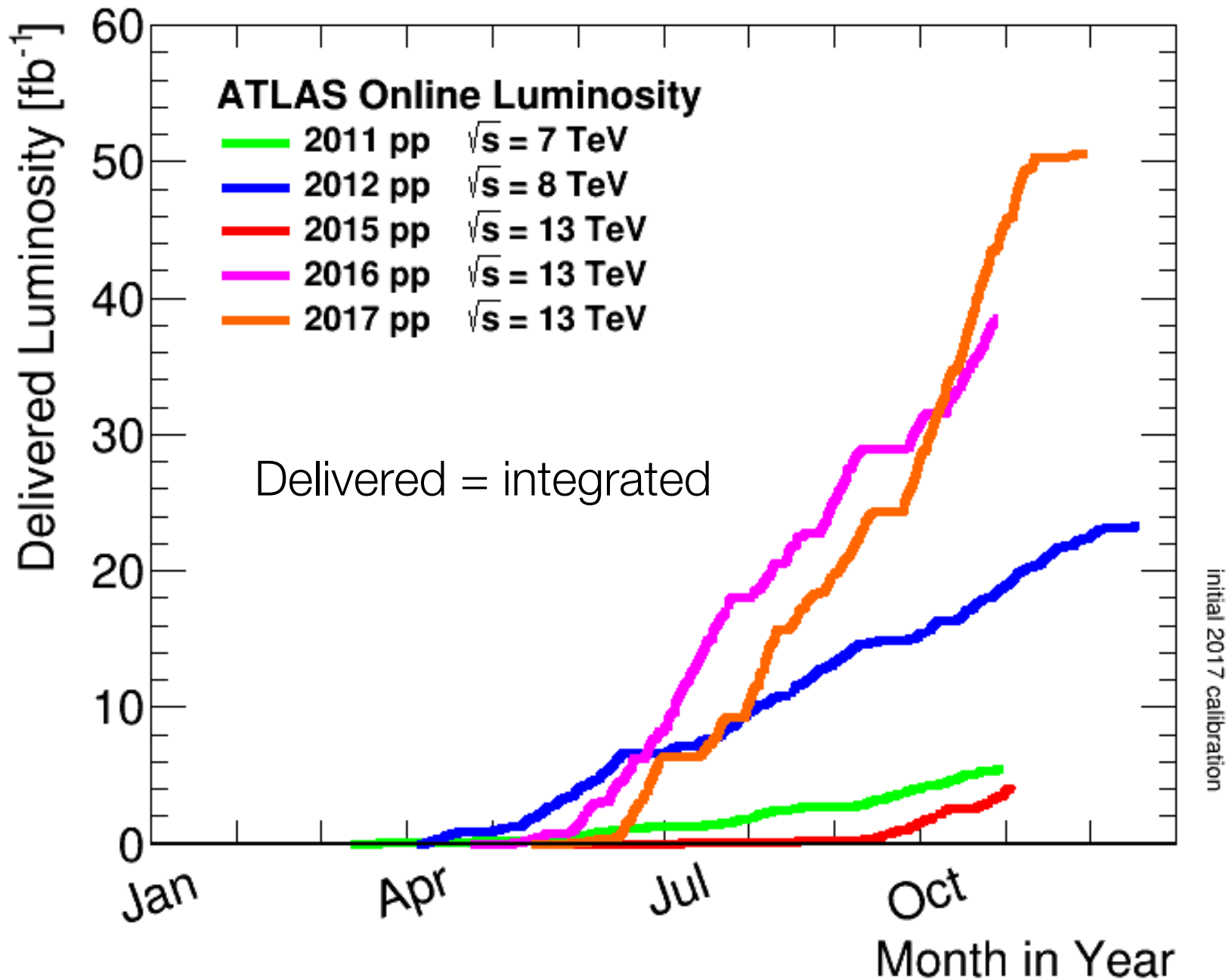
2017 2×6.5 TeV, $\beta^* = 0.3$ m, $L_{\text{peak}} = 2.1 \times 10^{34} \text{ cm}^{-2}\text{s}^{-1}$ $\int L dt = 50.4 \text{ fb}^{-1}$ 2544 bunches

2018 $\int L dt = 60 \text{ fb}^{-1}$ 2556 bunches

	LHC design	achieved
Momentum at collision, TeV/c	7	6.5
Luminosity, $\text{cm}^{-2}\text{s}^{-1}$	1.0E+34	2.1E+34
Dipole field at top energy, T	8.33	8.33
Number of bunches, each beam	3564	2544
Particles / bunch	1.15E+11	1.7E+11
Typical beam size in ring, μm	200 – 300	~300
Beam size at IP, μm	17	16



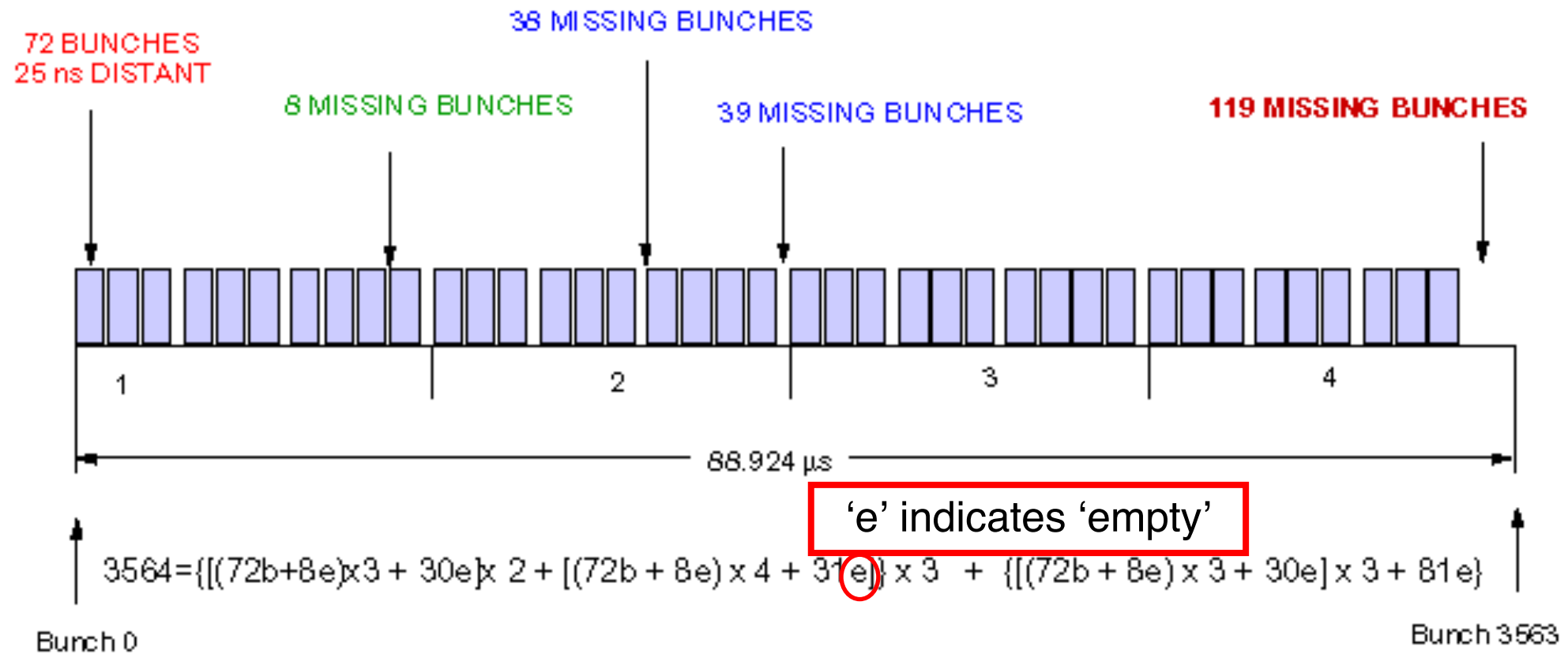
Luminosity delivered by LHC





LHC Nominal Bunch Structure

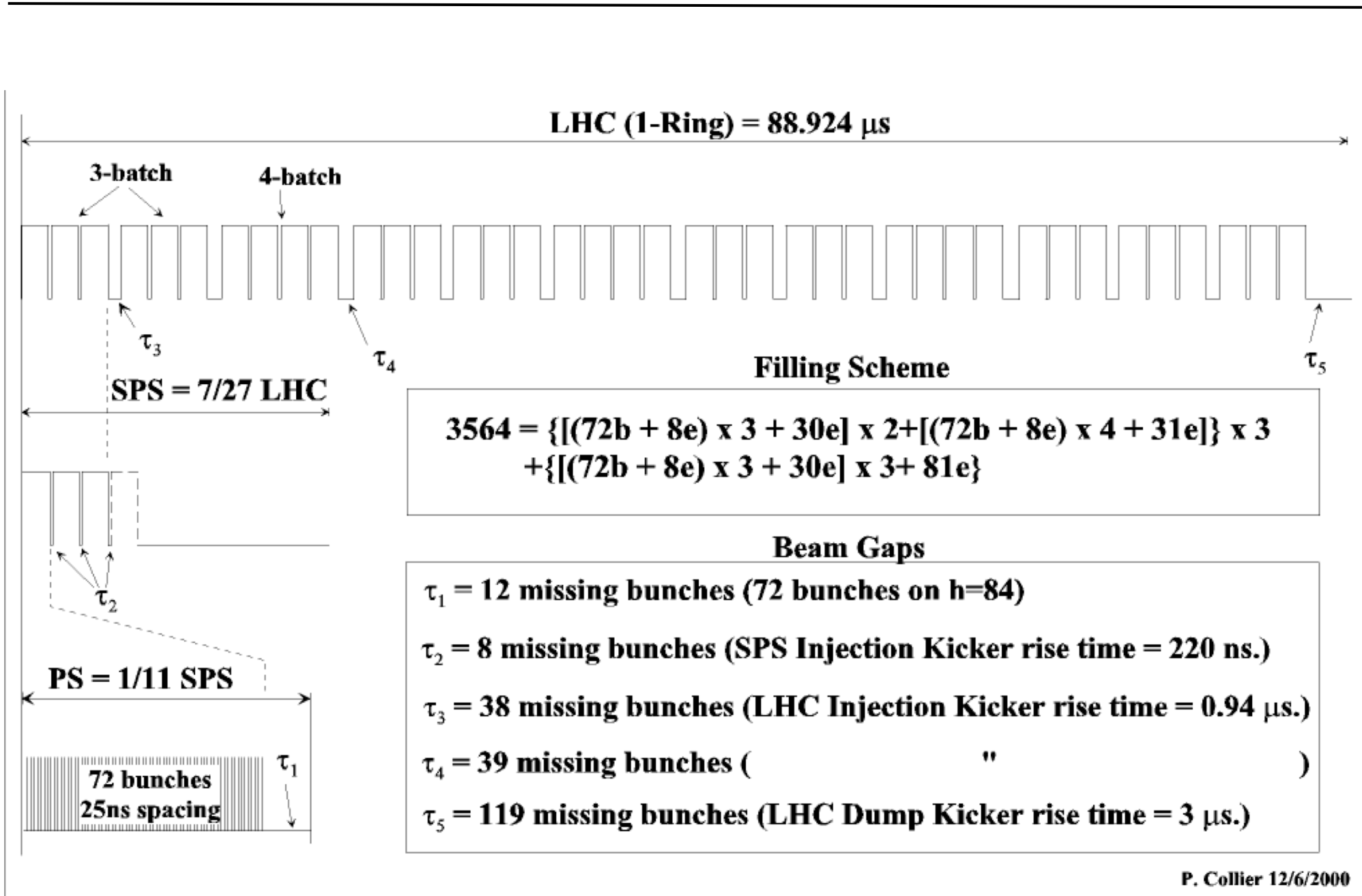
Not all bunches collide!



Filled bunches = 2808 = { [(72b)x3]x2 + [(72b)x4] }x3+{ [(72b)x3]x3 }

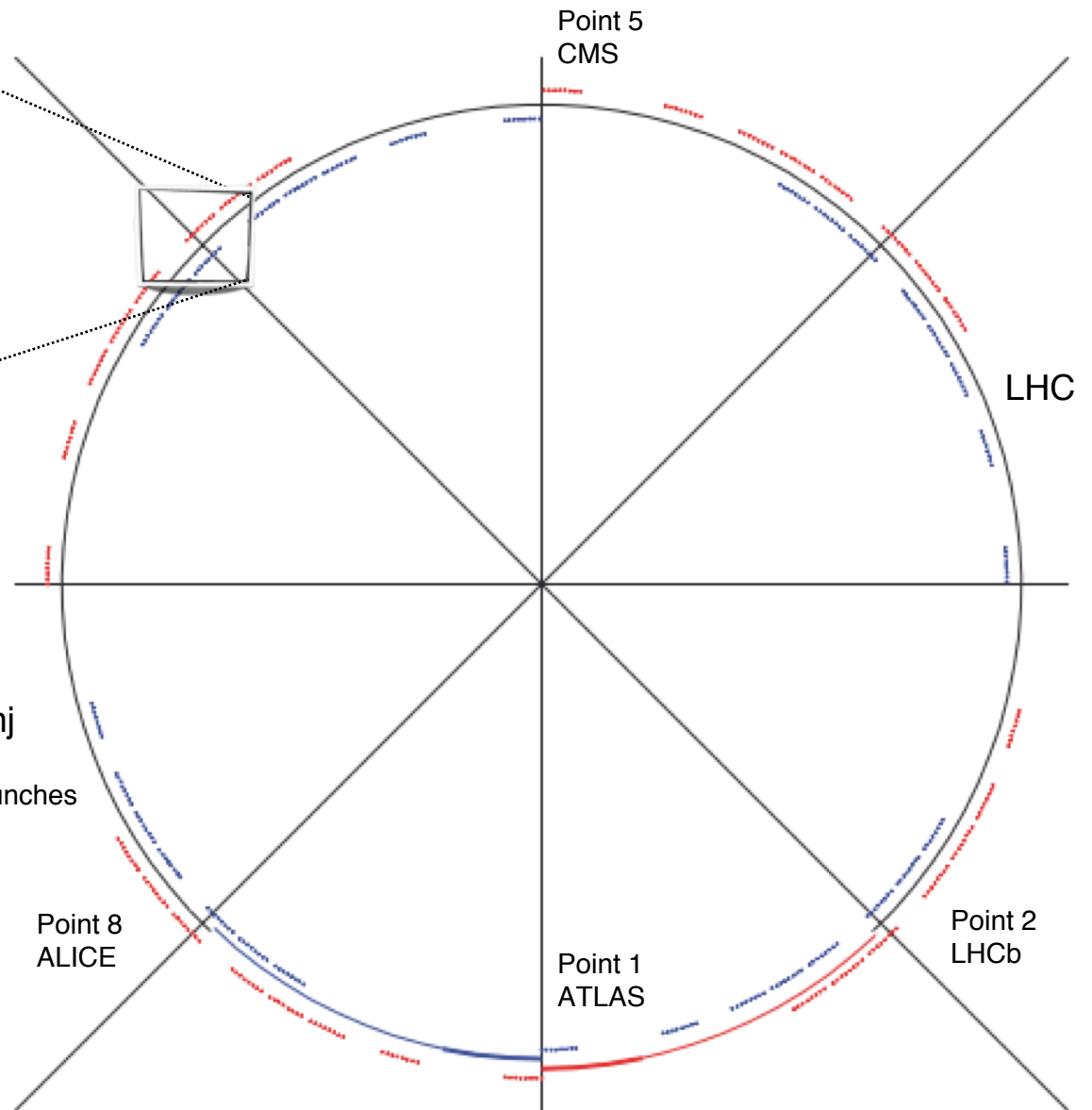
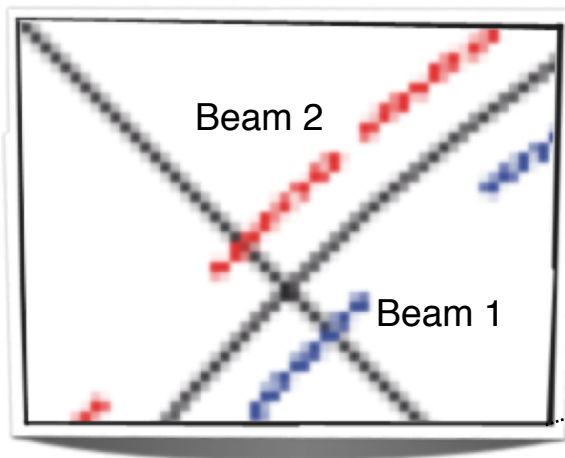


Bunch structures in LHC, SPS and PS





Present LHC Status



Present Bunch Structure:

150ns_248b_233_16_233_3x8bpi15inj

bunch distance

number of bunches

colliding bunches in points 1/5

colliding bunches in point 2

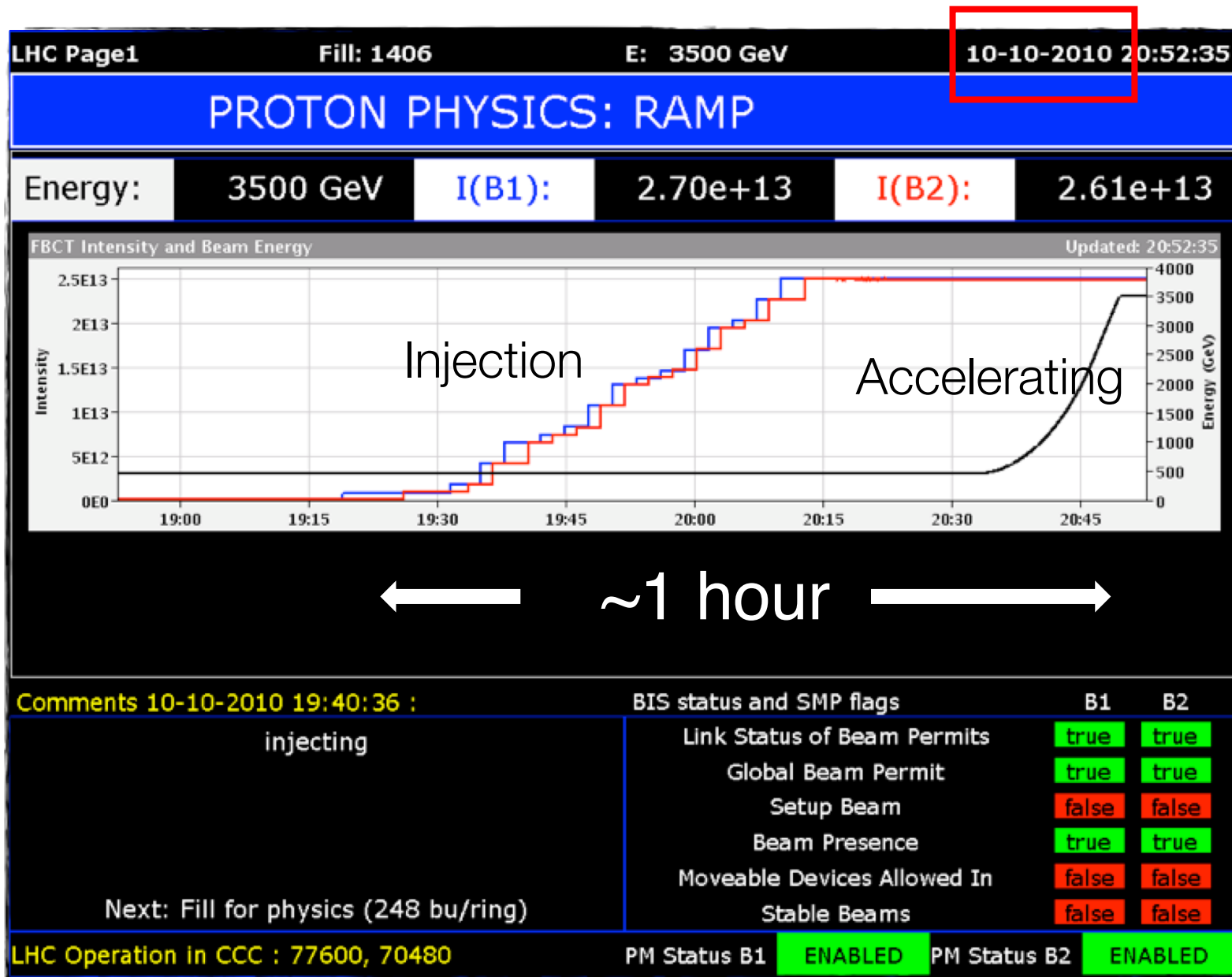
colliding bunches in point 8



LHC in Operation: what you see in Control Room

Toni Baroncelli Experimental High Energy Physics at Colliders 2019-20

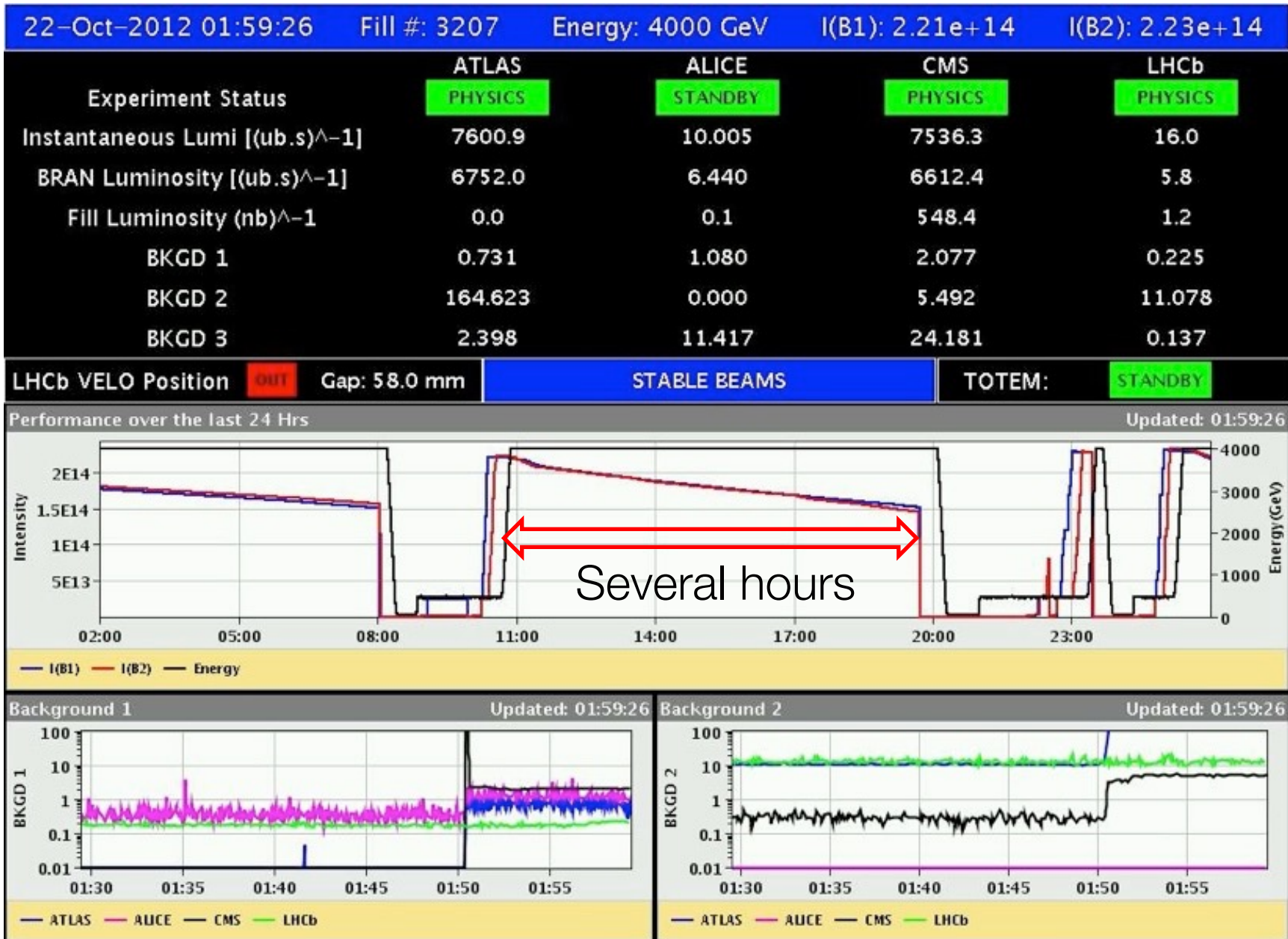
- Injection probe beam
- Injection
- Ramp
- Squeeze
- Adjust
- Stable Beams





LHC in Operation: what you see in Control Room-2

Toni Baroncelli Experimental High Energy Physics at Colliders 2019-20

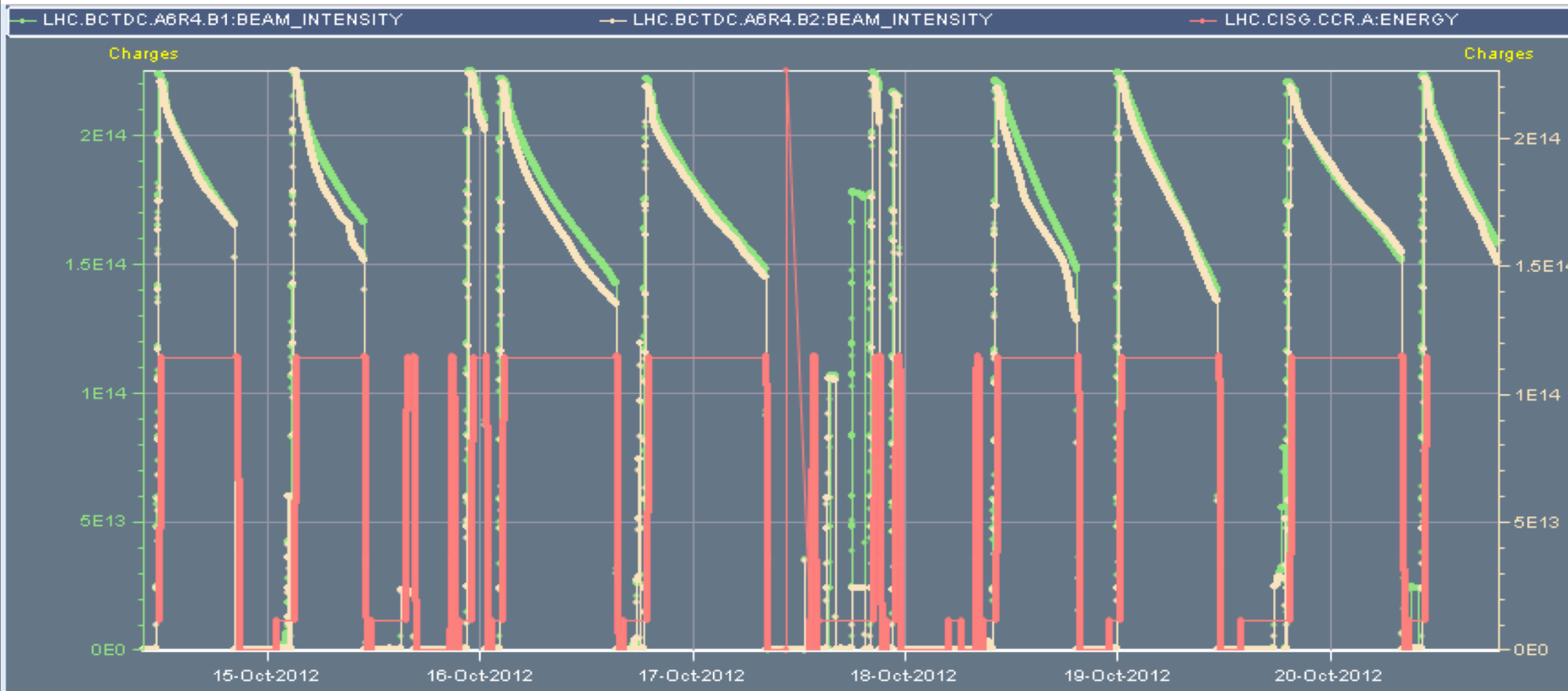


peak Luminosity $7.8 \times 10^{33} \text{cm}^{-2}\text{s}^{-1}$



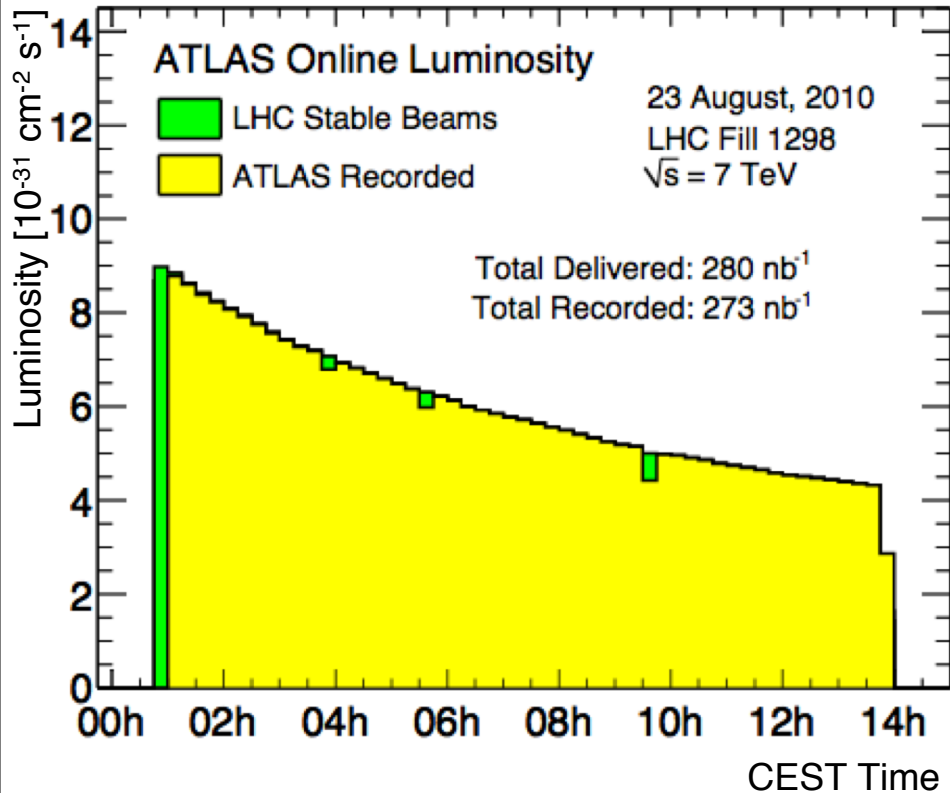
LHC typical week, Oct. '12, 1.2 pb⁻¹

Toni Baroncelli Experimental High Energy Physics at Colliders 2019-20



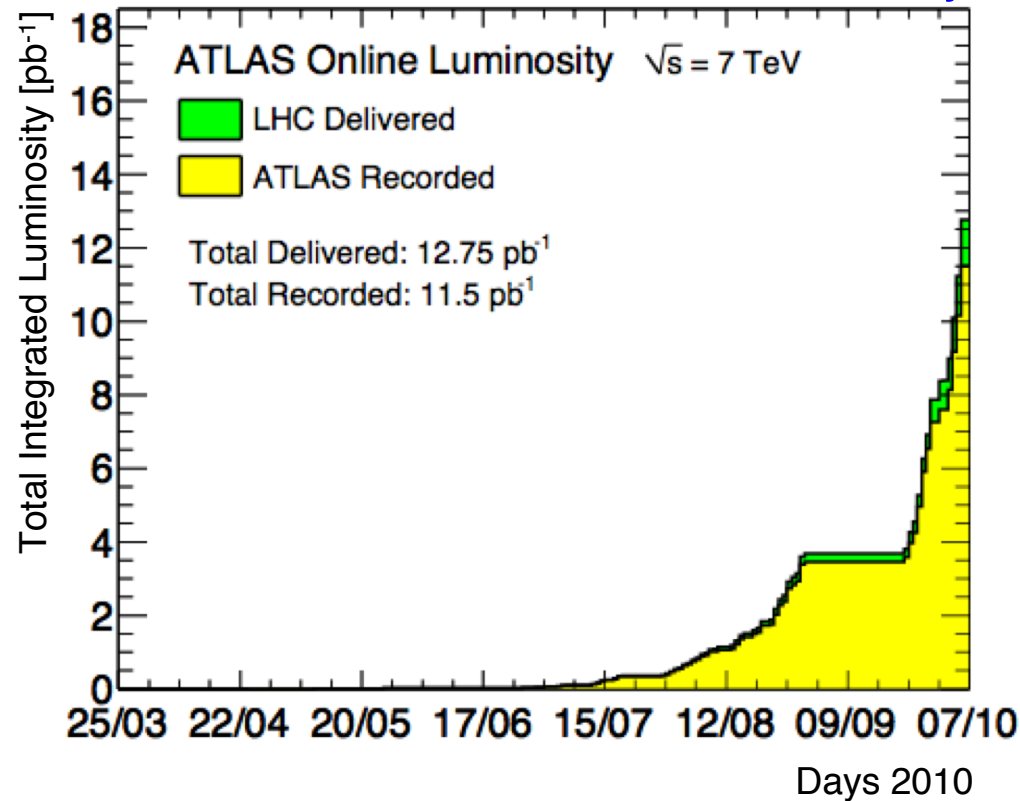


Present LHC Status



LHC Fill [August 2010]

Delivered and Recorded Luminosity



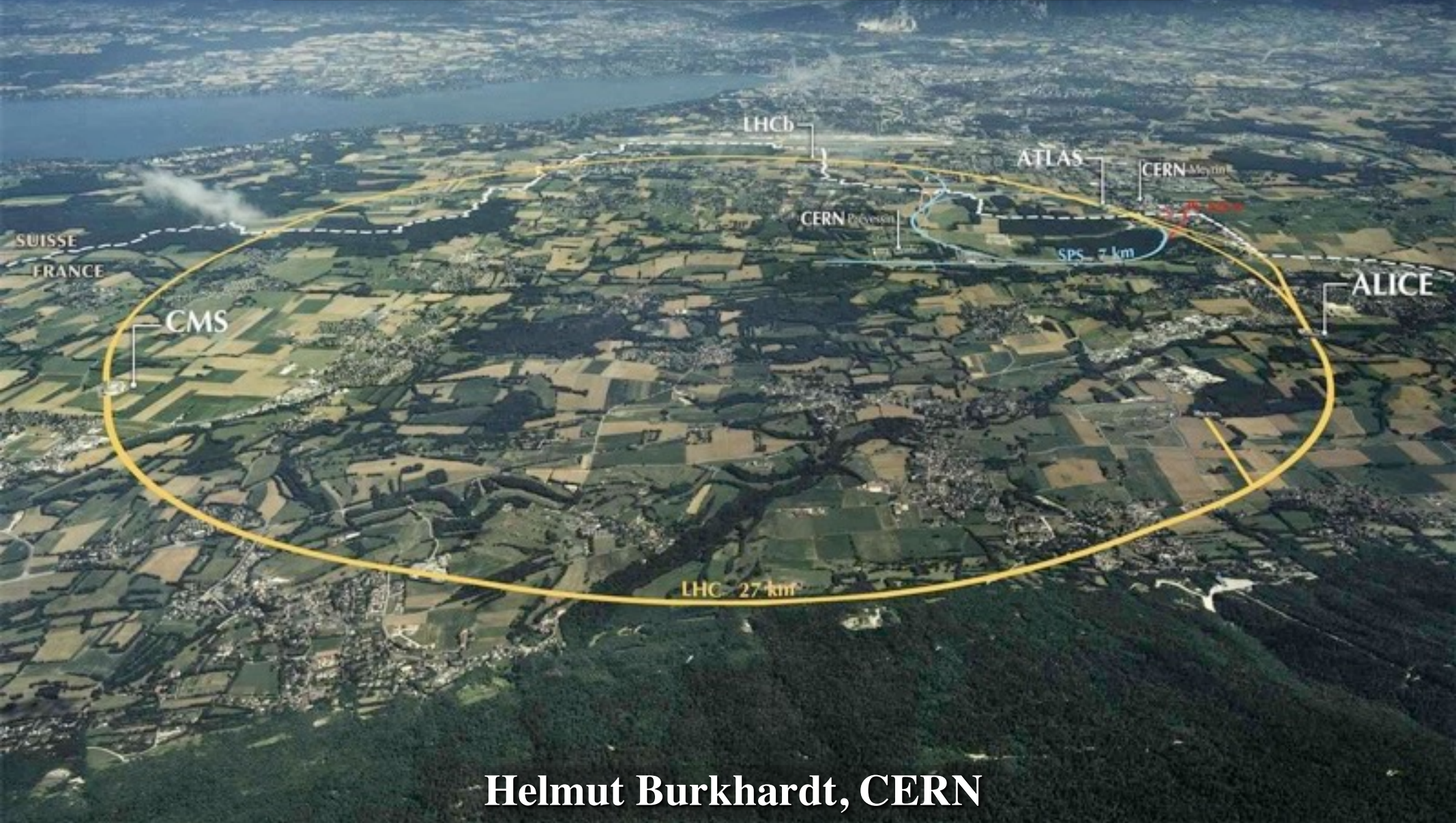
$$N = L \cdot \sigma$$

Number of Events

Integrated Luminosity

X-Sec.

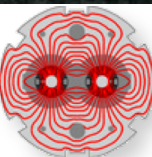
Introduction to Accelerators



Helmut Burkhardt, CERN



[ISEF 2013](#) 24 June 2013





Contents

- **Concepts: Energy Gain, E / B field. Units**
 - **Types of accelerators : Ring, Collider, Linac, e+e-, pp ; Cosmic**
 - **Components: Source, Magnets, resonant Cavities**
 - **Basic machine optics**
 - **Energy and Luminosity**
 - **Synchrotron Radiation**
 - **Limitations, current and future challenges**
-
- **Mixed with examples - mostly from CERN machines and in particular the LHC**

General, introductory refs. and books on Accelerators :

E. D. Courant and H. S. Snyder, *Theory of the Alternating-Gradient Synchrotron*, [pdf](#)

M. Sands, *Physics of Electron Storage Rings*, [SLAC Report No. 121](#); Wiedemann, *Particle Accelerator Physics* Bd. I,II

S.Y. Lee, *Accelerator Physics*, [World Scientific](#); M. Conte, W. MacKay, *Physics of Particle Accelerators*, [World Scientific](#)

CERN CAS yellow reports ; K. Wille, *The physics of particle accelerators*, Oxford University Press, 1996

Accelerators for Particle Physics, H. Burkhardt, in Handbook of Particle Detection and Imaging, [Ed. C. Grupen](#), Oct. 2011

The **L**arge **H**adron **C**ollider : O. Brüning, H. Burkhardt, S. Myers, [10.1016/j.pppnp.2012.03.001](#), [CERN-ATS-2012-064](#)

Accelerators and Colliders, Landolt-Börnstein New Series I/21C, [Springer 2013](#)



Accelerators at the Energy Frontier

Livingston plot

Exponential growth
of E_{cm} in **time**

Starting in 60's
with e^+e^- at about 1GeV

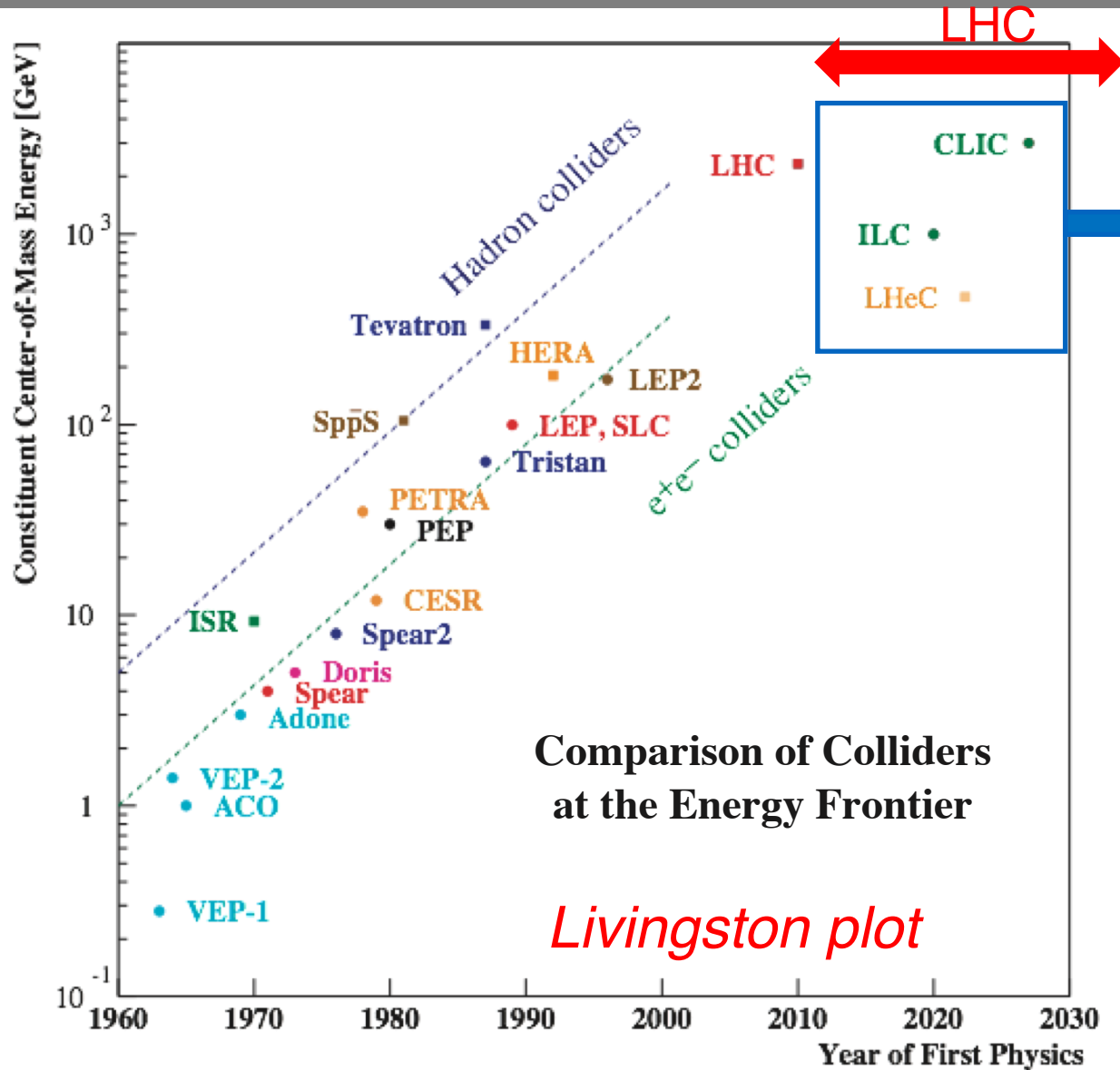
Factor 4 every 10 y

$pp, p\bar{p}$: $E_{cm} / 6$
still **5 x** above e^+e^- at
same time

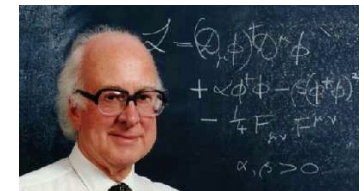
$pp, p\bar{p}$: **discovery**
 e^+e^- : **precision**

both required machines

+ ep : hadron structure, QCD
HERA, LHeC



The LHC is a major step forward
Discovery machine : Higgs ...





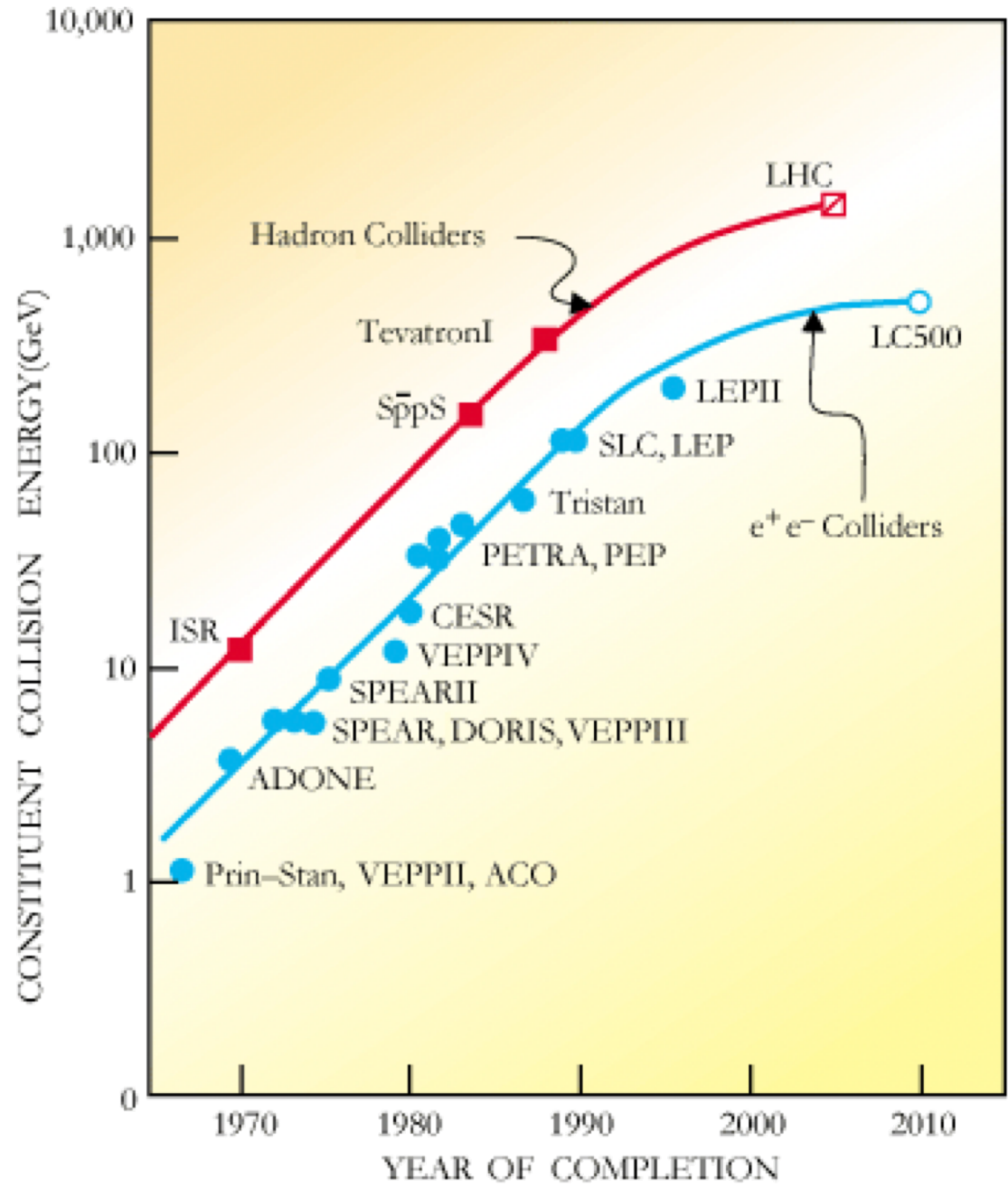
Livingstop plot

Livingston Plot:

Accelerator energy:
Energy reach has increased exponentially over the last 40 years

➔ Slow-down after 2000 (LHC and ILC)

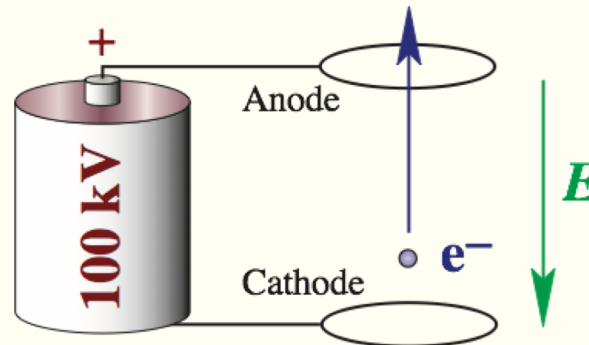
➔ Indication for limit of existing technologies!!





Basic concepts and units

Electric field :
Acceleration
 or rather
Energy gain
100 keV



Electric charge **e**
 and electric field
E

Special relativity, Lorentz transformation

$$E = \gamma mc^2 \quad p = \beta \gamma mc \quad \beta = \frac{v}{c} \quad \gamma = \frac{1}{\sqrt{1 - \beta^2}}$$

$$m_e \approx 0.511 \text{ MeV}/c^2 \quad m_p \approx 938 \text{ MeV}/c^2 \quad e \approx 1.602 \times 10^{-19} \text{ C}$$

C

For $E = 10 \text{ GeV}$:

Electron $\beta = 0.999\,999\,9987 \quad \gamma = 19569.5$

Proton $\beta = 0.995\,588\,4973 \quad \gamma = 10.6579$

Unit conversion

$$\frac{e^2}{4\pi\epsilon_0} = \alpha \hbar c = r_{\text{part}} m_{\text{part}} c^2 = 1.43996 \times 10^{-18} \text{ GeV m}$$

$$\hbar c = 197.327 \times 10^{-18} \text{ GeV m}$$

$$(\hbar c)^2 = 3.8938 \times 10^{-32} \text{ GeV}^2 \text{ m}^2 = 3.8938 \times 10^5 \text{ GeV}^2 \text{ nb}$$

for precise numbers see [PDG](#)

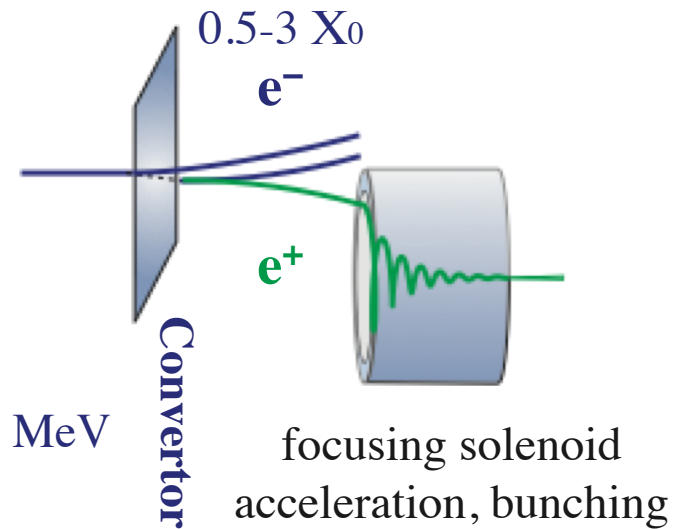
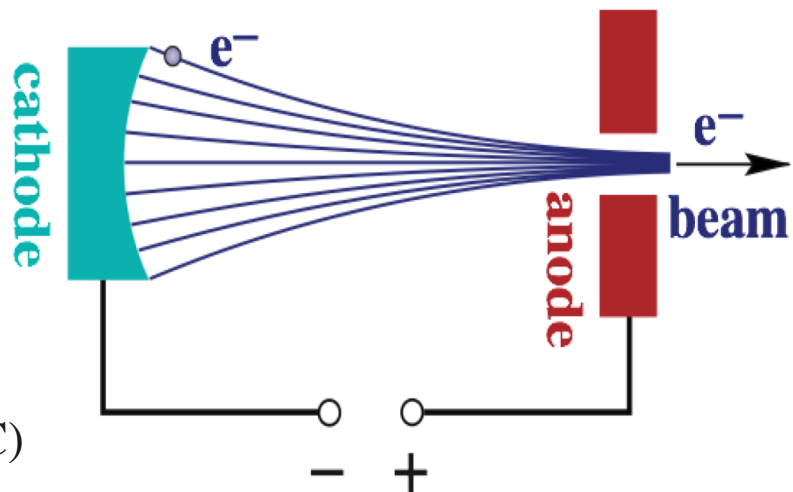
giga G = 10^9 tera T = 10^{12} peta P = 10^{15} exa E = 10^{18} zetta Z = 10^{21} yotta Y = 10^{24}



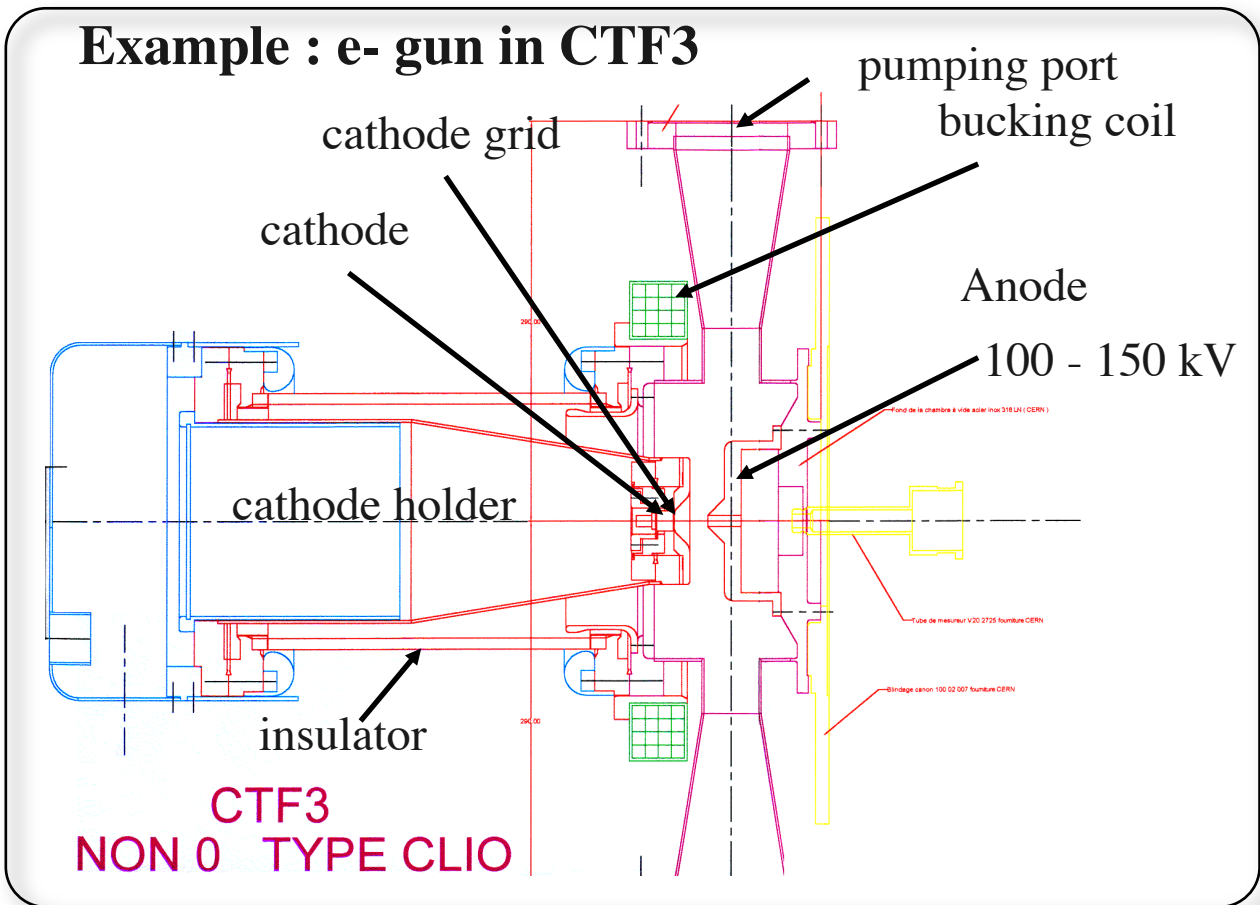
Particle sources

Thermionic electron source principle

same as cathode ray tube (significant for temperatures ~ 700 C)



Example : e- gun in CTF3



challenges :

high intensity

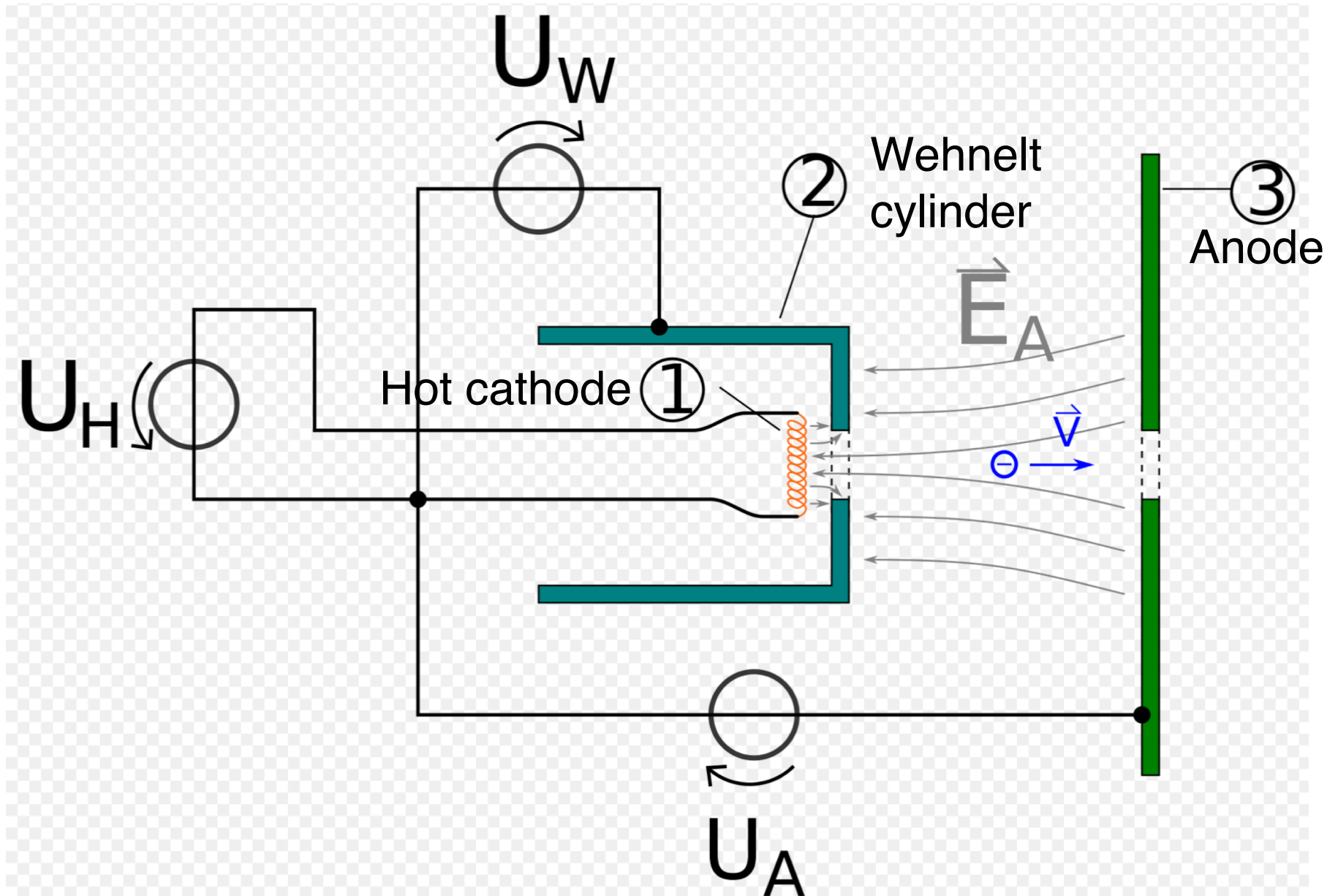
polarized e^- sources

damping rings for minimum emittance

undulator polarized e^+ sources



Electron source





Electron sources, details

A Wehnelt cap has the shape of a topless, hollow cylinder. The bottom side of the cylinder has an aperture (through hole) located at its center, with a diameter that typically ranges from 200 to 1200 μm . The bottom face of the cylinder is often made from platinum or tantalum foil.

Operation

A Wehnelt acts as a [control grid](#) and it also serves as a convergent [electrostatic lens](#). An electron emitter is positioned directly above the Wehnelt aperture, and an anode is located below the Wehnelt. The anode is biased to a high positive voltage (typically +1 to +30 kV) relative to the emitter so as to accelerate electrons from the emitter towards the anode, thus creating an electron beam that passes through the Wehnelt aperture. The Wehnelt is biased to a negative voltage (typically -200V to -300V) relative to the emitter, which is usually a [tungsten](#) filament or [Lanthanum hexaboride](#) (LaB_6) [hot cathode](#) with a "V" shaped (or otherwise pointed) tip. This bias voltage creates a repulsive electrostatic field that suppresses emission of electrons from most areas of the cathode.

The emitter tip is positioned near the Wehnelt aperture so that, when appropriate bias voltage is applied to the Wehnelt, a small region of the tip has a net electric field (due to both anode attraction and Wehnelt repulsion) that allows emission from only that area of the tip. The Wehnelt bias voltage determines the tip's emission area, which in turn determines both the beam current and effective size of the beam's electron source.

As the Wehnelt bias voltage increases, the tip's emitting area (and along with it, the beam diameter and beam current) will decrease until it becomes so small that the beam is "pinched" off. In normal operation, the bias is typically set slightly more positive than the pinch bias, and determined by a balance between desired beam quality and beam current.

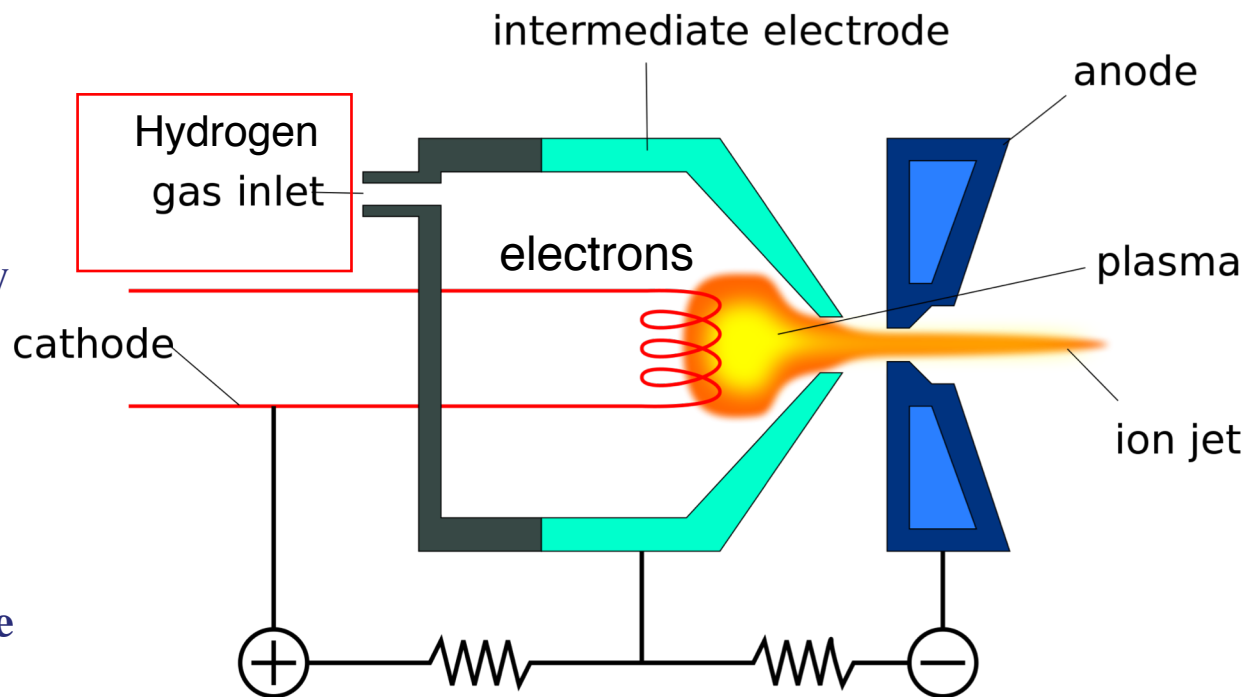
The Wehnelt bias controls beam focusing as well as the effective size of the electron source, which is essential for creating an electron beam that is to be focussed into a very small spot (for scanning electron microscopy) or a very parallel beam (for diffraction). Although a smaller source can be imaged to a smaller spot, or a more parallel beam, one obvious trade off is a smaller total beam current.



Proton and ion sources

Various methods exist to produce p (H^+), H^- (p with $2 e^-$) and heavy ions - heavier atoms, most electrons removed

Typically involves : **low pressure heated gas ionized gas / plasma**, inject H_2 to get protons, **or surface sputtering and electric and magnetic fields** to keep the electrons



CERN p-source and 50 MeV Linac

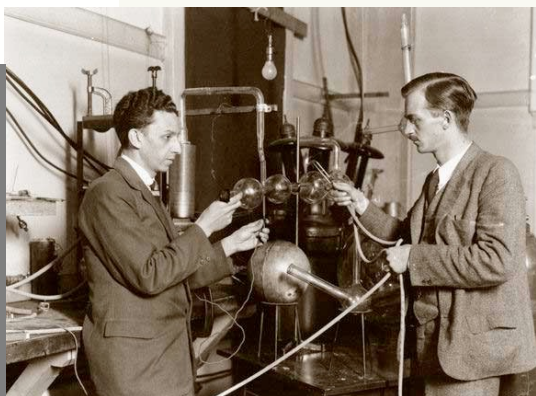




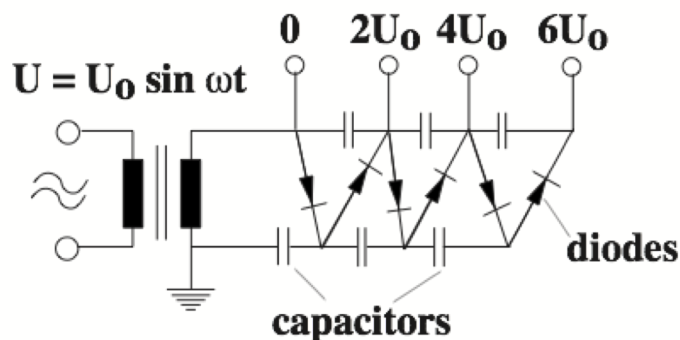
Linear Acceleration with Electrostatic Field

allows for DC, 100 % duty factor

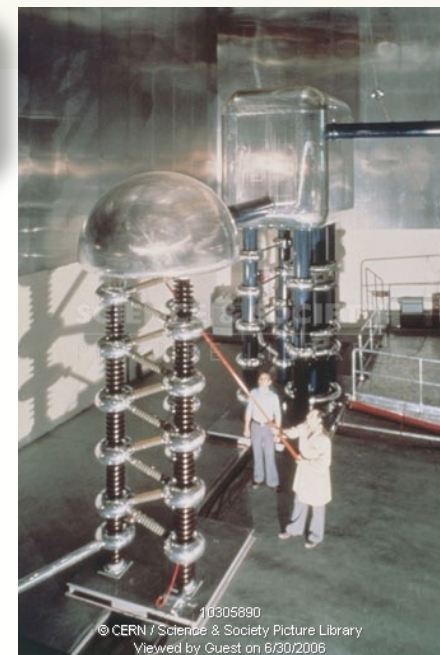
limited by HV-breakdown $\sim 1 \text{ MV} / \text{m}$



Cockcroft Walton
voltage multiplier

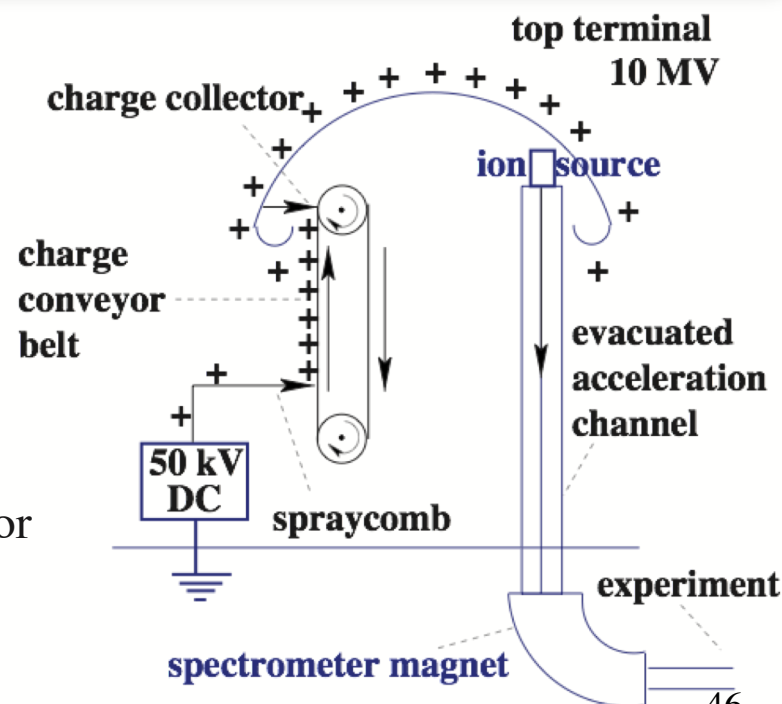


800 kV
proton pre-
injector
used at
CERN
until 1993



Van de Graaff generator
static electricity from belts

Oak Ridge Tandem Van de Graaff generator
reached 25.5 MV using pressurised SF₆





Time Varying Fields

Radio-Frequency or short RF acceleration

- allows for multiple passages
- bunched beams, reduced duty cycle
- higher RF frequencies allow for higher acceleration gradients

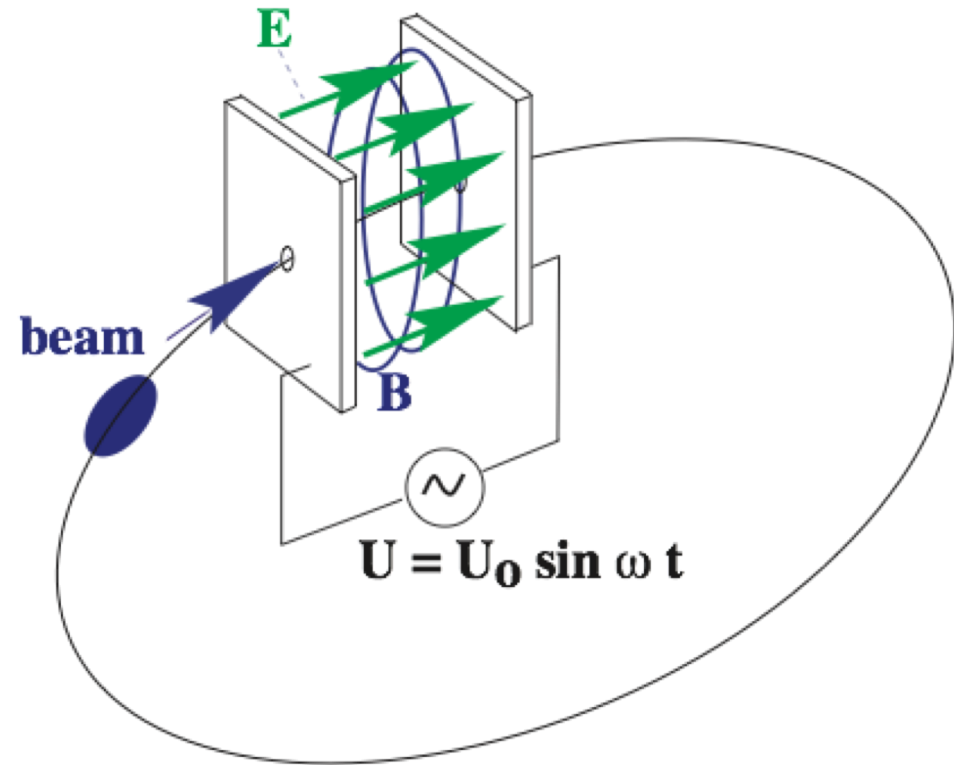
no time for breakdown / flashover

LEP , SC	8 MV / m at 352 MHz
Tesla / ILC, SC	31.5 MV / m at 1.3 GHz
CLIC	100 MV / m at 12 GHz

little gain above 12 GHz

SC limit ~ 50 MV/m, reached for single cell
 surface gradients higher than acceleration
 gradients, smooth structures

high f : shorter bunches - collective effects (peak current)
 and alignment more difficult
 less energy stored in structure





Basic parameters, Lorentz Force

$$\mathbf{F} = q (\mathbf{E} + \mathbf{v} \times \mathbf{B})$$

charge q , normally $q = e$; $q = Z e$ for ions

- Electric field \mathbf{E} provides the acceleration or rather energy gain
- The magnetic field \mathbf{B} keeps the particles on their path

ρ is the radius of curvature for motion perpendicular to the static magnetic field. Often called

- gyromagnetic or Larmor radius in astroparticle physics
- bending radius for accelerators

$B\rho$ known as magnetic rigidity, units Tm

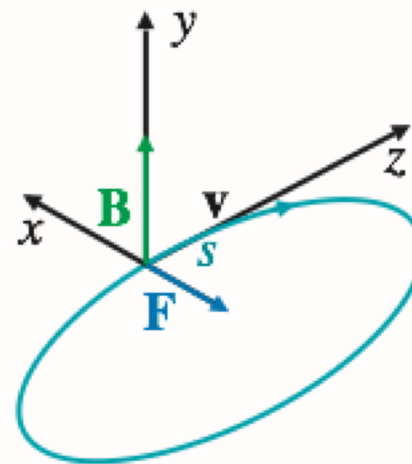
LHC

- Momentum $p = 7 \text{ TeV}/c$
- LHC bending radius $\rho = 2804 \text{ m}$
- Bending field $B = 8.33 \text{ Tesla}$
- magnets at **1.9 K, super-fluid He**

Circular motion for

$$\mathbf{E} = 0$$

$$\mathbf{v} \perp \mathbf{B}$$



$$B = \frac{p}{q \rho}$$

for $q = e$ numerically
 $B \text{ [T]} = p \text{ [GeV}/c] \cdot 3.336 \text{ m} / \rho$
 high energy, $v = c$ “ $p = E$ ”
 $E < E_H = q B \rho$ Hillas criterion

Astroparticle

units $10^{-4}\text{T} = 1\text{Gauss}$; a.u. = $1.5 \times 10^{11}\text{m}$

Solar system $B = 10 \mu\text{G}$ $E = 5 \text{ TeV}$ $\rho = 11 \text{ a.u.}$

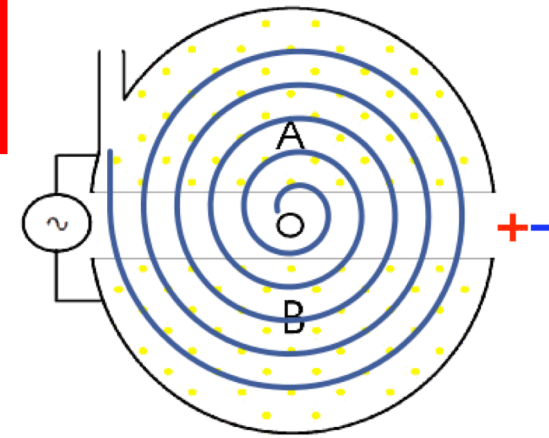
Intergalactic $B = 1 \text{ nG}$ $E = 5 \text{ PeV (knee)}$

$\rho = 1.7 \times 10^{19}\text{m}$ (4 % of galaxy-radius)

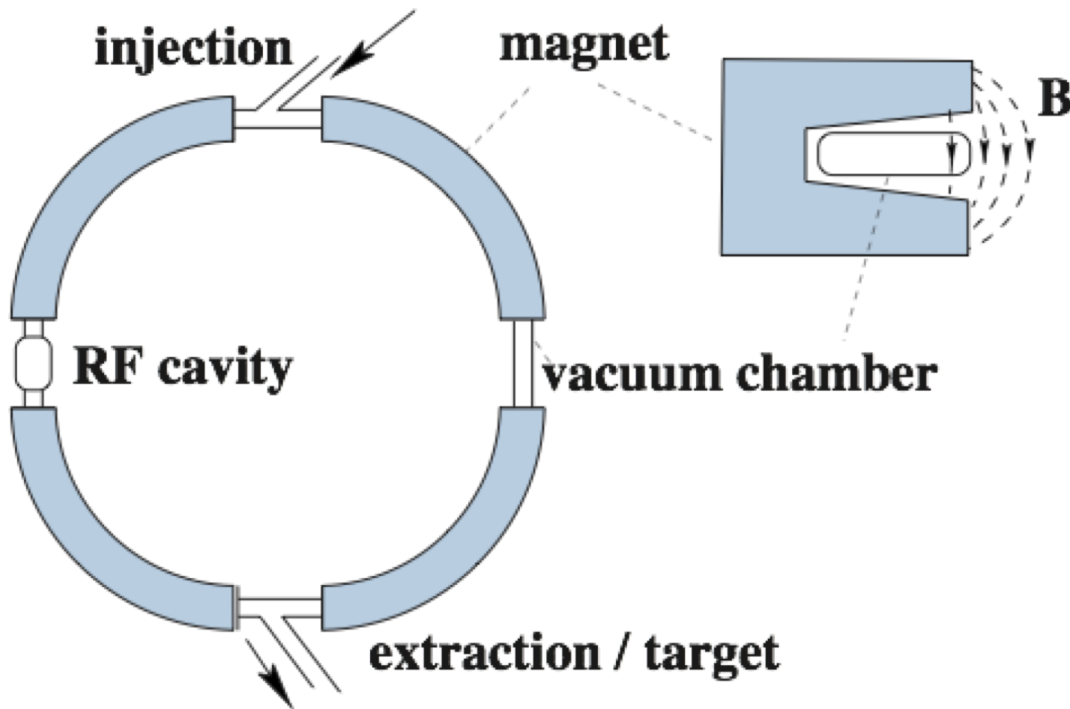


Circular Accelerator

Cyclotron : constant rf-frequency. Magnetic field radius ρ increases with energy. Used for smaller machines



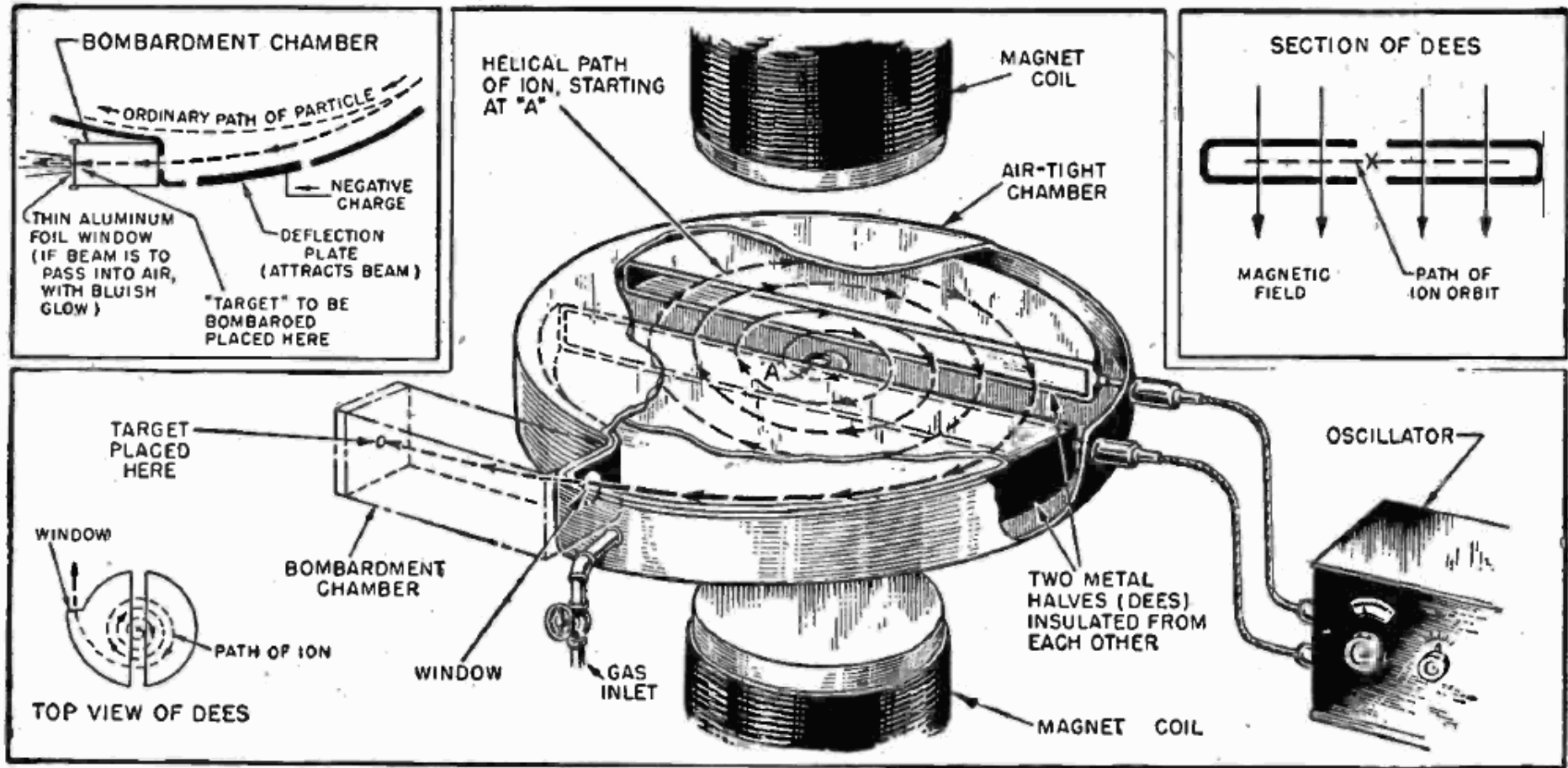
Cyclotron



Synchrotron : $\rho = \text{const.}$ B increased with energy. RF-frequency adjusted slightly ($\beta = 0.999 \dots 1.0$). Most HEP and all CERN ring accelerators PS, SPS, LEP, LHC of this type. Principle same for e, p, heavy-ion – PS, SPS – accelerate(d) all of these, in some cases switching within seconds



A sketch of an historical Cyclotron

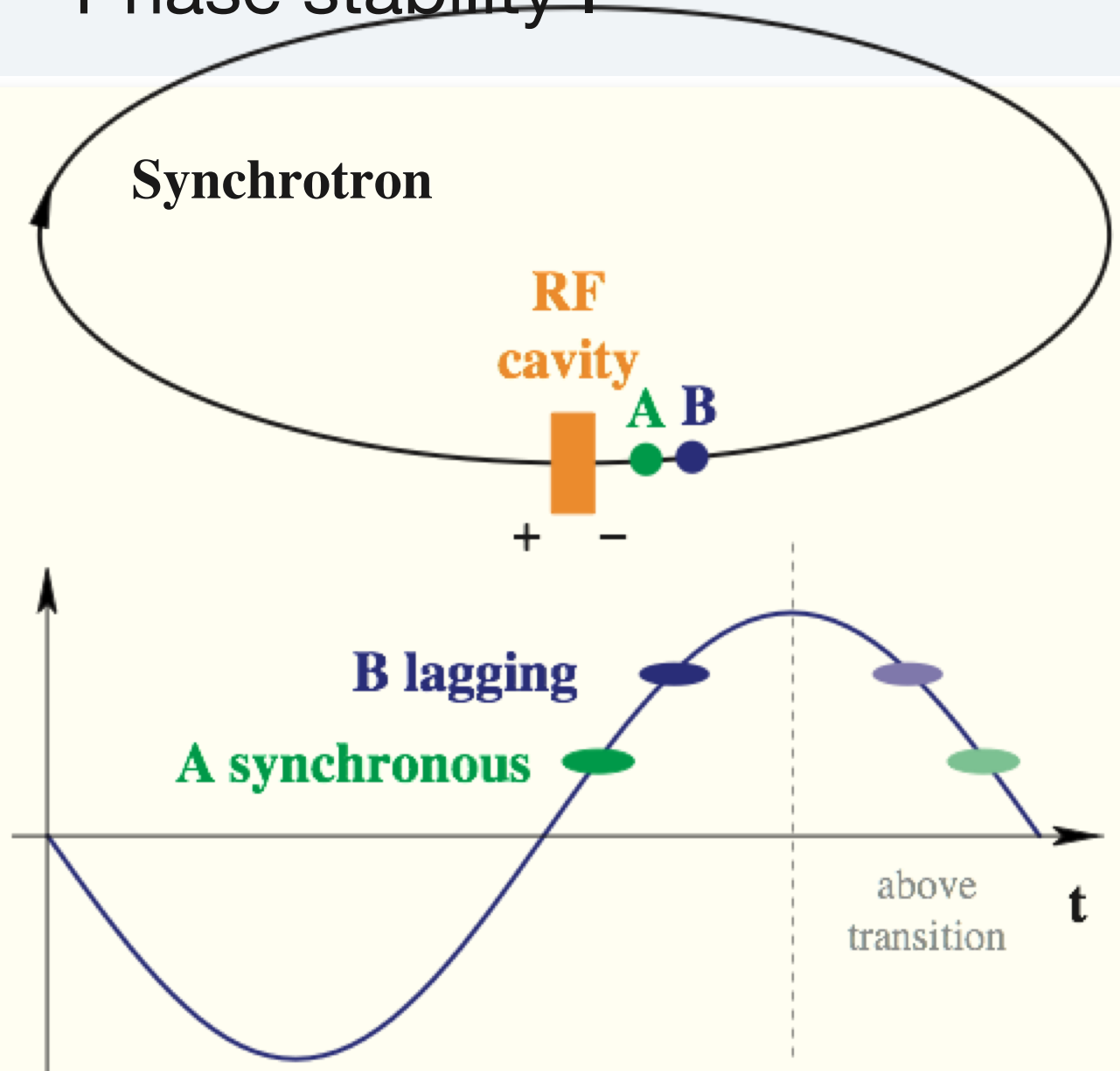




Phase stability I

acceleration,
ramping up in energy :

- allow for enough RF-voltage
- ramp up magnets
- particle adjust themselves in radius and phase to gain on average the right amount of energy



LHC nominal RF parameters

Voltage at injection 8 MV

top energy 16 MV

Revolution frequency $f_{rf} = h f_{rev}$

Circumference $L = v / f_{rev} = \beta c / f_{rev}$

$h = 35\,640$ $f_{rf} = 400.7896$ MHz $L = 26658.864$ m

$f_{rev} = 11.2455$ kHz 1 turn in 88.92446 μ s



Magnets and Power Consumption

Why super conducting magnets ?

$$P = R I^2$$

LEP

Lep = e⁺e⁻ machine

B = 0.1 T LEP2 ~ 100 GeV

(half) cells with each three 11.55 m long dipole magnets

I = 4.5 kA together **R = 1 mΩ** **P = 20 kW / cell**

488 cells **P = 10 MW**

if we would have kept the same magnets for the LHC

LHC **B ∝ I** **B = 8.38 T**

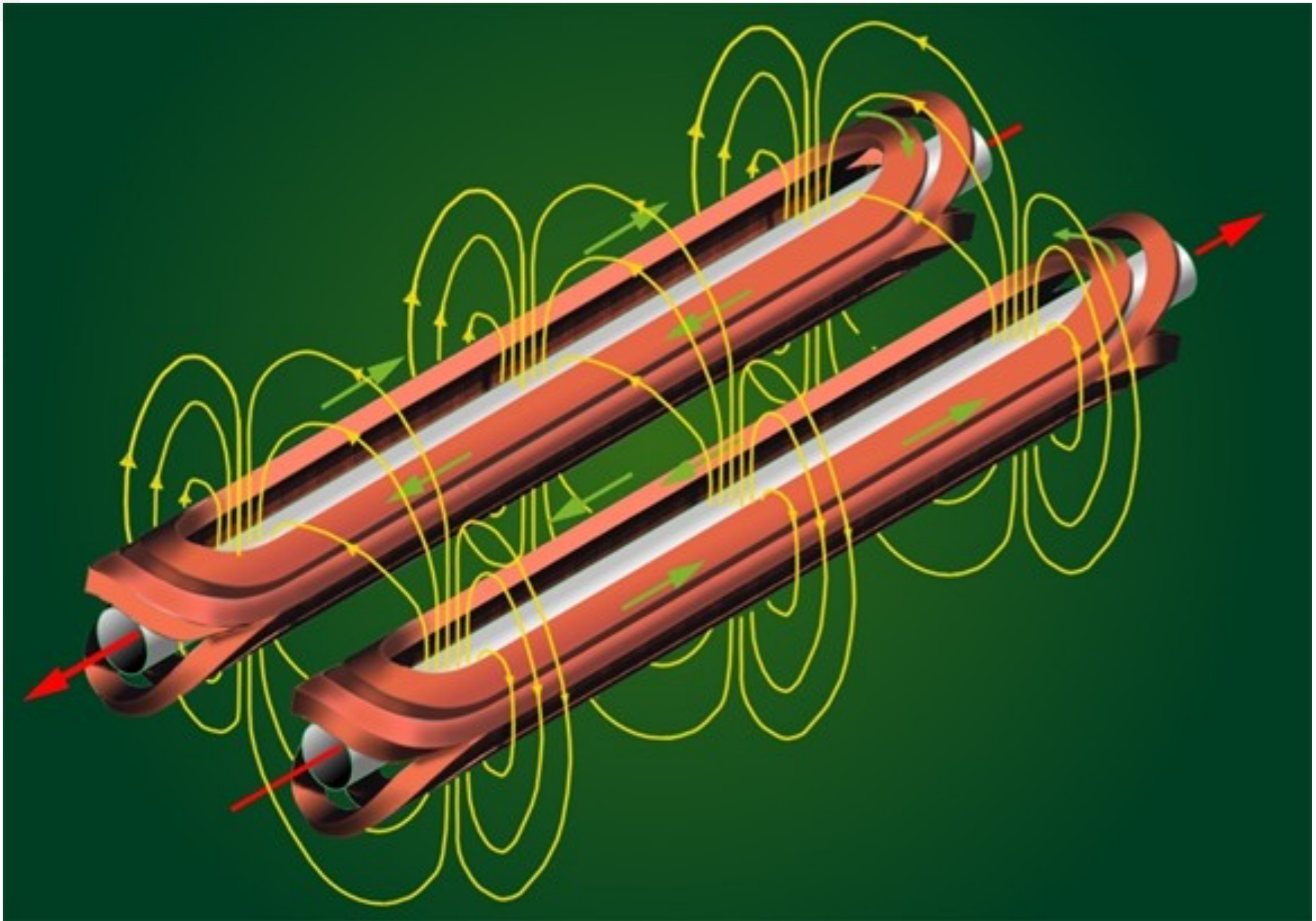
LHC = pp machine

would need now **I = 280 kA** with LEP magnets **R = 1 mΩ**

P = 78 MW / cell × 488 cells **total power P = 38 GW**

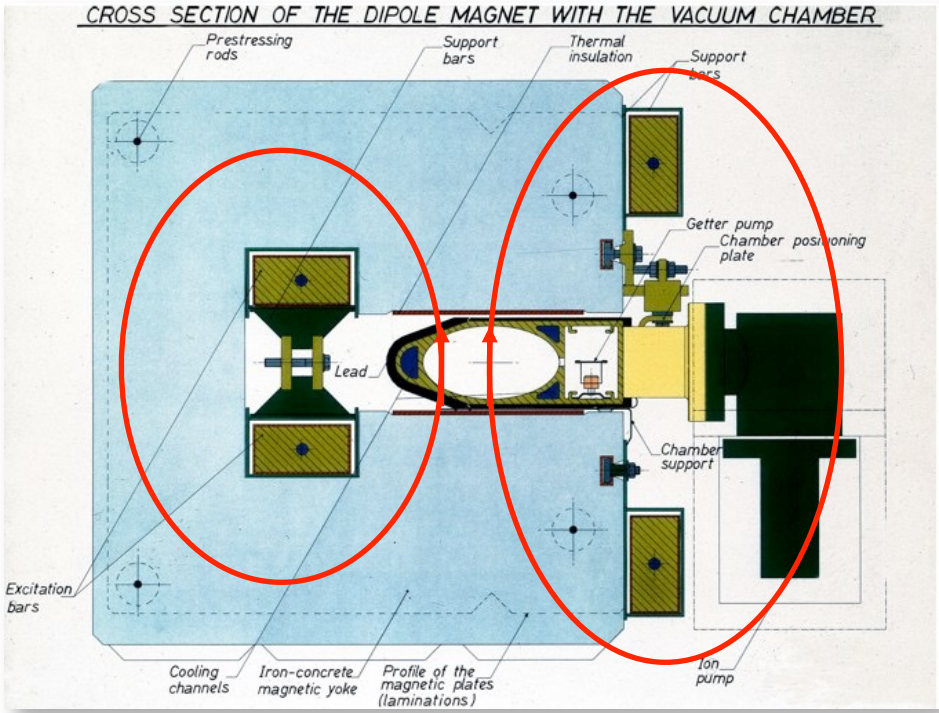


LHC dipoles

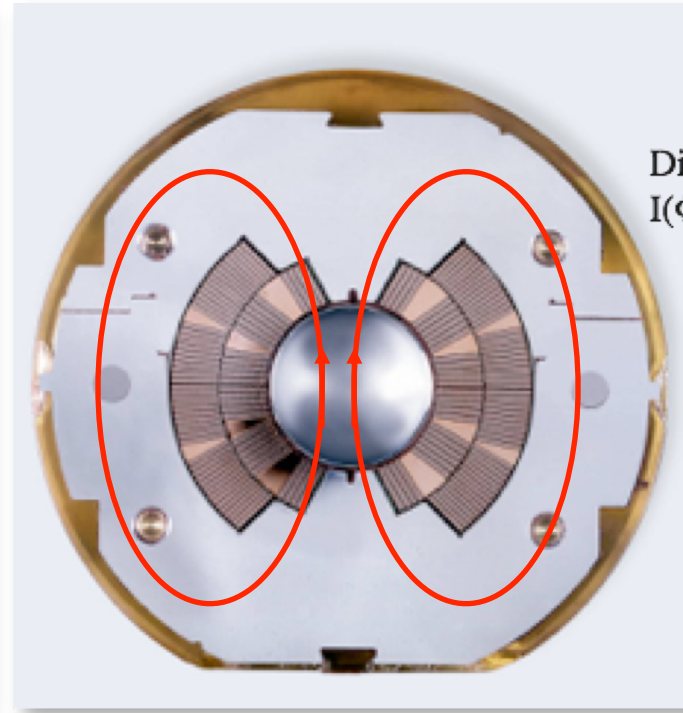


Magnet technology

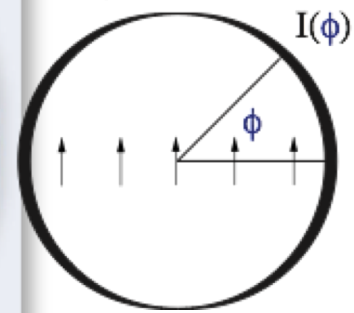
warm



cold



Dipole current distribution
 $I(\Phi) = I_0 \cos(\Phi)$



Toni Baroncelli Experimental High Energy Physics at Colliders 2019-20

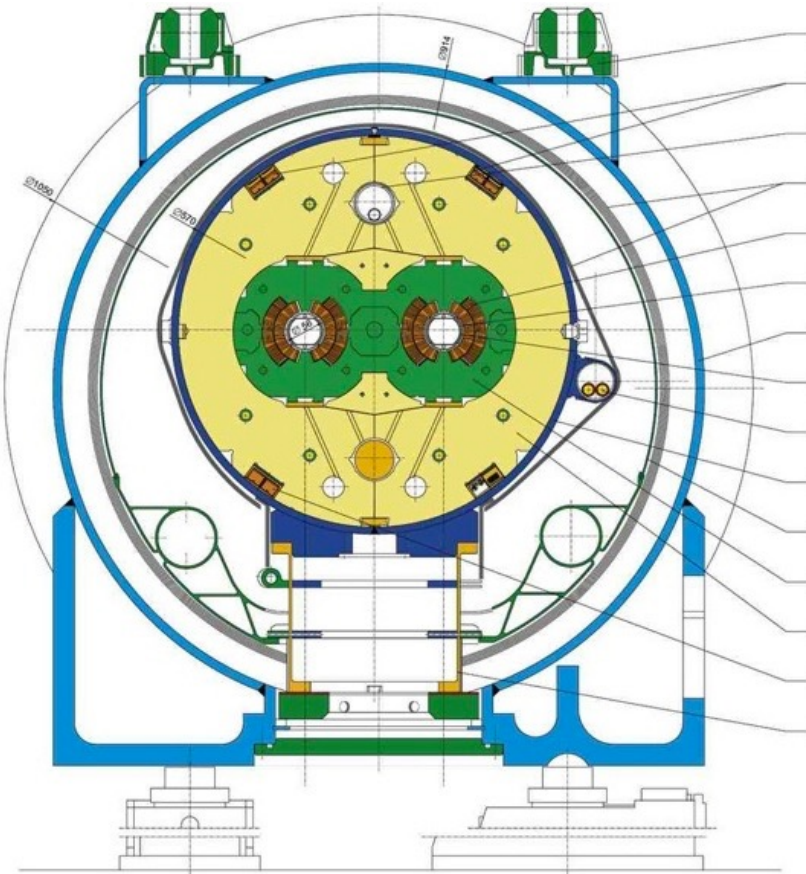
- field quality given by pole face geometry
- field amplified by Ferromagnetic material
- hysteresis and saturation ~ 2 T
- Ohmic losses for high magnet currents

- field quality given by coil geometry
- requires cooling to cryogenic temperatures
- persistent currents and snap back
- risk of magnet quenches

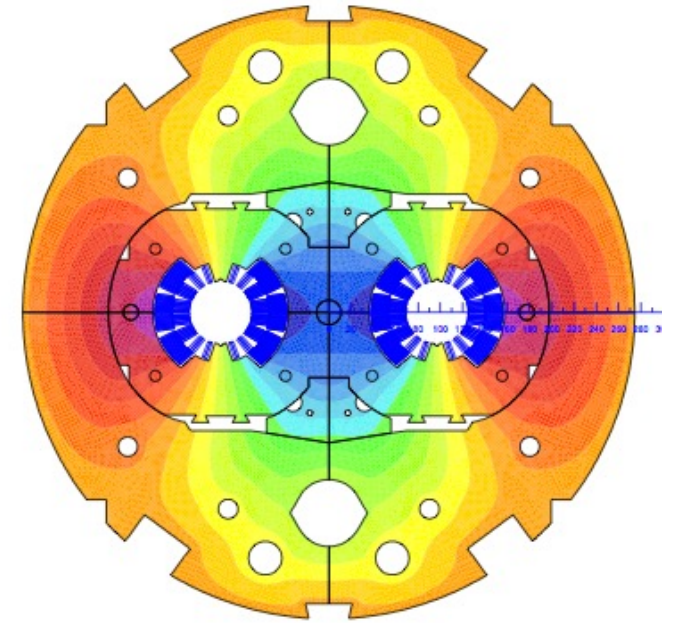


LHC dipole magnet

2-in-1 dipole magnet, 8.33 T field, 15 m long, mass 30 ton



- alignment target
- main quadrupole bus-bars
- heat exchange pipe
- superinsulation
- superconducting coils
- beam pipe
- vacuum vessel
- beam screen
- auxiliary bus bars
- shrinking cylinder / He I-vessel
- thermal shield (55 to 75 K)
- non-magnetic collars
- iron yoke (cold mass, 1.9 K)
- dipole bus-bars
- support post



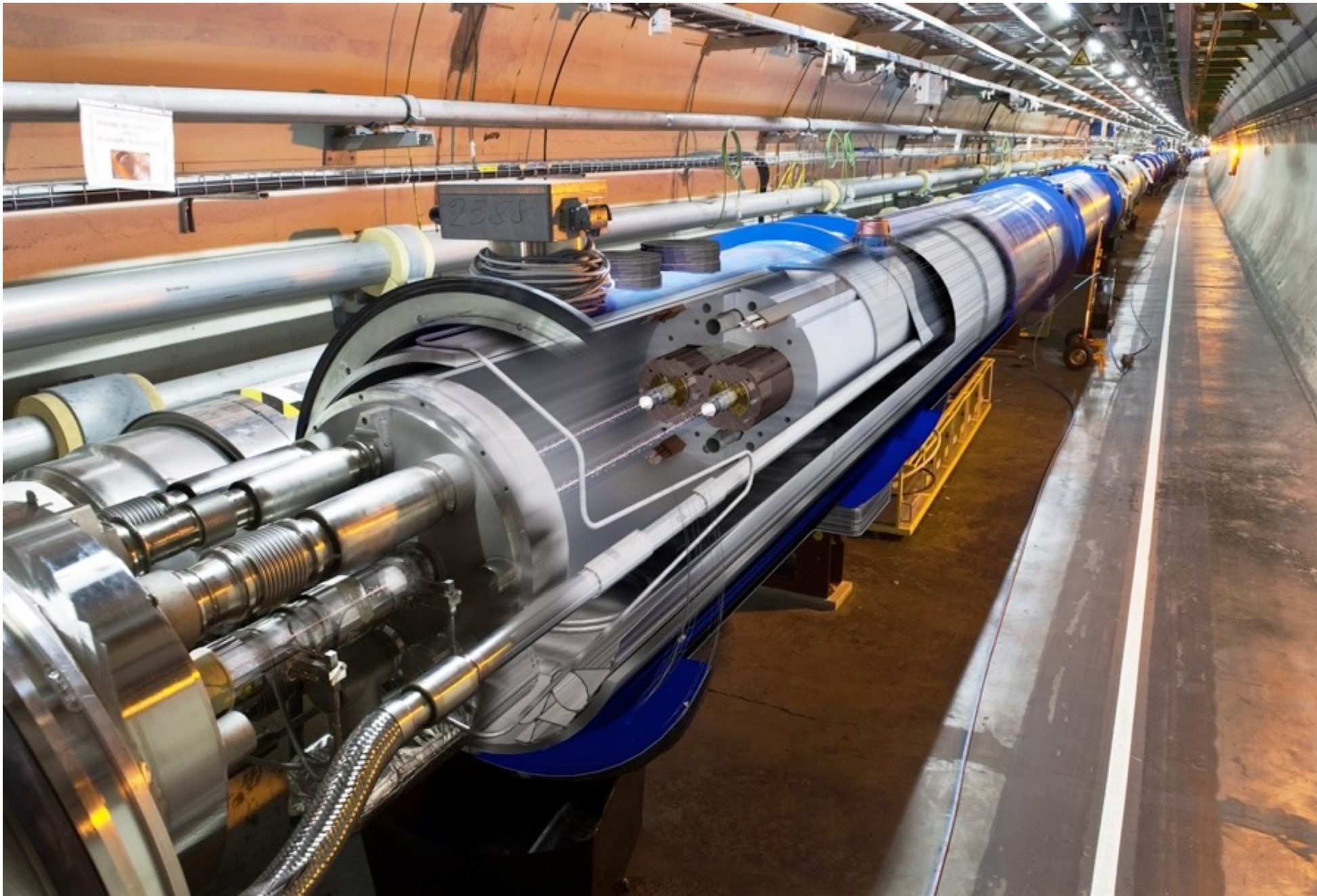
current distribution

LHC dipole magnet cross-section



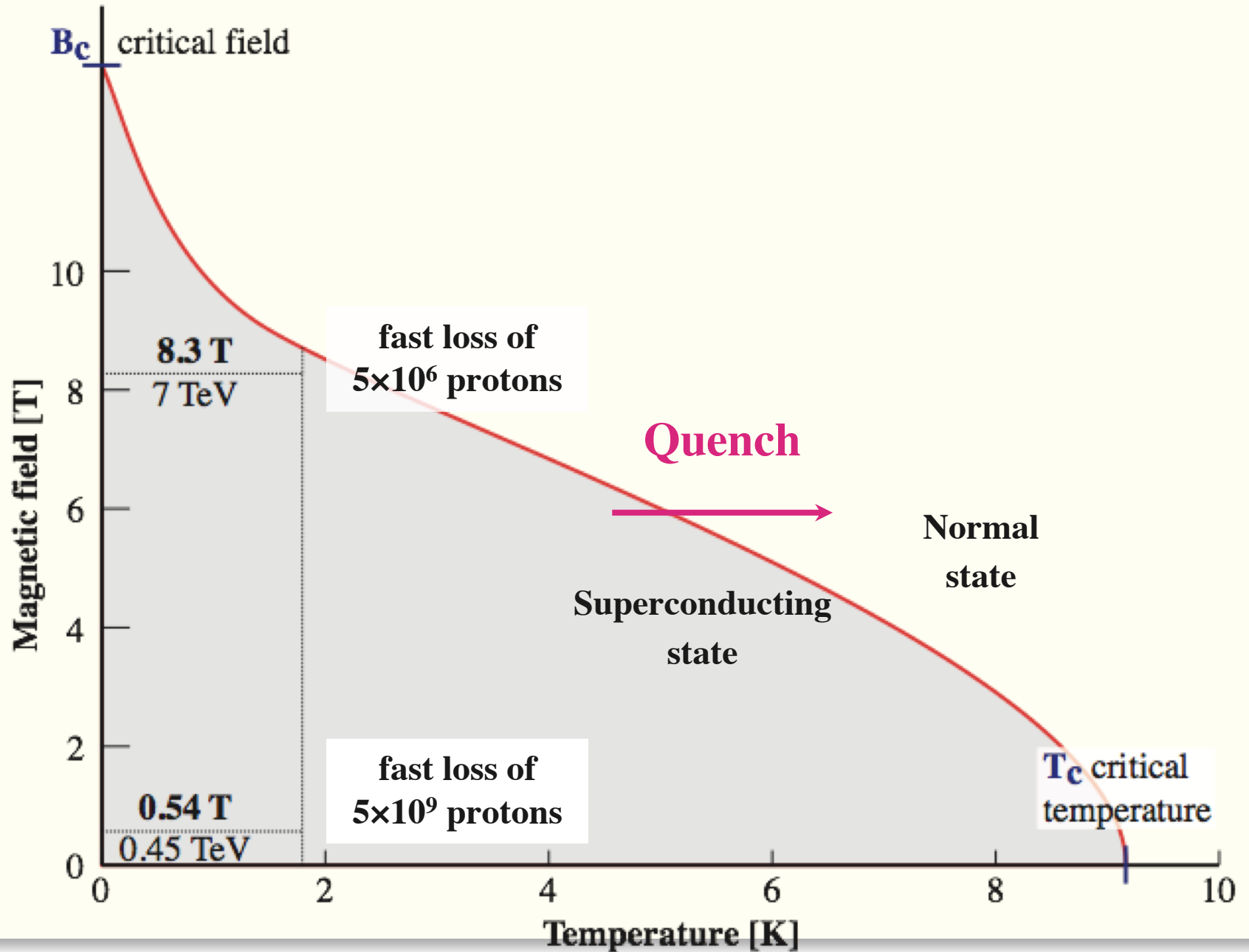
LHC magnets installed in the tunnel

Toni Baroncelli: Experimental High Energy Physics at Colliders 2019-20





Operational margin of a superconducting LHC dipole



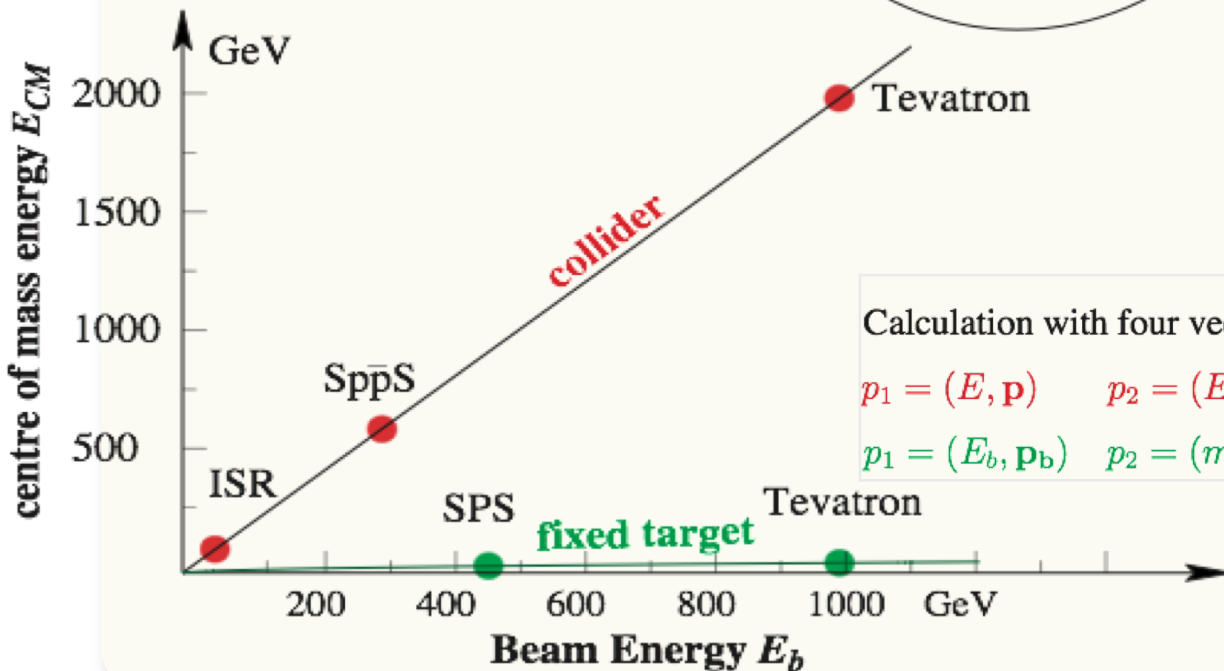
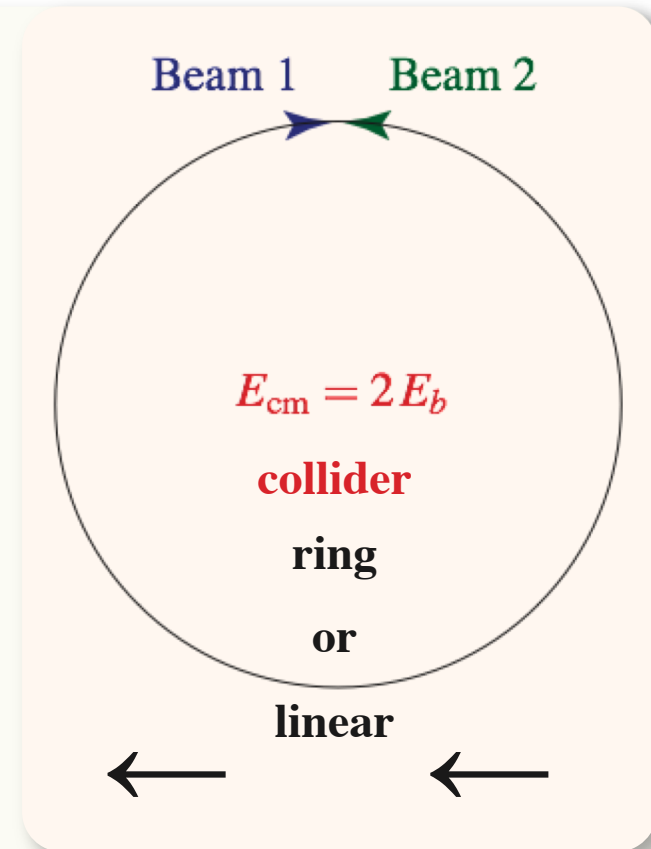
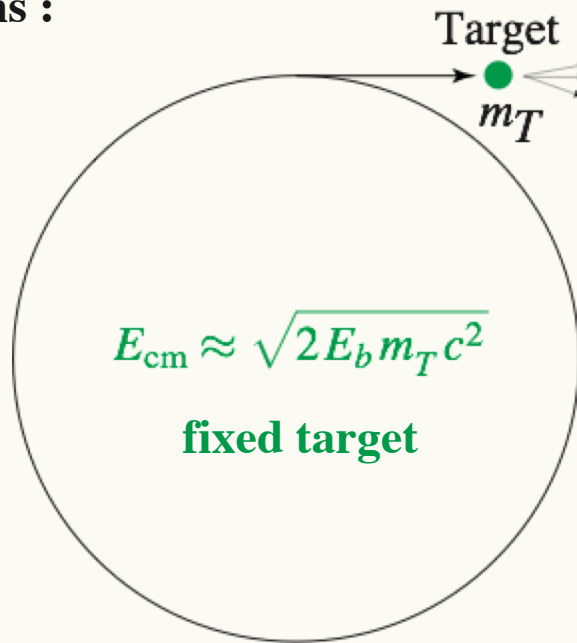


Fixed Target vs Collider

Fixed target, high energy collisions :
 Energy “lost” as kinetic energy

High Energy e^+e^- and
 very high energy pp gain
 a lot from **colliders**

Gain for LHC is by **x122**
 (14 TeV / 114.6 GeV)



Calculation with four vectors for $c = 1$ $E_{CM} = \sqrt{s}$ $s = (p_1 + p_2)^2$

$p_1 = (E, \mathbf{p})$ $p_2 = (E, -\mathbf{p})$ $s = 2m^2 + 2E^2 + 2p^2 = 4E^2$ **collider**

$p_1 = (E_b, \mathbf{p}_b)$ $p_2 = (m_T, \mathbf{0})$ $s = m_b^2 + m_T^2 + 2m_T E_b$ **fixed target**



Primary cosmic ray spectrum

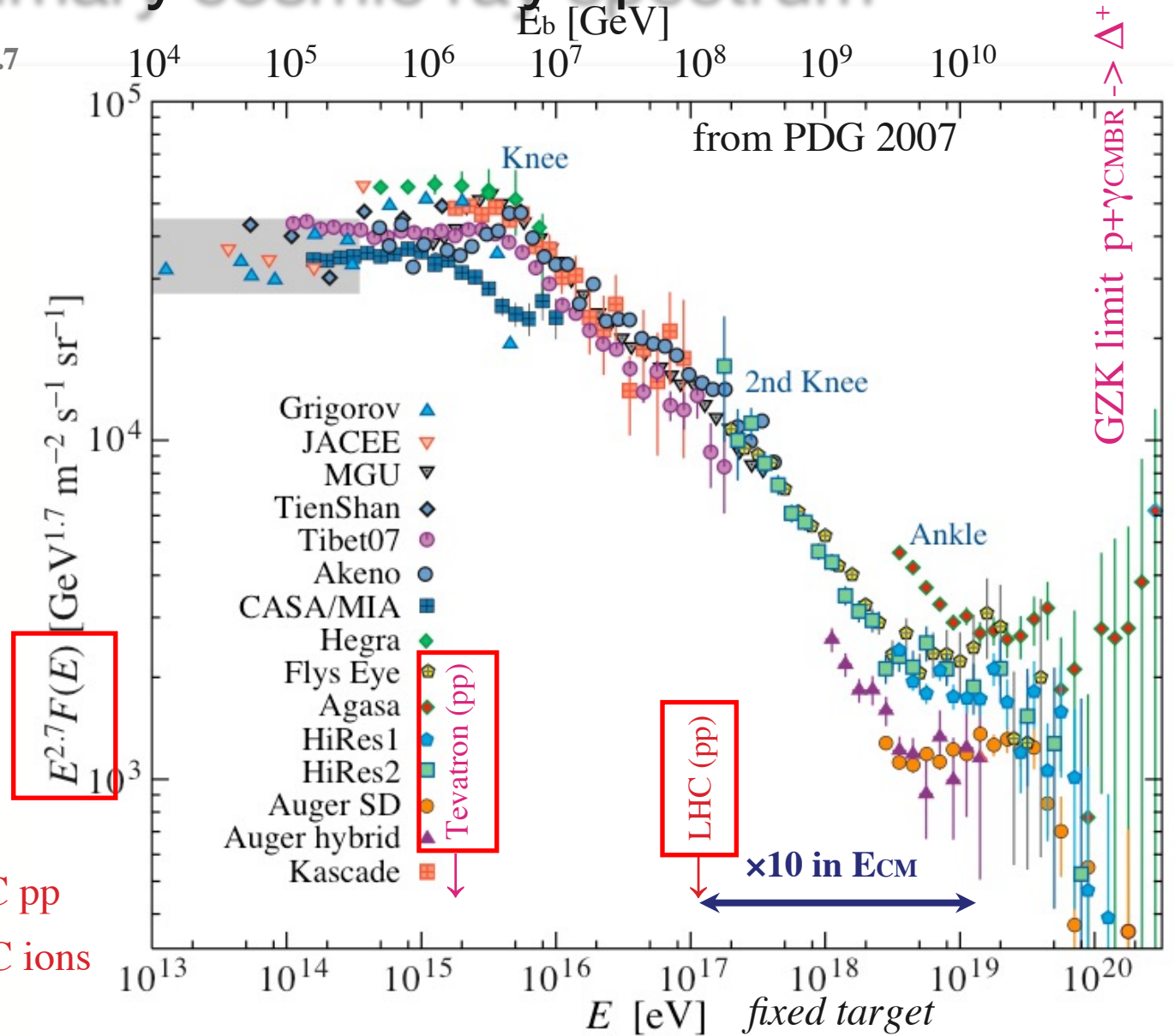
E spectrum falls as $E^{-2.7}$
 to knee at $E \approx 5e^{15}$ eV
 $= 5 \times 10^6$ GeV
 ~ 1 particle/(m² year)

origin galactic

above $\sim E^{-3}$

back to $E^{-2.7}$ at very
 highest energies
 conversion to E_{cm}

E_b [eV]	E_{cm} [TeV]
10^{13}	0.137
10^{15}	1.370
10^{17}	13.70 \approx LHC pp
10^{19}	137.0 \leftarrow LHC ions
10^{21}	1370.



Nature has much larger and more powerful **cosmic accelerators** than we can ever built.

With colliders we can get to these collision energies in clean laboratory conditions.

The LHC already gets us to within 1-2 orders of magnitude of the very highest cosmic rays.



Luminosity and collision rates

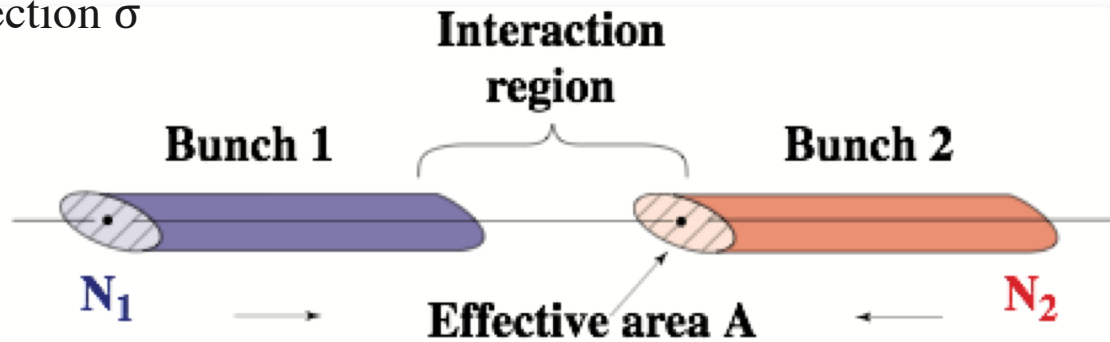
Event rate for process with cross section σ

$$\dot{n} = \mathcal{L} \sigma$$

Luminosity from bunch

crossings at frequency $f = f_{\text{rev}} n_b$

$$\mathcal{L} = \frac{N_1 N_2 f}{A}$$



for Gaussian bunches with rms sizes $\sigma_x \sigma_y$ $A = 4 \pi \sigma_x \sigma_y$

High **Luminosity** : $N \uparrow$ collide many particles, $A \downarrow$ squeezed in small bunches

LHC 1.15×10^{11} protons, $n_b = 2808$ ($f \uparrow$ crossings at 25 ns intervals)

Beams squeezed using strong

large aperture quadrupoles

around the interaction points

from ~ 0.2 mm to

$$\sigma_x = \sigma_y = 17 \mu\text{m}$$



$$\langle \beta_{\text{arc}} \rangle = 80 \text{ m}$$

$$\beta_{\text{IP}} = 0.5 \text{ m}$$

Rare new processes, like Higgs production can have very small cross section,

like $1\text{fb} = 10^{-39}\text{cm}^2$. LHC designed for very high Luminosity $\mathcal{L} = 10^{34} \text{cm}^{-2}\text{s}^{-1}$

Event rate for such rare processes : ~ 1 new particle every 28h.

Instead pp $\sigma_{\text{tot}} \approx 0.1$ barn 30 / crossing



Alternate gradient focusing

Quadrupole lens focusing in x, defocusing in y or vice versa

$$\mathbf{F} = e (\mathbf{v} \times \mathbf{B})$$

here

$$\begin{aligned} \mathbf{F} &= e (0, 0, v) \times (B_x, B_y, 0) \\ &= e (-v B_y, +v B_x, 0) \end{aligned}$$

Combine F D

Defocusing when at

small amplitude

Overall focusing

Normal (light) optics :

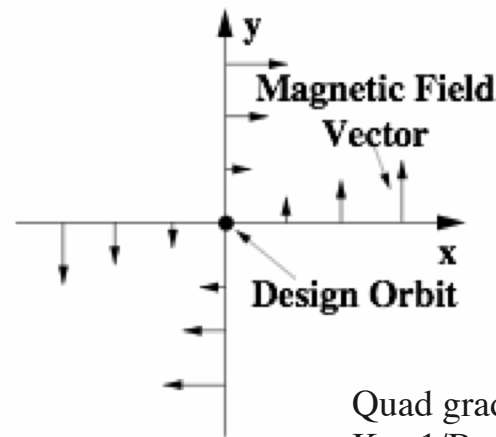
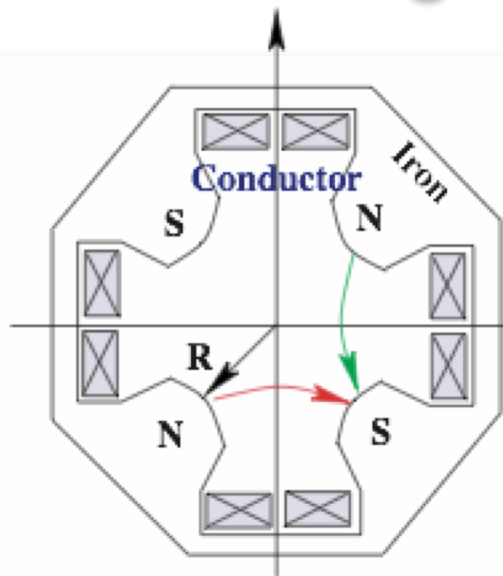
Focal length of two lenses at distance D

$$1/f = 1/f_1 + 1/f_2 - D/f_1f_2$$

is overall focusing

with $1/f = D/f^2$

for $f = f_1 = -f_2$



$$B_x = k y$$

$$B_y = k x$$

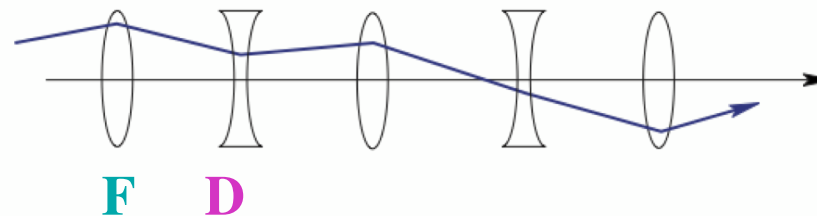
$$B_z = 0$$

$$\nabla \times \mathbf{B} = \mathbf{0}$$

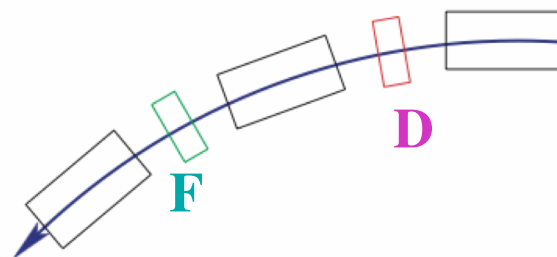
Quad gradients in the LHC

$$K = 1/B_0 \partial B_y / \partial x \approx 200 \text{ T/m}$$

alternate gradient focusing



together with bending magnets FODO lattice



N. C. Christofilos, unpublished manuscript in 1950 and patent

Courant, Snyder in 1952, Phys. Rev. 88, pp 1190 - 1196 + longer review in [Annals of Physics 3 \(1958\)](#)



Betatron motion

Equation of motion of particles in a ring (with bending fields) **and quadrupoles** (field gradients $\propto \partial B / \partial r$)

In both transverse planes, here written with x for x, y : known as Mathieu-Hill equation

$$x''(s) + k(s) x(s) = 0,$$

derived in 1801 to describe planetary motion

Generalised oscillator equation with position dependent, periodic restoring force $k(L+s) = k(s)$ given by the quadrupole gradients (+ the small weakly focusing bending term in the ring plane)

Solution : $x(s) = \sqrt{\epsilon \beta(s)} \cos(\mu(s) + \phi)$

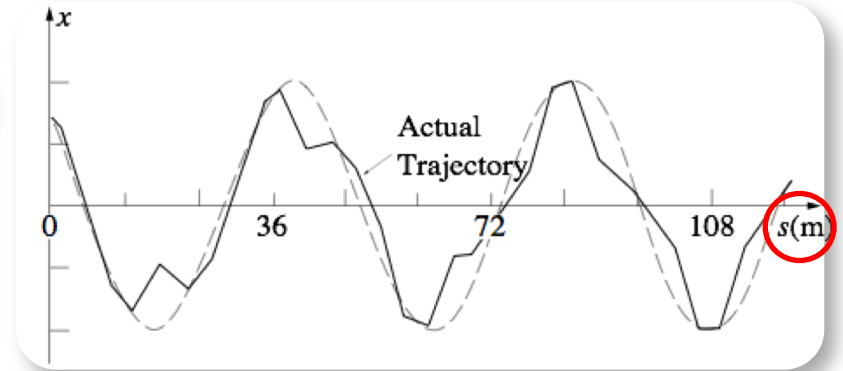
Phase advance

Lyapunov-Floquet Transformation

$$\mu(s) = \int_0^s \frac{ds}{\beta(s)}$$

Tune # of betatron oscillations

$$Q = \mu / 2\pi$$



motion $x/\sqrt{\beta}$ plotted with phase advance normalised coordinates - becomes simple cos

$\beta(s)$ **beta function**, describes the focusing properties of the magnetic lattice

ϵ invariant, together with $\beta(s)$ amplitude. "single particle emittance"

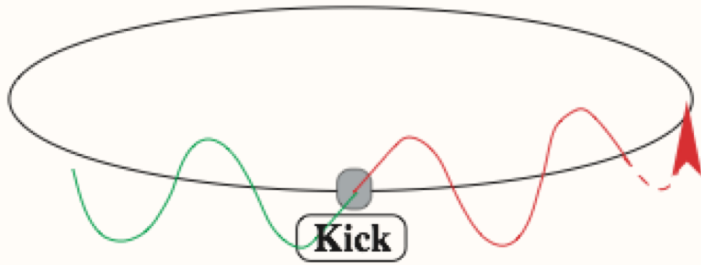
Motion conveniently described in phase space (x, x') where $x' = p_x / p$ and linear optics elements as matrices ; with simple case for M, applies for IP to IP

$$\begin{pmatrix} x(s) \\ x'(s) \end{pmatrix} = \mathbf{M} \begin{pmatrix} x(s_0) \\ x'(s_0) \end{pmatrix} \quad \mathbf{M} = \begin{pmatrix} \cos 2\pi Q & \beta \sin 2\pi Q \\ -\frac{1}{\beta} \sin 2\pi Q & \cos 2\pi Q \end{pmatrix}$$

Accelerator design : starts with magnet lattice based on linear beam optics ; MAD program



Orbit stability and tune



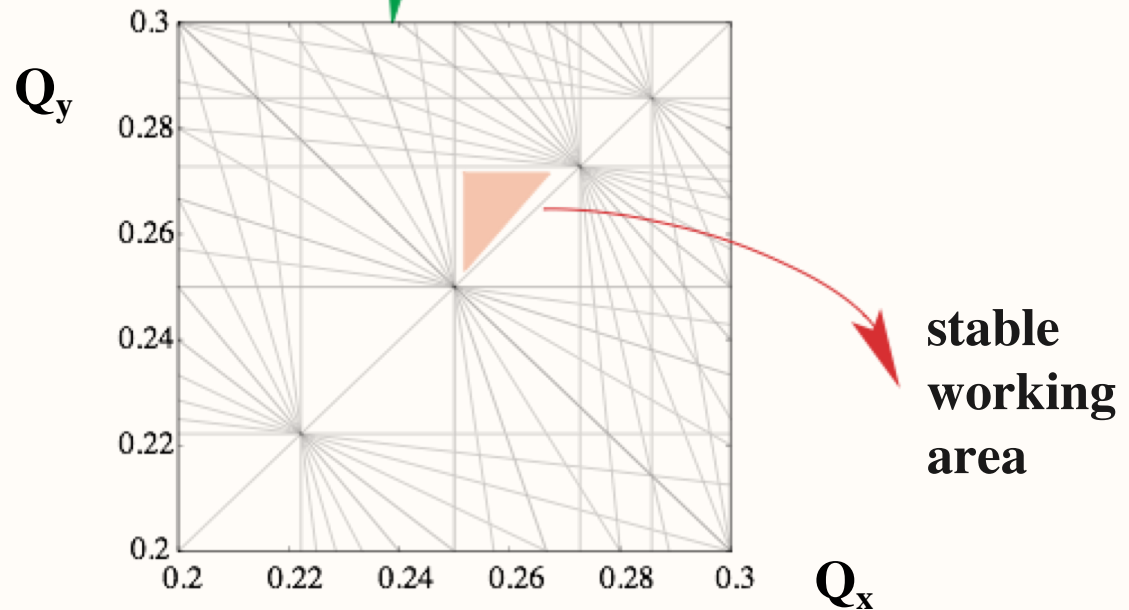
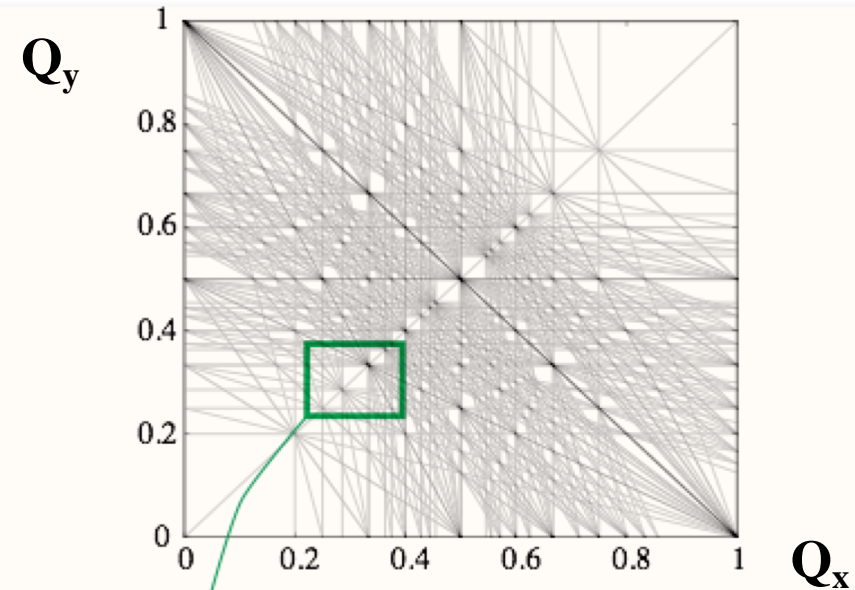
Misalignments and dipole field errors

→ **orbit perturbations**

would add up on successive turns
for integer tune $Q = N$

Higher order field errors,
Quad., Sext. perturbations.
Avoid simple fractional tunes
 $nQ_x + m Q_y + m Q_s = \text{int.}$

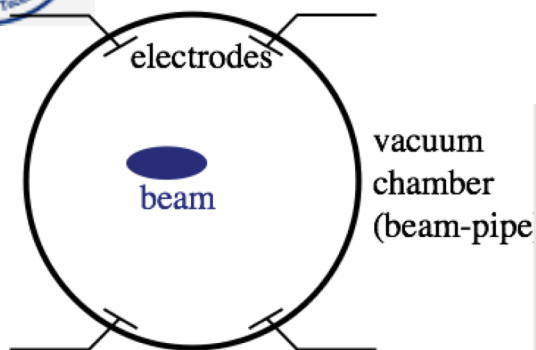
Minimise field and alignment
errors



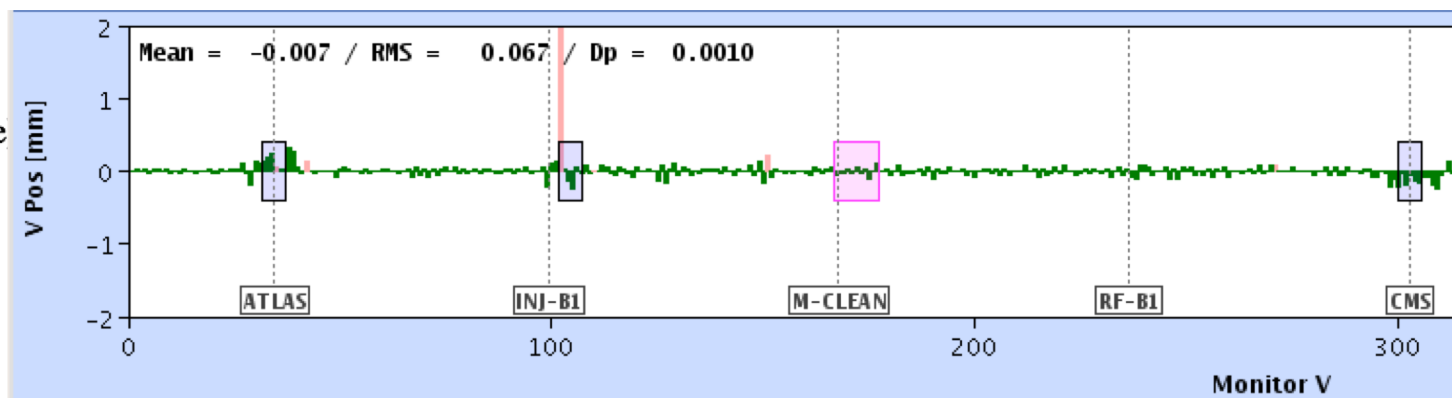


Orbit, tune measurement and peak beam current

vertical orbit, June 2011, 1st half of LHC shown



Beam Pickup Monitor



$\langle I_b \rangle$ average ring and \hat{I} local peak current

$$\hat{I} = \frac{\langle I_b \rangle L}{\sqrt{2\pi} \sigma_z}$$

Typical numbers, for a single bunch

$$\langle I_b \rangle = n e f_{rev}$$

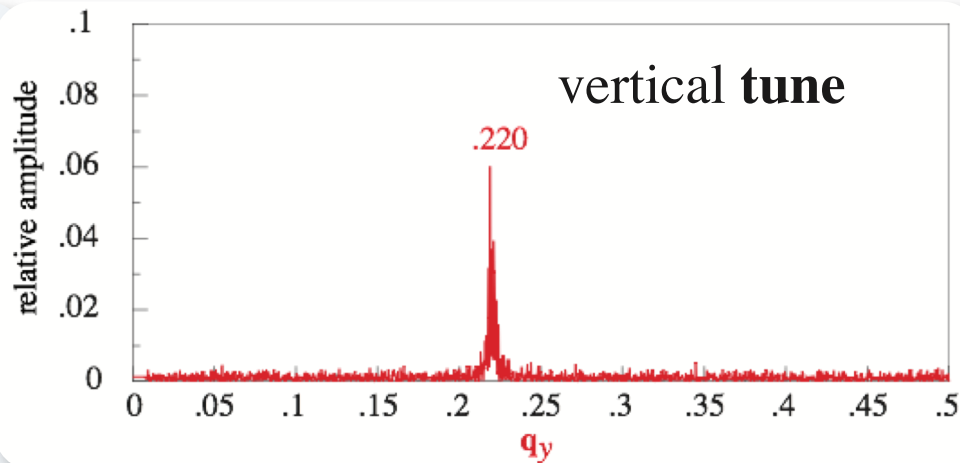
LEP $n = 4 \times 10^{11}$ $\langle I_b \rangle = 0.72 \text{ mA}$ $\sigma_z = 2 \text{ cm}$ $\hat{I} = 960 \text{ A}$

LHC $n = 1.15 \times 10^{11}$ $\langle I_b \rangle = 0.21 \text{ mA}$ $\sigma_z = 7.55 \text{ cm}$ $\hat{I} = 73.2 \text{ A}$

$f_{rev} = 11245 \text{ kHz}$, $L = 26658.9 \text{ m}$

**Bunch peak currents are many Amperes !
Strong signals, used to monitor beam position and oscillations**

Also source of undesirable effects :
wake fields, heating, instabilities





Transverse beam size and emittance

consider : beam of many particles on stable orbit and
simple case : dispersion and slope $\beta' = 0$ by default at IP - relevant for experiments

beam size, r.m.s.

$$\sigma(s) = \sqrt{\epsilon\beta(s)}$$

beam divergence, r.m.s.

$$\theta(s) = \sqrt{\epsilon/\beta(s)}$$

product

$$\epsilon = \sigma(s)\theta(s)$$

β - function : local machine quantity - focusing of lattice

Emittance ϵ : beam quantity - the average action

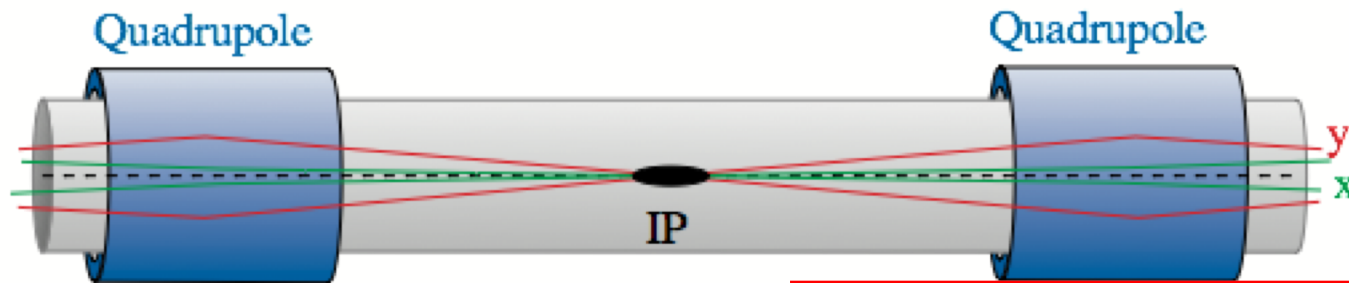
related to phase space density or kind of beam temperature

given by initial conditions (injected beam)

or equilibrium of quantum excitation and damping - 2nd lecture

in ideal machine : x, y, z motion uncoupled, 3 emittances $\epsilon_x, \epsilon_y, \epsilon_z$

IP: squeeze β to a minimum, called β^* \Rightarrow maximum of divergence, needs aperture



LHC $\epsilon_N = \epsilon \beta\gamma = 3.75 \mu\text{m}$, at top $E_b = 7 \text{ TeV}$: $\epsilon = 0.503 \text{ nm}$, $\beta^* = 0.55 \text{ m}$, $\sigma^* = 16.63 \mu\text{m}$, $\theta^* = 30 \mu\text{rad}$

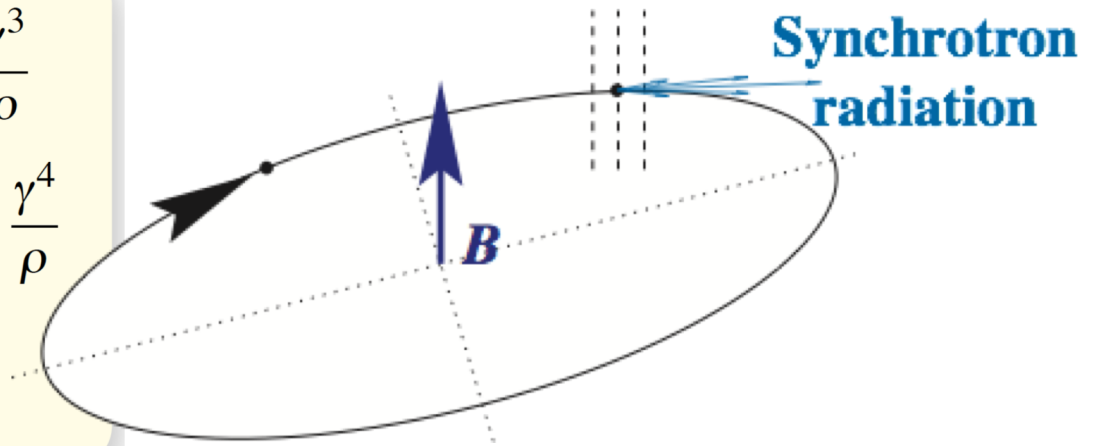


Standard Synchrotron Radiation

$$E_c = \frac{3}{2} \frac{\hbar c \gamma^3}{\rho} = 2.96 \times 10^{-7} \text{ eV m} \frac{\gamma^3}{\rho}$$

$$U_0 = \frac{e^2}{3\epsilon_0} \frac{\gamma^4}{\rho} \approx 6.0317 \cdot 10^{-9} \text{ eV m} \frac{\gamma^4}{\rho}$$

$$P_b = \frac{U_0 I_b}{e}$$



		E GeV	γ	ϱ m	U_0 MeV	E_c keV	τ_d s	N 10^{12}	I mA	P_b MW	B T
RHIC	Au	$A \times 10^0$	107.4	242.8	21×10^{-6}	1.5×10^{-6}	4.9×10^6	0.06	60	1.3×10^{-12}	3.42
LHC	p	7000	7460.5	2804	0.0067	0.044	61729	646	1163	0.0072	8.33
LEP1	e	45.6	89237	3026	126	69.5	23×10^{-3}	2.22	4	0.5	0.05
LEP2	e	104.5	204501	3026	3490	836	1.9×10^{-3}	2.8	5	18	0.115

Same beam energy E and radius ϱ : electron instead of proton $U_0 \sim \gamma^4 : (m_p/m_e)^4 = 1.13 \times 10^{13}$

Electrons, $E \gg 100$ GeV needs linear collider (ILC / CLIC)

Damping time E / U_0 turns or $\tau_d = t_{rev} E / U_0$ revolution time LEP/LHC $t_{rev} = 88.9 \mu\text{s}$

Gold ions Au⁷⁹⁺ A=197 $\langle E_\gamma \rangle = 8/(15\sqrt{3}) E_c$ $8/(15\sqrt{3}) \approx 0.308$



Synchrotron light monitor

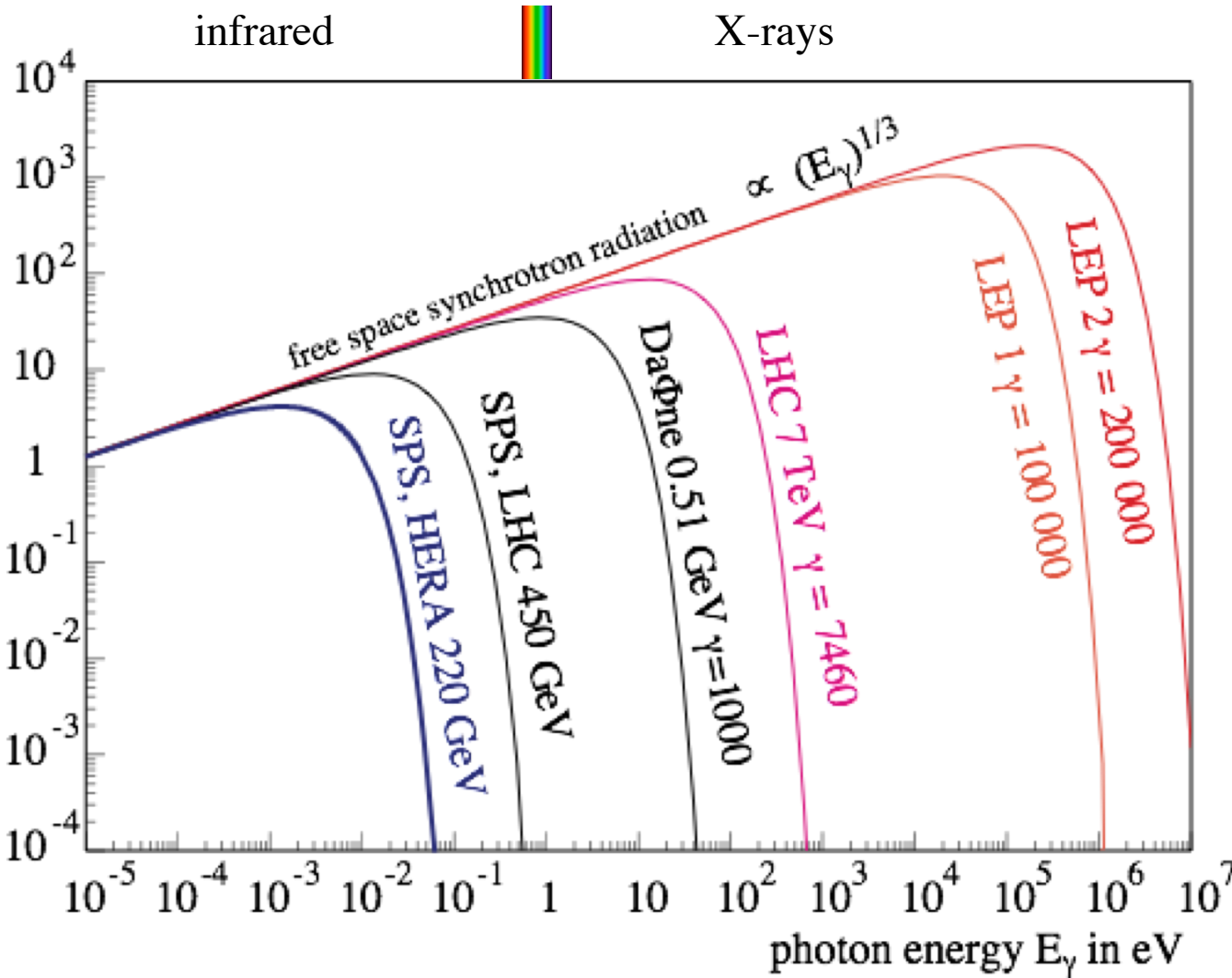
**Picture from LEP. Typical
transverse
rms beam size 0.15 mm
vertical 1.5 mm horiz.**



**Mirror, small slit, telescope and camera : beams continuously visible.
Now also used for protons in the LHC.**



Power Spectrum, Free space, Cutoff and CSR



$$\frac{f_{\text{cutoff}}}{f_{\text{rev}}} = \sqrt{\frac{2}{3}} \left(\frac{\pi \rho}{h} \right)^{3/2}$$

ρ bending radius
 h chamber height
 cutoff relevant
 for $\gamma \approx 100$

12 orders of magnitude
 in E_γ and λ

10^{-5} eV $\lambda = 0.124$ m

10^{+7} eV $\lambda = 124$ fm

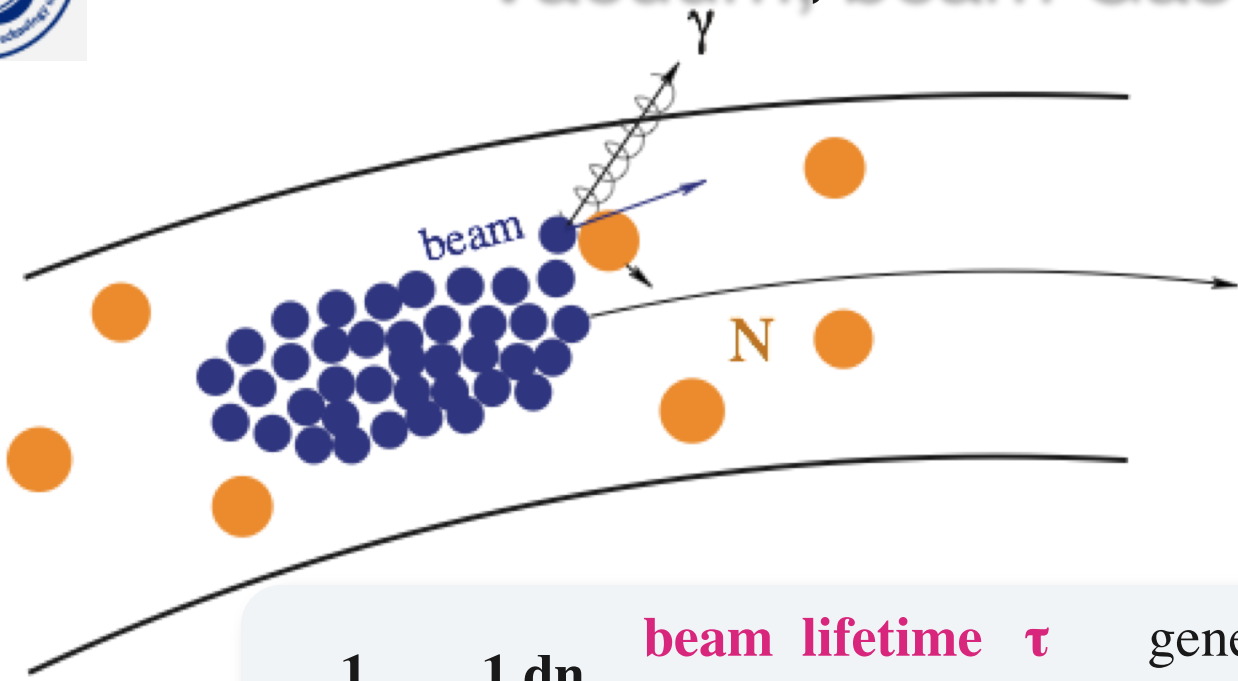
Effects which can modify the low energy, long wavelength spectrum :

- i) **Coherent Synchrotron Radiation CSR** increases radiation and loss
- ii) **Boundary conditions - cutoff by conducting chamber** decreases radiation and loss

Energy Loss of Gold Ions in RHIC, [EPAC 2008](#)



Vacuum, beam Gas - lifetime



Beam blow up, core + halo
 Background to experiments
 loss, radiation, beam and
 Luminosity lifetime

Minimize effect :
 Good vacuum
 O(nTorr or 10^{-9} mb)
 Collimation

$$\frac{1}{\tau} = - \frac{1}{n} \frac{dn}{dt}$$

beam lifetime τ general expression
 average time between collisions leading to beam loss
 inverse normalised loss rate

$$p = 1 \text{ ntorr} = 1.33 \times 10^{-7} \text{ Pa}$$

$$\rho_m = \frac{p}{kT} = 3.26 \times 10^{13} \text{ molecules / m}^3$$

typical cross section $\sigma = 6 \text{ barn} = 6 \times 10^{-28} \text{ m}^2$

collision probability $P_{\text{coll}} = \sigma \rho_m = 1.96 \times 10^{-14} / \text{m}$

$$\tau = \frac{1}{P_{\text{coll}} c} = 1.7 \times 10^5 \text{ s} = 47 \text{ hours} \quad \text{for } v \approx c$$



Damage potential : confirmed in controlled SPS experiment

controlled experiment with beam extracted from SPS at 450 GeV in a single turn, with perpendicular impact on Cu + stainless steel target

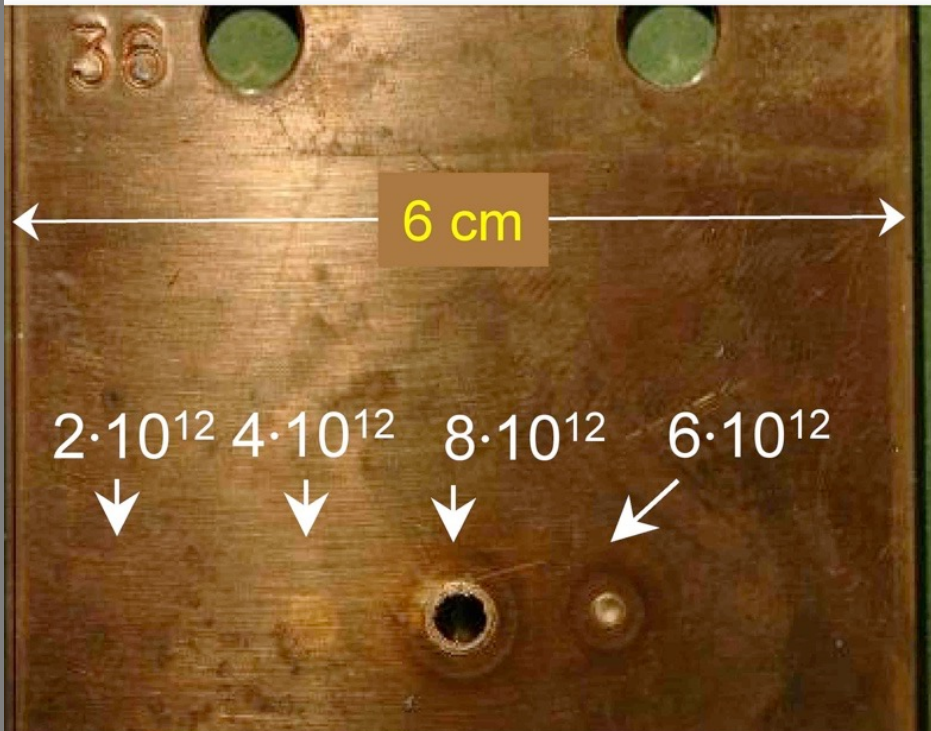
450 GeV protons →

r.m.s. beam sizes $\sigma_{x/y} \approx 1$ mm



Cu and stainless steel sandwich
108 plates

25 cm



6 cm

$2 \cdot 10^{12}$ $4 \cdot 10^{12}$ $8 \cdot 10^{12}$ $6 \cdot 10^{12}$

SPS results confirmed :

$8 \cdot 10^{12}$ clear damage

$2 \cdot 10^{12}$ below damage limit

for details see V. Kain et al., PAC 2005 [RPPE018](#)

For comparison, the LHC nominal at 7 TeV :

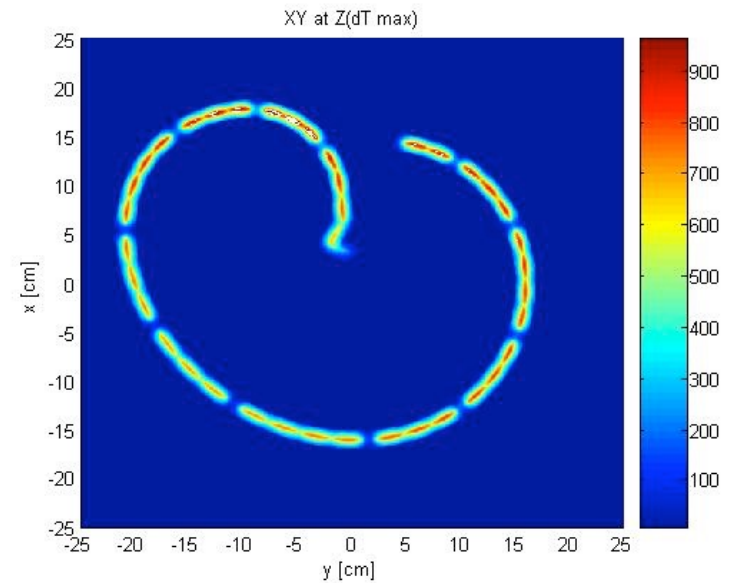
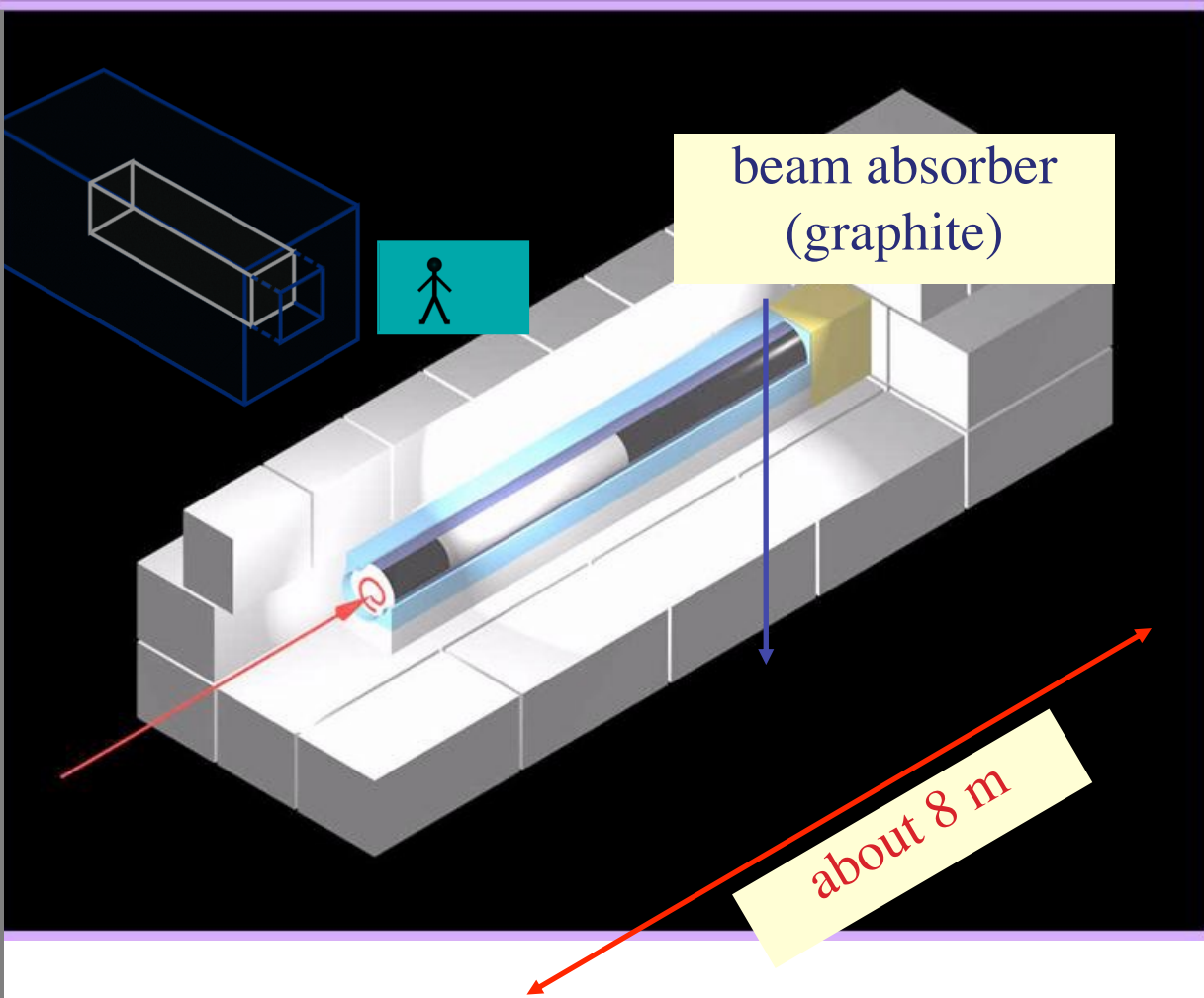
$$2808 \times 1.15 \times 10^{11} = 3.2 \times 10^{14} \text{ p/beam}$$

at $\langle \sigma_{x/y} \rangle \approx 0.2$ mm

over 3 orders of magnitude above damage level for perpendicular impact

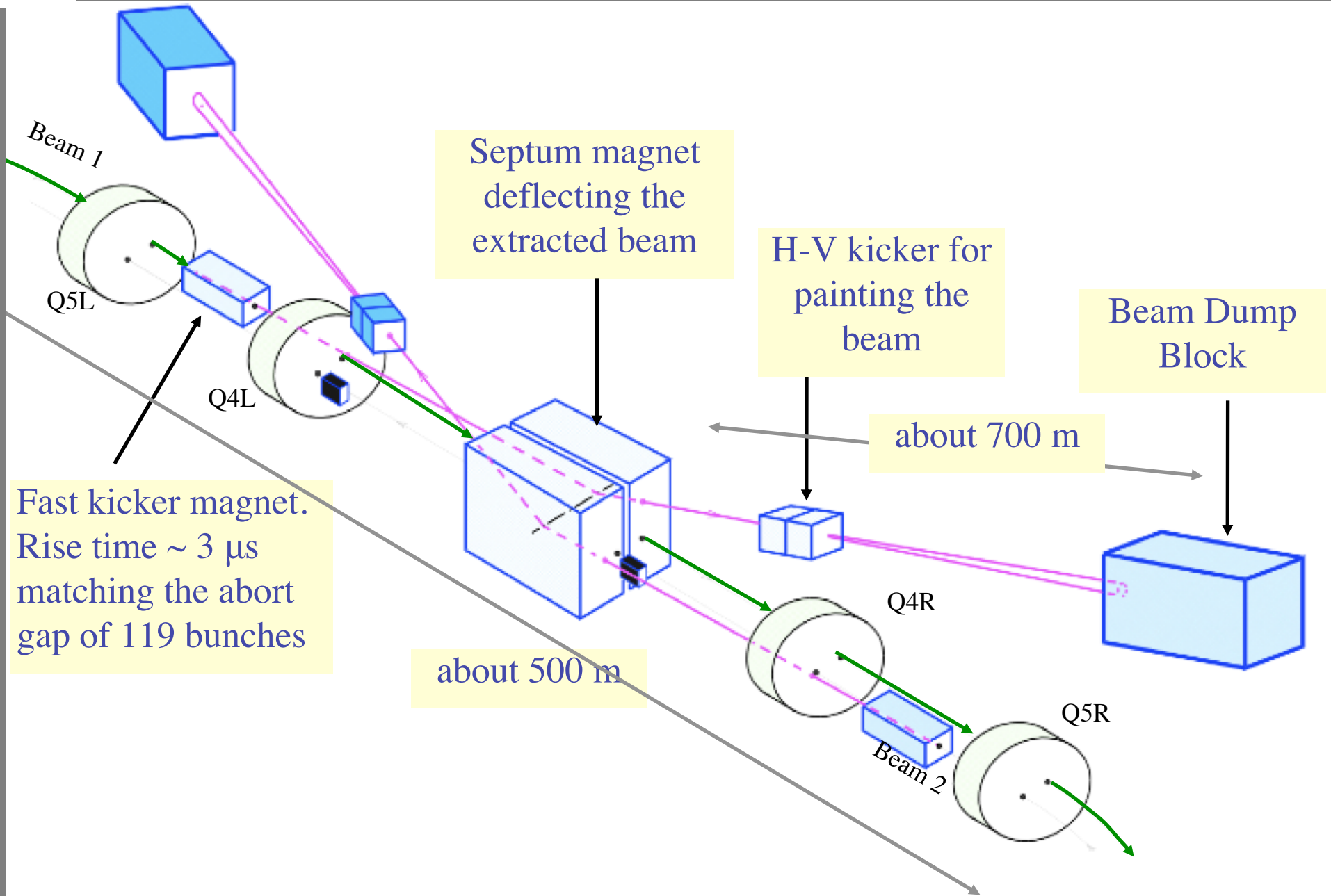


Dumping the LHC beam





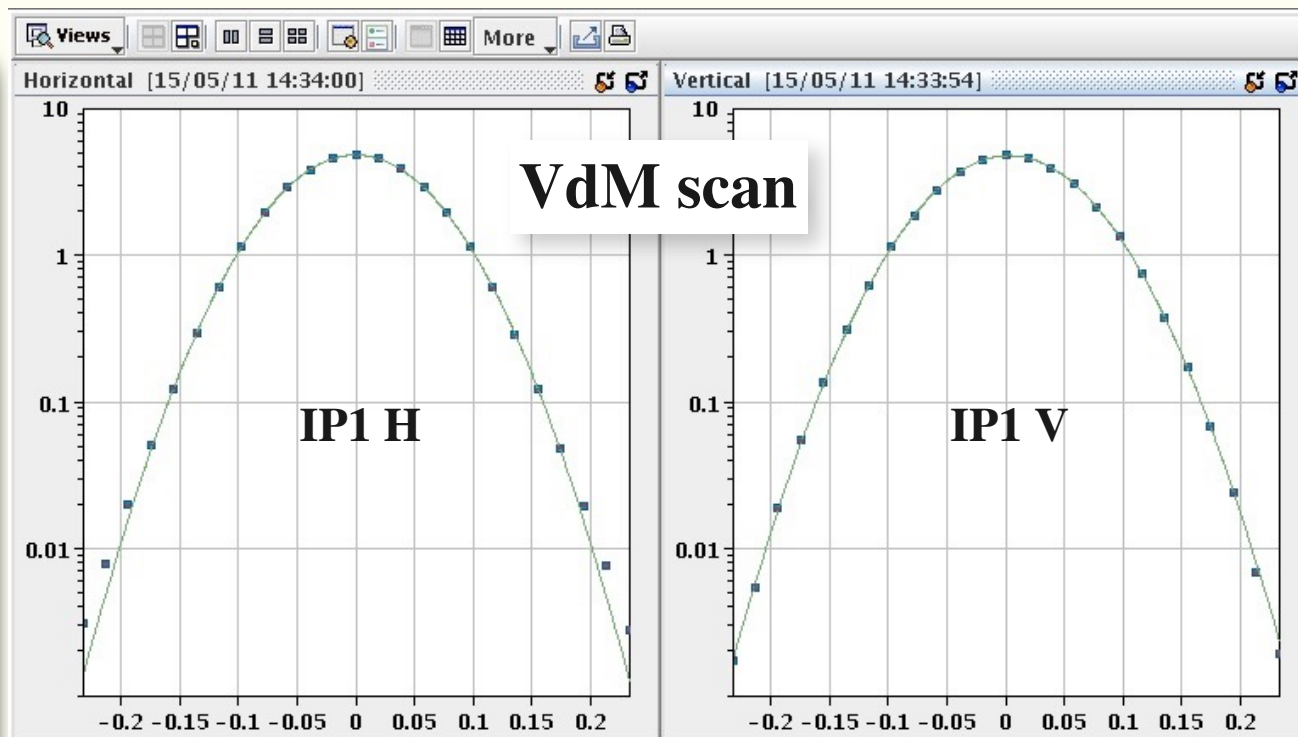
Schematic layout of beam dump system in IR6





Precision front - high quality of LHC beams

- **absolute luminosity normalization**
 - **low, well understood backgrounds**
 - **precision optics for ATLAS-ALFA and TOTEM**
- $\beta^* = 1000$ m, Oct.'12



precise measurement of the luminous region + beam intensity --> absolute luminosity and cross section calibration

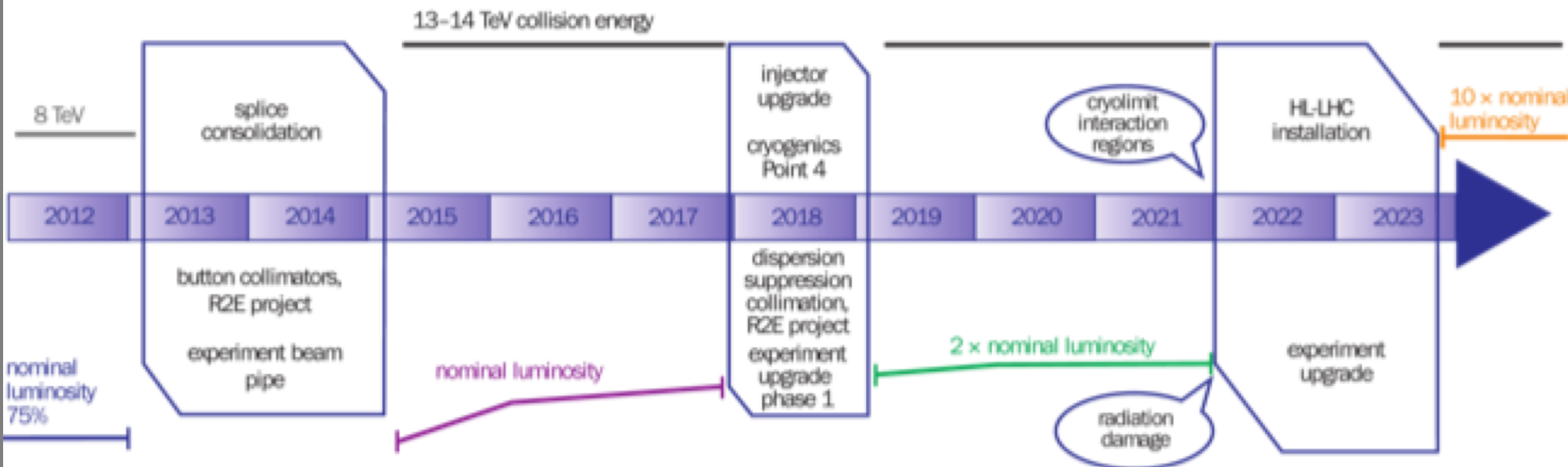
currently ~ 3 % level (Tevatron had ~ 15 %)



HL-LHC Timeline

Toni Baroncelli: Experimental High Energy Physics at Colliders 2019-20

The LHC is still a rather young machine
Operation planning + upgrade studies (HL-LHC) extend to ~ 2030



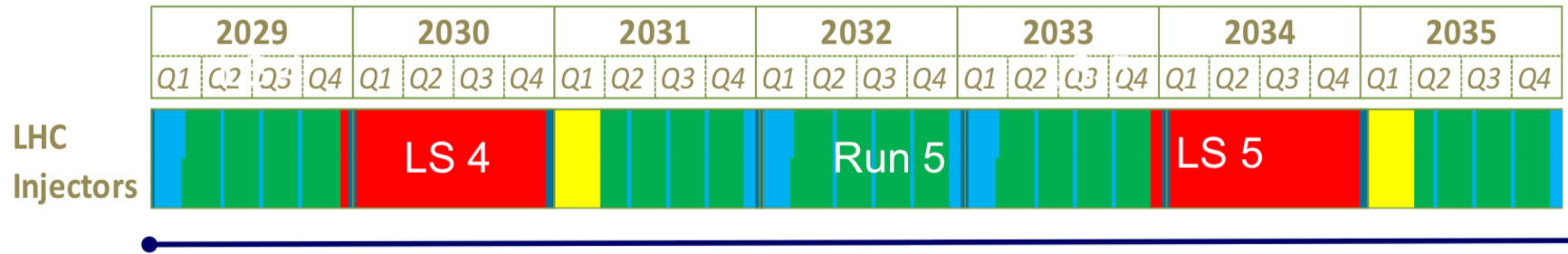
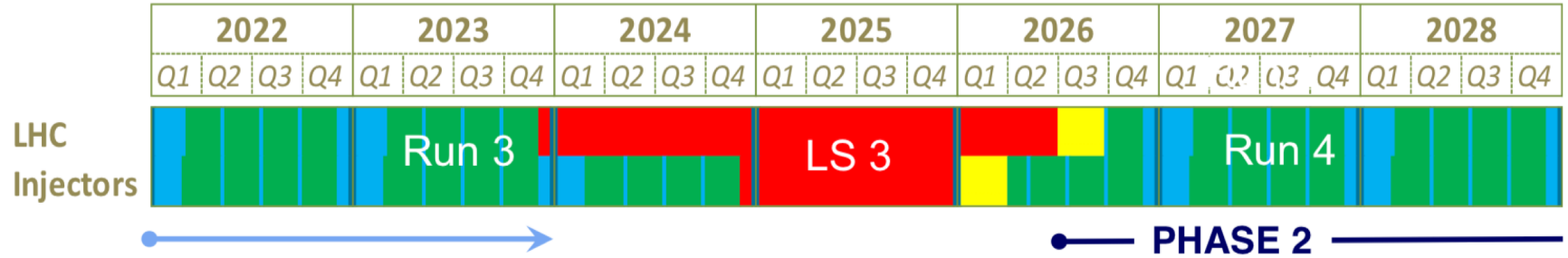
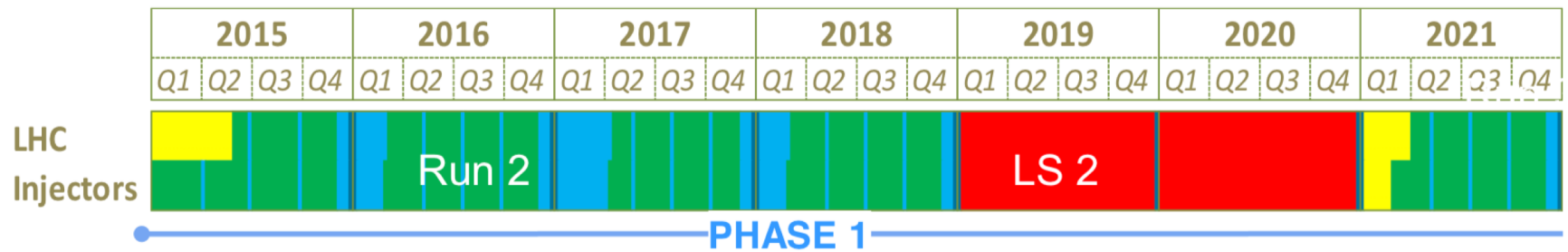
Further ideas already exist (HE-LHC, LHeC, TLEP)
We also study other machines, and in particular CLIC →



Up-to-date LHC schedule

LHC roadmap: according to MTP 2016-2020 V1

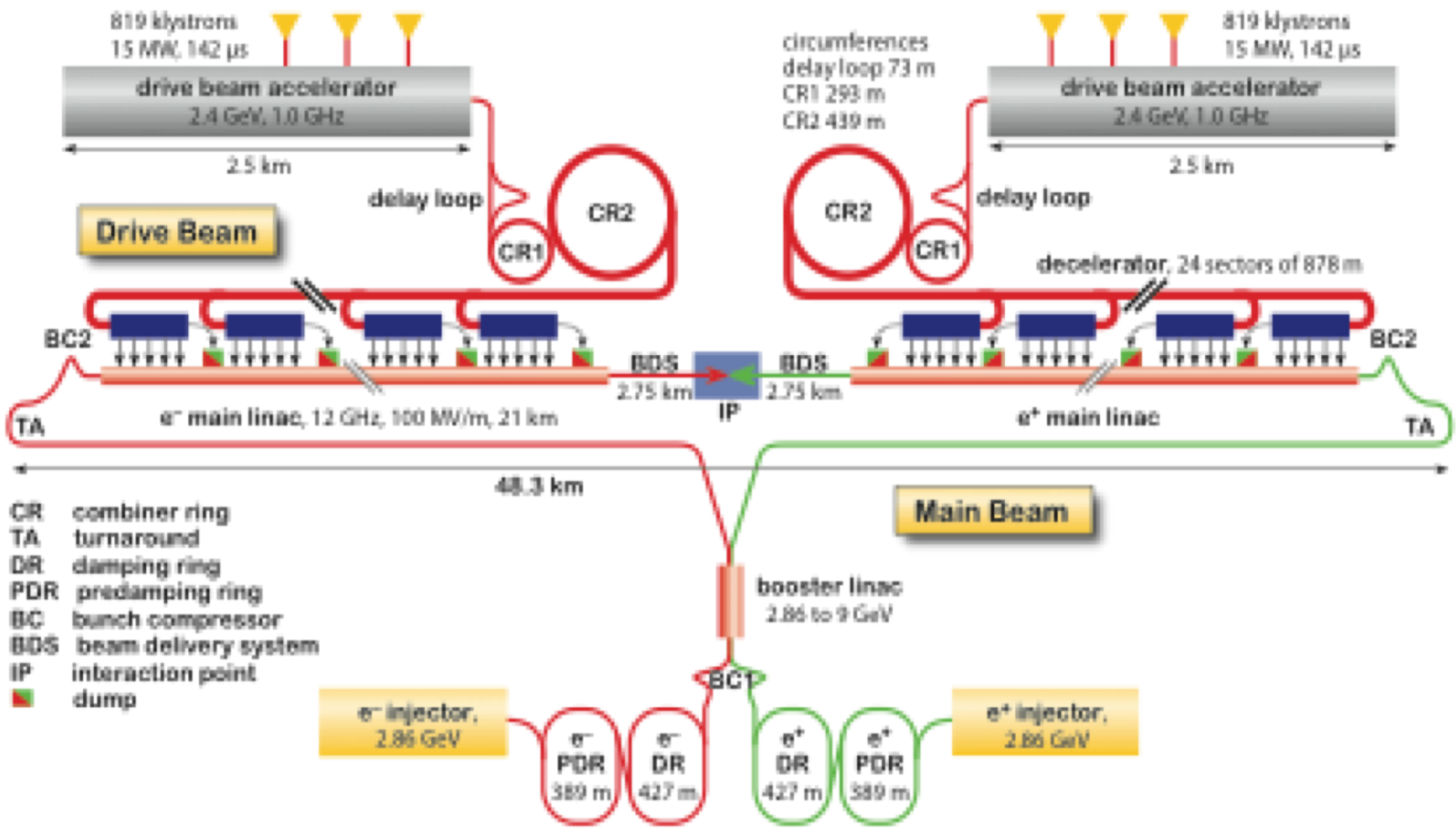
LS2 starting in 2019 => 24 months + 3 months BC
 LS3 LHC: starting in 2024 => 30 months + 3 months BC
 Injectors: in 2025 => 13 months + 3 months BC





CLIC

Toni Baroncelli: Experimental High Energy Physics at Colliders 2019-20



Overview of the CLIC layout at $\sqrt{s} = 3$ TeV

The machine requires only one drive beam complex for stages 1 and 2.



Accelerator applications and R&D

- **The largest flag-ship accelerator is the LHC here at CERN**
 - **By now many more accelerators outside particle physics**
- #Accelerators in the world : O (30 000) mostly smaller for medical and industrial applications
- **Broad range of particle accelerator types and applications**

Large research facilities for :

Synchrotron light, UV, X-Ray (electron accelerators)

High intensity proton accelerators + neutron spallation sources

condensed matter, material science and biology research,

accelerator driven subcritical fission (energy production & radioactive waste incineration)

Yearly international accelerator conferences IPAC, last one in May'13 in [Shanghai](#)

Some of the hot-subjects and keywords :

- **Free electrons lasers FEL, X-FEL, Laser induced coherent SR**
- **Advanced LINACS -- including recirculation and energy recovery ERL**
- **New acceleration techniques :**
 - **Dielectric, LASER, Plasma driven**



Reserve



Radiation of an accelerated charge

General concept - power radiated by an accelerated charge. Relativistic version of Lamor's formula, derived by Lienard in 1898, before relativity was known.

Photon spectrum : J. Schwinger Phys. Rev. 75 (1949) pp. 1912-1925

Here written with formulas in SI units. More info + references in my paper on MC generation of [SynRad](#) CERN-OPEN-2007-018

power radiated by an accelerated charge

$$P = \frac{e^2 \gamma^2}{6\pi \epsilon_0 m^2 c^3} \left[\left(\frac{d\mathbf{p}}{dt} \right)^2 - \beta^2 \left(\frac{d\mathbf{p}}{dt} \right)^2 \right]$$

relativistic
Lamor formula

results in a major energy loss for a ring at high γ

$\mathbf{v} \perp \dot{\mathbf{v}}$

$$\underbrace{\left(\frac{d\mathbf{p}}{dt} \right)^2 - \beta^2 \left(\frac{d\mathbf{p}}{dt} \right)^2}_0 = \dot{\mathbf{p}}^2 \quad P = \frac{e^2}{6\pi \epsilon_0 m^2 c^3} \gamma^2 \dot{\mathbf{p}}^2$$

Perpendicular acceleration, B-field (or E_{\perp} field). Motion in circular machine.

$\mathbf{v} \parallel \dot{\mathbf{v}}$

$$\left(\frac{d\mathbf{p}}{dt} \right)^2 = \left(\frac{d\mathbf{p}}{dt} \right)^2 \quad \left(\frac{d\mathbf{p}}{dt} \right)^2 - \beta^2 \left(\frac{d\mathbf{p}}{dt} \right)^2 = \dot{\mathbf{p}}^2 (1 - \beta^2) = \frac{\dot{\mathbf{p}}^2}{\gamma^2}$$

$$P = \frac{e^2}{6\pi \epsilon_0 m^2 c^3} \dot{\mathbf{p}}^2$$

Parallel acceleration, E-field, Linac case
cancellation, $1/\gamma^2$

The energy loss for linear acceleration is very small.

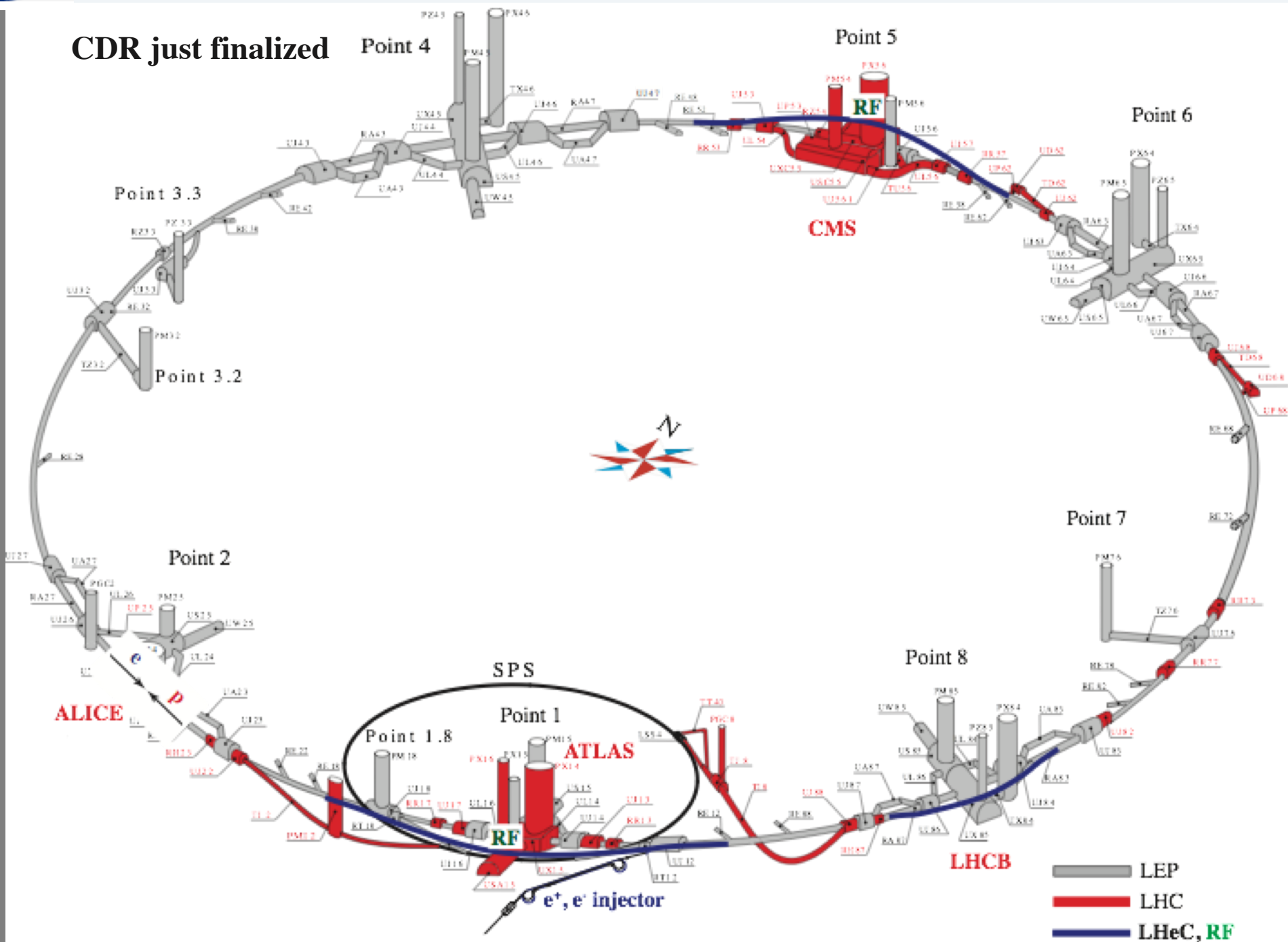
Example: CLIC gradient 100 MV/m. Loss is 11 keV/s or only 0.4 eV for a 1 TeV 10 km Linac



LHeC

Toni Baroncelli Experimental High Energy Physics at Colliders 2019-20

CDR just finalized

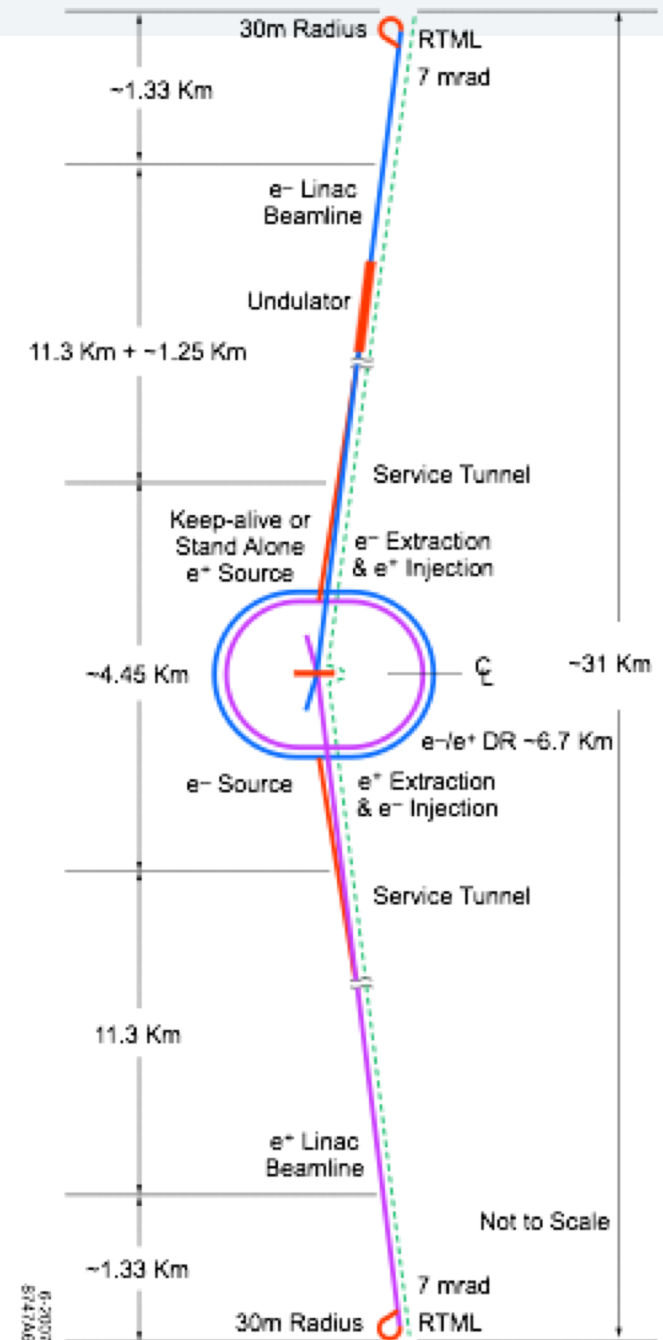
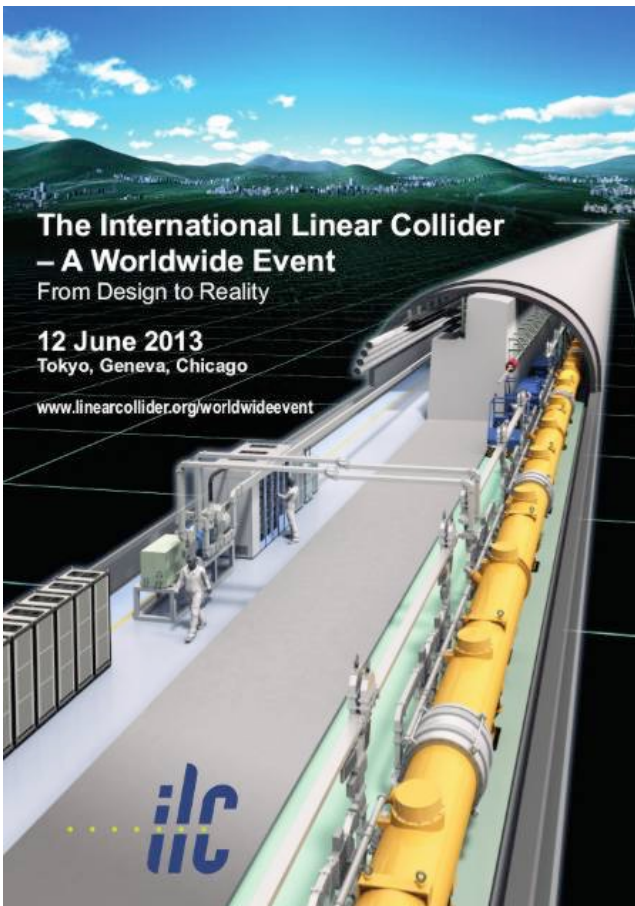




ILC

ILC TDR Handover, 12 June 2013

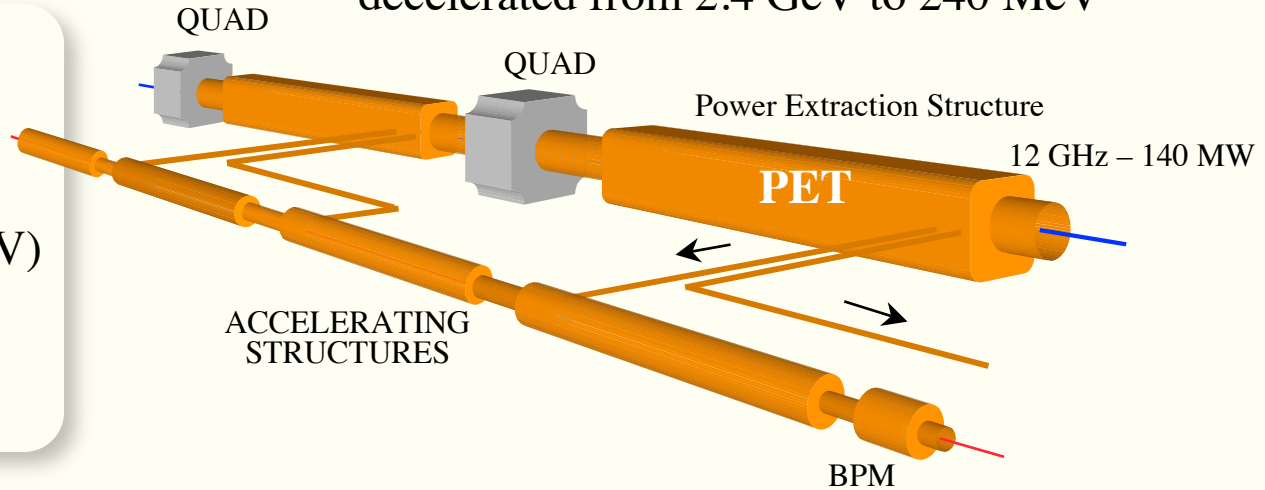
- 200-500 GeV centre-of-mass, 31 km long
- Luminosity: $2 \times 10^{34} \text{ cm}^{-2}\text{s}^{-1}$
- Based on accelerating gradient of 31.5 MV/m
1.3 GHz superconducting RF





CLIC

Drive beam - 100 A, 240 ns
decelerated from 2.4 GeV to 240 MeV



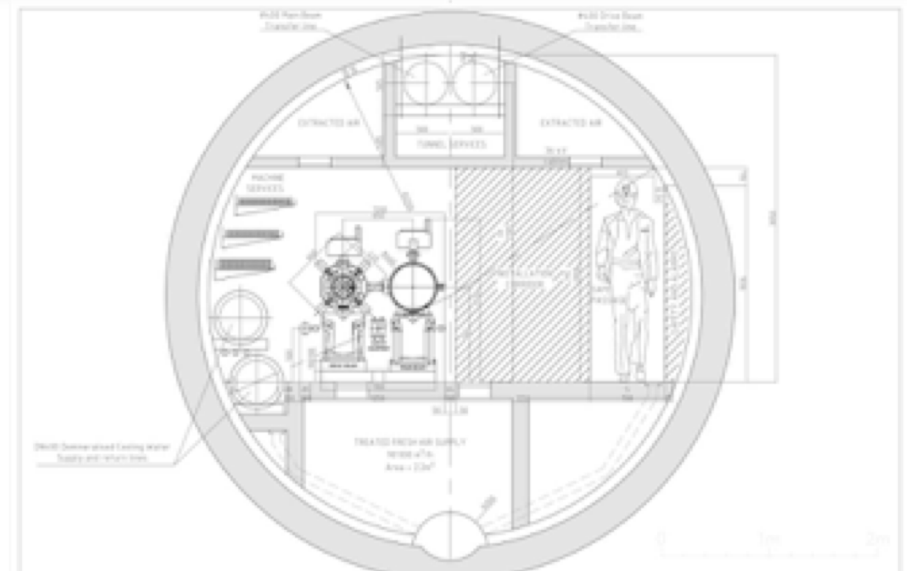
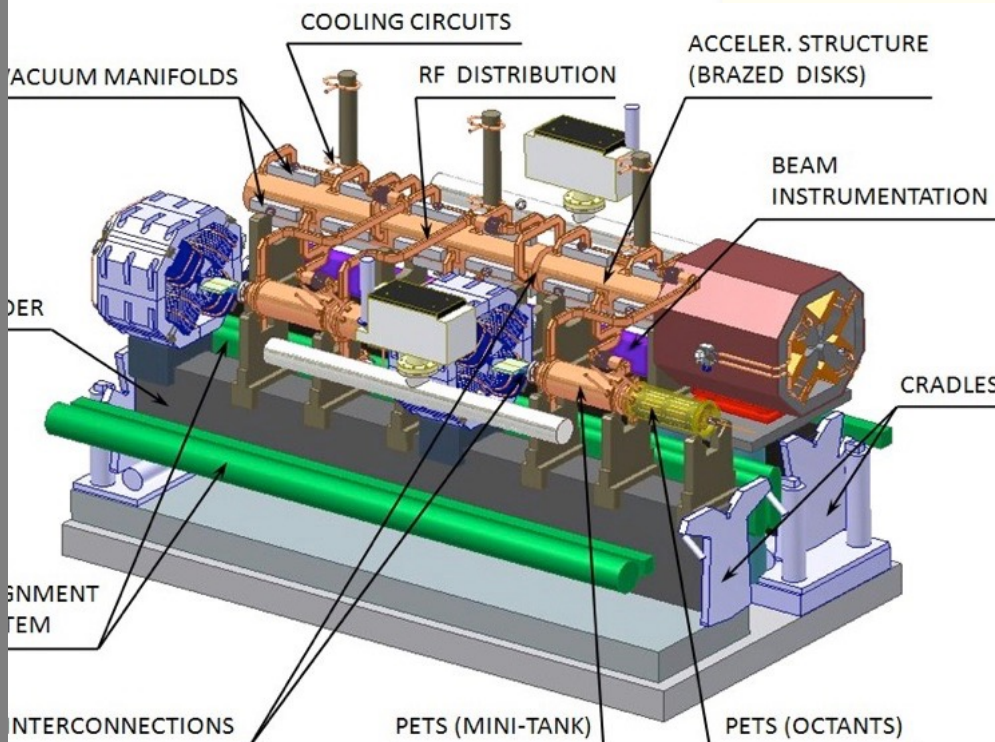
Two Beam Scheme

Drive Beam supplies RF power

- 12 GHz bunch structure
- low energy (2.4 GeV - 240 MeV)
- high current (100A)

warm (not superconducting) RF

Main beam - 1.2 A, 156 ns bunch trains
accelerated from 9 GeV to 1.5 TeV





ILC and CLIC parameters

ILC: Superconducting RF

CLIC: normal conducting copper RF

500 GeV

3 TeV

accelerating gradient:

31.5 MV/m

100 MV/m

35 MV/m target

RF Peak power:

0.37 MW/m , 1.6 ms, 5 Hz

275 MW/m, 240 ns, 50 Hz

RF average power:

2.9 kW/m

3.7 kW/m

total length:

31 km

48.4 km

site power :

230 MW

392 MW

Beam structure:

particles per bunch:

20×10^9

3.7×10^9

2625 bunches / pulse of

0.96 ms

312 bunches / pulse of 156 ns

bunch spacing

369 ns

0.5 ns



The main 2013-14 LHC consolidations

1695 Openings and final reclosures of the interconnections

Complete reconstruction of 1500 of these splices

Consolidation of the 10170 13kA splices, installing 27 000 shunts

Installation of 5000 consolidated electrical insulation systems

300 000 electrical resistance measurements

10170 orbital welding of stainless steel lines

18 000 electrical Quality Assurance tests

10170 leak tightness tests

4 quadrupole magnets to be replaced

15 dipole magnets to be replaced

Installation of 612 pressure relief devices to bring the total to 1344

Consolidation of the 13 kA circuits in the 16 main electrical feed-boxes